U.PORTO
FEUP FACULDADE DE ENGENHARIA
UNIVERSIDADE DO PORTO

Faculdade de Engenharia da Universidade do Porto

Departamento de Engenharia Mecânica

Condition Monitoring of Gearbox Faults with Acoustic and Vibration Signals

Alexandre Mauricio

Master's Degree Dissertation presented to

Faculdade de Engenharia da Universidade do Porto

Dissertation supervised by

Professor Jose Dias Rodrigues — Associate Professor of FEUP

Engineer Carina Freitas — Researcher of Siemens PLM

Porto, 2017

LaTeX

FEUP-U.PORTO

Alexandre Mauricio

2017

To my father João Mauricio,
in hope to see the man proud.

Acknowledgments

With the conclusion of the Master's Degree Dissertation comes the time to mention some of the people who helped me throughout this final project.

I express my deepest appreciation to my supervisor, Eng. Carina Freitas, for the guidance during the execution of this work and for the inspiration she represents. That's something I aspire for my future. I also show my recognition to Dr. José F. D. Rodrigues for encouraging me on the pursuit of excellence.

A special thanks to all of Siemens PLM (Research Technology and Development) for the support: Jacques Cuenca for the inspiration of an expert and patient support; Kilian Hendricks and Claudio Colangeli for the added interesting topics that added value to my research; Joao Araújo for being a part of the research; Andrea Renno for the friendship the support he provided; and every one else for the good environment they created around me.

At the end of the Master's Degree in Mechanical Engineering, a special reference to Faculdade de Engenharia da Universidade do Porto for these amazing years and resources put at the disposal of its students in order to provide them a superior education, professional and personally. In particular, a special thanks to Eng. César Soares for the dedication and friendship he gave when I most needed it.

On a personal note, I express my gratitude to my girlfriend Teresa Brissos, for all the love, understanding and dedication she provided me during these years, and particularly during the conclusion of this dissertation.

Last, but not least, my family. The ones who believed in me, gave me comprehension and means to conclude the degree. My intention for my professional and personal future is most and foremost to make them proud.

Keywords

Condition Monitoring of Gears

Gear with Chipped Tooth

Gear with Missing Tooth

Acoustic Signals

Cyclic Spectral Correlation

Principal Components Analysis

Vibration Signals

Palavras-Chave

Monitorização de Condição de Engrenagens

Pinhão com Dente Lascado

Pinhão com Dente Partido

Sinais Acústicos

Cyclic Spectral Correlation

Análise de Componentes Principais

Sinais Vibratórios

Abstract

The increase of repair costs alongside the waste of time generated by the replacement of damaged mechanical components has generated an increasing global interest by companies regarding the investigation of processes that allow a correct prediction and maintenance of mechanical components. Condition monitoring is clearly an emerging area in obtaining such answers.

Gearbox faults are a topic that has been extensively studied, resorting mainly to Vibration Analysis and, in a smaller scale, to acoustic analysis. Both of them can describe the nature of a working gearbox; however, there is no consensus among the academia on a global functioning diagnosis for all gearbox signals, even less one that is automatized.

The fact that such diagnosis are inescapably done by an expert in the field makes this process rather expensive. Following that reasoning, this dissertation focused on the assessment of vibration and acoustic signals of a gearbox with two different kinds of damage.

In order to do so, two faults inserted in the gearbox were analyzed: pinion with a missing tooth, and pinion with a chipped tooth. Both were compared with a healthy gearbox. The necessary signal processing method for obtaining the impulses was Envelope Analysis, being the filter selection done semi-automatically through Cyclic Spectral Correlation.

From the obtained results, it was concluded that for vibration signals, the filter selection was correct, and the Wavelet Analysis clearly states the different cases, specially the impulse present in the missing tooth case. Regarding the acoustic signals, it was seen that the impulsive band of frequencies is hard to obtain for one case, for the gearbox with the missing tooth.

It is also demonstrated that the Principal Components Analysis (PCA) distinctly classifies the two different faults regarding the vibration signals, whereas the PCA for the acoustic signal allows the classification for the chipped tooth case, by automatic selection from the Cyclic Spectral Correlation. The missing tooth case is also classified, but human intervention is needed through the choice of the acoustic filter. Overall, even though the PCA is an unsupervised method, without no label attached, it provides a good distinction between the faults.

Resumo

O aumento de custos de reparação juntamente com a perda de tempo em substituição dos componentes mecânicos que roturam, gerou um interesse global conjunto por parte das empresas em investigação de processos que permitam a correta previsão e manutenção de componentes mecânicos. Desta investigação observa-se uma área notoriamente emergente na obtenção destas respostas, o Condition Monitoring.

A falha de caixas de engrenagens é um tópico extensamente estudado, principalmente por Análise de Vibrações , e em menor degrau por Análise Acústica. Ambas conseguem descrever a natureza da caixa de engrenagens em funcionamento. Contudo não existe consenso sobre um correto diagnóstico de rotura global, e muito menos automático. O facto deste diagnóstico ser invariavelmente feito por um analista experiente nesta área torna o processo dispendioso.

Nesse sentido, esta dissertação teve como principal objectivo a avaliação de sinais de vibrações e acústicos de caixa de engrenagens com dois tipos de dano.

Para tal, foram analisadas as seguintes duas falhas inseridas na caixa de engrenagens: pinhão com dente partido; pinhão com dente lascado. Estas foram comparadas com a caixa de engrenagens saudável. O processamento de sinal necessário para a obtenção dos impulsos foi o Envelope Analysis, e para tal a seleção do filtro é concluída de forma semi-automática pelo Cyclic Spectral Correlation.

Dos resultados obtidos, concluiu-se que para sinais de Vibraçao, a seleção do filtro é correta, e a Análise por Wavelet claramente denota os diferentes casos, especialmente o impulso do dente partido. Para o sinal acústico, verificou-se que a banda de frequências impulsiva está dissimulada, apenas para o caso do dente partido.

Conclui-se, tambem, que a Análise dos Componentes Principais (PCA) classifica de maneira clara as duas diferentes falhas, para os sinais de vibração. O PCA do sinal acústico permite a classificação do dente rachado, para o processo automático. O dente partido também é classificado, mas para isso intervenção humana é necessária na escolha do filtro acústico. Em suma, mesmo o PCA sendo um método não supervisionado, sem informação dos diferentes estados, devolve uma boa distinção entre as diferentes falhas.

Nomenclature

Latin characters

Variable	Description	Units
A_i	Magnitude of the i_{th} component	m^2
E	Expected value	-
e	Distance from axis centerline to the center of gravity	m
f	Frequency	Hz
f_r	Shaft rotation speed	Hz
$\tilde{\mathrm{M}}$	Variance of healthy signal	-
N_a	Greatest common factor	-
R_{xx}	Autocorrelation function	-
S_x	Covariance matrix	-
s_C	Carrier wave	-
s_m	Modulating wave	-
T	Period	s
t	Time	s
X_w	Fourier Transform	-
W	Window function	-
w	angular speed	rad/s
Z_1	Pinion number of teeth	-
Z_2	Driven Gear number of teeth	-

Greek characters

Variable	Description	Units
τ	time-lag	s
α	Cyclic frequency	Hz

Note: The variables units are presented according to the International System of Units (SI). Throughout the text other units may be used to allow an easier interpretation.

Acronyms

CF	Crest Factor
CI	Condition Indicator
CSC	Cyclic Spectral Correlation
GFD	Gearbox Fault Diagnosis
GMF	Gear Mesh Frequency
HTF	Hunting Tooth Frequency
RMS	Root Mean Squared
PCA	Principal Component Analysis
SK	Spectral Kurtosis
$STFT$	Short Time Fourier Transform
TSA	Time Synchronous Averaging

Contents

Abstract ix

Resumo xi

Nomenclature xvi

List of Figures xx

List of Tables xxi

1 Introduction 1
- 1.1 Condition Monitoring . . . 1
- 1.2 Motivations . . . 2
- 1.3 Objectives . . . 3
- 1.4 Document Outline . . . 3

2 Gearbox Fundamentals 5
- 2.1 Signal Classification . . . 5
- 2.2 Common types of faults in a gearbox . . . 10
  - 2.2.1 Frequent Component Signals . . . 12
- 2.3 Rolling Element Bearing Signals . . . 14
- 2.4 Gear Signals . . . 16
  - 2.4.1 Distributed Defects . . . 17
  - 2.4.2 Localized Defects . . . 18

3 Data Processing Techniques 21
- 3.1 Signal Representation Methods . . . 21
  - 3.1.1 Time Domain . . . 21
  - 3.1.2 Frequency Domain . . . 23
  - 3.1.3 Time-Frequency Domain . . . 25
  - 3.1.4 Angular Domain . . . 27
- 3.2 Signal Processing Methods . . . 28
  - 3.2.1 Cepstrum . . . 28
  - 3.2.2 Time Synchronous Averaging (TSA) . . . 28
- 3.3 Envelope Analysis . . . 29
- 3.4 Filter Selection Techniques . . . 30
  - 3.4.1 Spectral Kurtosis . . . 30
  - 3.4.2 Kurtogram . . . 30
  - 3.4.3 Wavelet Analysis . . . 31
  - 3.4.4 Cyclostationary Analysis . . . 32
- 3.5 Fault Indication . . . 34

4 Condition Diagnosis **37**
4.1 Classification Features . . . 37
4.2 Feature Analysis . . . 41
4.2.1 Single Features . . . 41
4.2.2 Principal Component Analysis (PCA) . . . 42
4.2.3 Adopted Procedure . . . 44

5 Experimental Tests and Results **45**
5.1 Experimental Setup . . . 46
5.2 Gearbox Raw Vibration Signals . . . 47
5.2.1 Spectrum . . . 48
5.2.2 Wavelet Analysis . . . 49
5.2.3 Cyclostationary Analysis . . . 51
5.2.4 Hunting Tooth Diagnosis . . . 53
5.3 Vibration Signal Filtered at 4500 Hz . . . 54
5.4 Vibration Signal Filtered at 8500 Hz . . . 61
5.5 Gearbox Raw Acoustic Signal . . . 65
5.6 Acoustic Signal Filtered at 1500 Hz . . . 66
5.7 Acoustic Signal Filtered at 8500 Hz . . . 67
5.8 Features Extraction . . . 68
5.8.1 Filter Influence . . . 68
5.8.2 Principal Component Analysis . . . 69

6 Conclusion **73**
6.1 Conclusions . . . 73
6.2 Future Works . . . 74

Bibliography **79**

Appendices **79**

Appendix A Tutorial : Gearbox Fault Diagnosis **81**
A.1 Raw Data Analysis . . . 82
A.2 Pre-Processing . . . 83
A.3 Processed Data Analysis . . . 84

List of Figures

1.1 Sensors representation of a) Microphone for Acoustic Signals, and b) Accelerometer for Vibration Signals . . . 2

2.1 Signal Classification . . . 6
2.2 Periodic Classification of a Signal . . . 7
2.3 Periodic Spectrum of a Triangular Wave . . . 7
2.4 Example of amplitude modulated white noise . . . 10
2.5 Gearbox typical signals . . . 11
2.6 Expected Healthy Spectrum of a Gearbox . . . 12
2.7 Frequent Gearbox Faults . . . 12
2.8 Shaft Misalignment . . . 13
2.9 Gear with Backlash . . . 13
2.10 Hunting Tooth Gear Spectrum . . . 14
2.11 Rolling element bearings geometry . . . 14
2.12 Rolling element bearings fault signals . . . 15
2.13 Gear Tooth Mesh and Load Fluctuation . . . 16
2.14 Progression of Gear Wear and typical Spectrum . . . 17
2.15 Crack related faults on gears . . . 18

3.1 Modulation Process . . . 22
3.2 Transient Signal . . . 23
3.3 Time-Domain of two Signals . . . 24
3.4 Spectrum of Simulated Signal . . . 25
3.5 Waveform, Spectrum and Spectrogram using Short Time Fourier Transform. 26
3.6 Order Tracking Process . . . 27
3.7 Time Synchronous Averaging . . . 29
3.8 Envelope Analysis Procedure . . . 30
3.9 Fast Kurtogram. . . . 31
3.10 Wavelet Analysis of Generated Signal with noise. . . . 32
3.11 Cyclic Analysis with Spectral Correlation . . . 34

4.1 Two Features Classifying Faulty case (red) from Healthy case (blue). a) Sideband Power Factor with bad classification, and b) Crest Factor with good classification. . . . 42
4.2 Two Features Classifying Faulty case (red) from Healthy case (blue) . a) Root Mean Square with Robust classification, and b) Crest Factor with Unreliable classification. . . . 42
4.3 Principal Component Analysis example of dimension reduction [1]. . . . 43
4.4 Adopted Procedure. . . . 44

5.1 SpectraQuest Machine Fault Simulator (MFS) . . . 45

5.2 Experimental Setup Diagram . . . 46
5.3 Three pinions for the experimental test . . . 46
5.4 Missing tooth raw time signal . . . 47
5.5 Chipped tooth raw time signal . . . 48
5.6 Spectra of Raw Vibration Signals . . . 49
5.7 Wavelet Analysis of Missing Tooth . . . 50
5.8 Wavelet Analysis of Missing Tooth . . . 51
5.9 Cyclic Spectral Correlation of Missing Tooth . . . 51
5.10 Cyclic Spectral Correlation of three cases . . . 52
5.11 Impulsive Transients of the signals . . . 53
5.12 Waveform and Spectrum without signal demodulation . . . 54
5.13 Healthy Envelope Signal for Filter 1 . . . 55
5.14 Chipped and Missing Tooth Envelope Signals for Filter 1 . . . 56
5.15 Healthy Envelope Spectrum for Filter 1 . . . 56
5.16 Chipped Tooth Envelope Spectrum for Filter 1 . . . 57
5.17 Missing Tooth Envelope Spectrum for Filter 1 . . . 57
5.18 Wavelet Analysis of Healthy Envelope for Filter 1 . . . 58
5.19 Wavelet Analysis of Missing Tooth Envelope for Filter 1 . . . 59
5.20 Impulse deviation phenomenon and correction for TSA . . . 59
5.21 Unphased impulse after TSA correction . . . 60
5.22 Comparison of TSA method . . . 61
5.23 Healthy Envelope Signal for Filter 2 . . . 61
5.24 Envelope Spectrum for Filter 2 . . . 62
5.25 Zoom of the Missing Tooth Envelope Spectrum for Filter 2 . . . 63
5.26 Order Tracked Envelope of Missing Tooth . . . 63
5.27 Order Tracked of the healthy pinion and missing tooth pinion . . . 64
5.28 Order Tracked of faulty signal on different components . . . 65
5.29 Raw Acoustic Signals . . . 66
5.30 Wavelet Analysis of the Acoustical filtered signal around 1500 Hz band . . . 66
5.31 Wavelet Analysis of the Acoustical filtered signal around 8500 Hz band, for healthy and chipped . . . 67
5.32 Wavelet Analysis of the Acoustical filtered signal around 8500 Hz band, for the missing tooth . . . 67
5.33 Effect of Envelope Analysis on Features . . . 68
5.34 PCA of the Acoustical Signals for 1500 Hz bandpass filter . . . 69
5.35 PCA of the Acoustical Signals for 8500 Hz bandpass filter . . . 70
5.36 PCA of the Raw Vibration Signals for 1500 Hz bandpass filter . . . 70
5.37 PCA of the Raw Vibration Signals for 4500 Hz bandpass filter . . . 70
5.38 PCA of the Raw Vibration Signals for 8500 Hz bandpass filter . . . 71

A.1 GFD main interface . . . 81
A.2 GFD main interface . . . 82
A.3 Cyclostationary Analysis . . . 83
A.4 Save Processed Data . . . 83
A.5 Processed Data Analysis . . . 84
A.6 Principal Component Analysis . . . 85

List of Tables

5.1 **Frequencies of Interest for Different Speeds** 47
5.2 Filter Parameters. 53
5.3 Magnitude of Frequencies of Interest for the three cases. 58

CHAPTER 1

Introduction

1.1 Condition Monitoring

> "The implementation of Condition based maintenance can prevent machine failures, increase reliability of the system and decrease maintenance cost. Thus Condition Monitoring is becoming widely utilized in many real industrial applications such as helicopter transmission systems and wind turbines" [2]

Preventive vs. Predictive Maintenance

The dynamic nature of machines require correct maintenance to perform reliably at peak performance. Before this premise was known, the maintenance commonly performed was Run-To-Failure method, where mechanical machinery developed faults with time until it led to a complete breakdown, demanding replacement of said machinery. This is undesirable as it results in a loss of productivity that is easily prevented by technicians with experience to detect the state of the machines with touch, sound and visually. Preventive Maintenance takes this experience into account and applies it to routine minor checks that have great influence of the machines. It is ensued with the objective of Preventing machine breakdown.

Instead of prevention, the correct prediction of the development of machine components to provide the correct maintenance at the appropriate time, greatly increases the productivity. This is the Preventive Maintenance, and has been consistently growing in the industry due to the presented advantage that make companies more competitive, specially in industries where the losses for breakdown are extremely high and also when the machine is essential for production.

Vibration and Acoustic Signals

The physical phenomenon under investigation is often translated by a transducer into an electrical equivalent, and thus referring to a continuous (or analogue) signal. The displacement in time of a structure around a mean neutral position generates the wave signals that are dependent on the parameters of the structure. When a fault happens it changes these parameters and thus it is inferred that the vibration signal is an indicator of the nature of a structure and its condition.

Acoustic waves are simply disturbances involving mechanical vibrations in solids, liquids, or gases. The Acoustic signals capture the pressure changes correspondent to these disturbances at a point in an acoustic field, by the displacement of the diaphragm, which in turn generates an electrical current. Figure 1.1 a) represents this typical microphone layout.

Vibration signals are captured by sensors voltage variations from a vibration transducers. When a force is applied to a piezoelectric material in the direction of its polarization an electric charge is developed between its surfaces, giving rise to a potential difference on the output terminals. The charge (and voltage) is proportional to the force applied, or the mass displacement due to accelaration. The same phenomenon will occur if the force is applied to the material in the shear mode. Both modes are used in practical accelerometer design, which is shown in Figure 1.1 b).

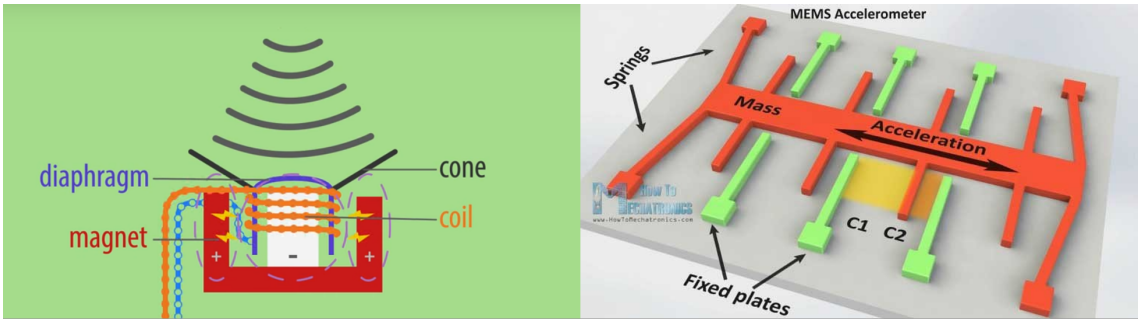

Figure 1.1: Diagrams for sensors [3]

So, theoretically both the signals capture the vibration of the structure, where the only difference is the medium by which they are transported. The accelerometers are extensively shown in the literature to provide better results, as they measure directly the displacement of the structure they are consolidated with. They are more sensitive to the structural modes carrier frequencies that generate the impulse transients [4]. Microphones are insensitive to these structural modes/resonances, but they are equally affected by the mechanical background noise. Microphones are susceptible to ambient noise and conditions must be met to ensure a clean signal. The work on noise reduction on acoustics is more critical than for accelerometer signals. The greatest advantages of microphone are the fact that they do not need to be physically mounted on the structure, where they can be obtained from afar, and are generally cheaper than the accelerometers. These reasons make the microphones extremely desirable to implementations in complicated locations.

1.2 Motivations

Gearboxes, as one of the most frequent mechanical structure that plays a crucial part of rotating machines, are the main focus of this dissertation. Thus appropriate maintenance is critical in avoiding catastrophic results to rest of the structure machines, and if implemented on a production line, usually results in a less cost that would otherwise go to repairs and delays that result from it.

For the maintenance, the market is turning to vibration analysts to detect and monitor these faults. However, this type of analysis is complex by nature and requires some years of training and expertise. The challenging part is to provide a method that allows the correct

gearbox condition analysis in an automated way, and most importantly, in a simple manner that can allow any technician to understand the analysis with as little time as possible.

An easy way of assessing the condition is based on the analysis of simple statistical features, such as the standard deviation and kurtosis. Those vary however from case to case, and depend upon many variables to perform a correct diagnosis. The most interesting challenge would be to combine different features that could translate the condition of the gearbox for the acoustic signals, whose have a greater noise component than that of the accelerometer signals. With this in mind, some objectives were defined for this thesis which are enumerated as follows.

1.3 Objectives

- Understand the fundamentals of condition monitoring, through different techniques, and the state of the art of the technology.
- Review the current state of the art on gearbox diagnosis, for missing and chipped tooth faults, and understand the procedures performed to obtain and process correctly vibration and acoustical signals that contain the gearbox condition information.
- Study the processing techniques available and clarify their advantages.
- Develop a vibration signal and acoustical signal based fault feature extraction, using advanced signal processing methods.
- Selection of the correct features which can provide the correct classification of gearboxes for several operating speeds.
- Semi-automation of the process, and simplification of the obtained results by labeled cluster points correspondent to chipped tooth and missing tooth faults.

1.4 Document Outline

This text is structured in six chapters.

The next two expose the fundamental theory on the condition monitoring. Namely Chapter 2 provides the literature review on gearbox expected behavior for different configuration on rotating machines. The topic of diagnosis of gearboxes and the common defects and interferences are exposed, as well as the common faulty components and their correspondent signal analysis.

Chapter 3 details the data processing techniques available for condition analysis and effective procedures to clear and enhance both the healthy and faulty signals, namely by the Cyclic Spectral Correlation and the Wavelet Analysis.

In Chapter 4 are presented the features studied and the correlation conducted between them, in particular by the Principal Component Analysis, that allows the visualization of all the features in an intuitive way.

Chapter 5 present the results obtained for the *three* levels of fault on gearboxes, processed with both envelope analysis and features extraction.

In the final part of this thesis, Conclusion, is dedicated to take the necessary conclusions about the work and future work suggestions, respectively.

CHAPTER 2

Gearbox Fundamentals

The condition of rotating machinery can be measured by their vibration signal, making the vibration the most regularly measured condition parameter in modern rotating machinery. Vibration can be described as the system motion in which the system oscillates about a certain equilibrium position. That system motion is represented as a waveform, where the position in time relative to the equilibrium point is plotted at each point in time. This time-domain representation captures the characteristics of vibration measurements that yield information regarding the machine's condition and any mechanical fault. The time-domain events are usually masked and hard to understand, making representations of the vibration signals in other domains a common practice, ensuring a better understanding of the nature of the signals.

The most common domains for the representation of the vibration signals are time, frequency, time-frequency, and lately the frequency-frequency domain used mostly in Cyclostationary Analysis. Also the representation of these signals can be done in hertz, a linear representation in time, or in orders, a linear function of the shaft speed. This transformation in relation to one shaft revolution, the so called order domain (e.q. angular sampling) is another common representation, that gives further intuition to the vibration signals and to those events that depend on the shaft speed, which are the nature of the gear vibration signals.

The two premises of condition monitoring are that every failure mode has a distinct vibration frequency of interest that can be measured, and that each failure mode amplitude will remain constant unless a change occurs, such as a fault. There is a common knowledge that these frequencies of interest are usually hidden by the noise, other mechanical generated signals and transmission path through the structure. Therefore, many algorithms are implemented numerically to process the signal in order to obtain the frequency correspondent to the faults directly.

2.1 Signal Classification

A fundamental difference is whether a signal is deterministic or random, and the analysis methods are considerably different depending on the nature of the signal. The correct classification of the signals generated by a component is of the utmost importance, as it dictates the processing that should be applied.

Generally, signals are mixed, so the classifications of Figure 2.1 may not be easily applicable, and thus the choice of analysis methods may not be apparent. In many cases some prior knowledge of the system (or the signal) is very helpful for selecting an appropriate method. [5]

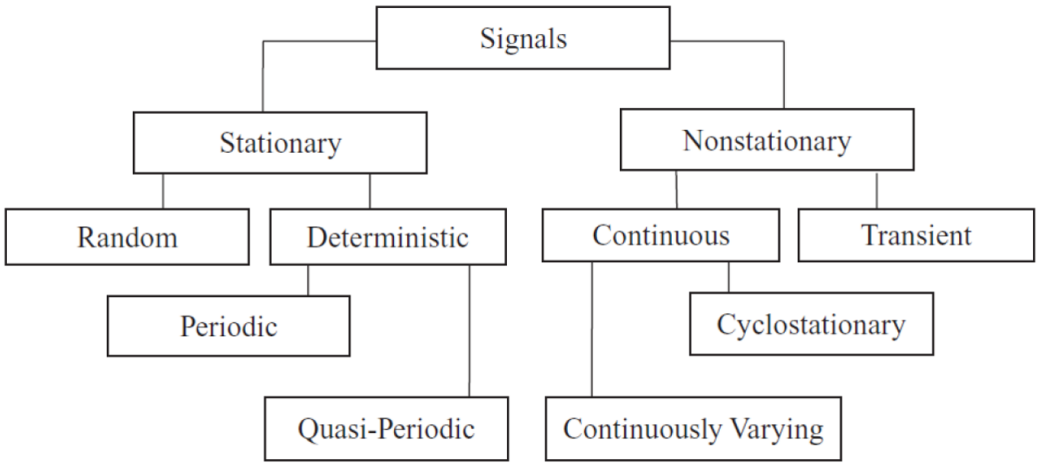

Figure 2.1: Signal Classification [6].

Deterministic signals are those whose behavior can be predicted exactly, which is the supposed behavior of gear signals, as they are forced to mesh a certain number of times per revolution and each time a tooth meshes with the other, an impulse occurs. So the deterministic signals are assumed to be composed from discrete frequency sinusoids,and their frequency spectrum consists then of prominent discrete lines at those sinusoids [5].

Nonstationary signals are those whose behavior cannot be exactly predicted, which is the theoretical behavior of rolling bearing elements, as they rotate the axis of rotation slips, and the embedded fault may or may not generate constant number of impulses per revolution [7]. Impulse signals are Transients, which are also nonstationary. These appear in both gear and rolling element fault signals, as the impulses excite certain resonant frequencies that rapidly decay, and thus contain critical information on the condition of both machine components. It is important to differentiate the nature of the signals to obtain the desired components for a correct diagnosis, for the presented reasons.

The classification of data as being deterministic or random might be debatable in many cases and the choice must be made on the basis of knowledge of the physical situation. In practice, signals are modeled as being a mixture of both random and deterministic signals. Considering a pair of gears meshing, even though the frequency derived from the meshing of gears is deterministic, other components of the signal are random as they derive from other components (such as bearings), the transmission path error and inherent noise.[8]

Stationary Deterministic Signals

Periodic signals are defined as those whose waveform repeats exactly at regular time intervals.

The simplest example is a sinusoidal signal as shown in Figure 2.2(a), where the time interval for one full cycle is called the period T_P (in seconds) and its reciprocal $f_p = 1/T_P$ is called the frequency (in Hertz).

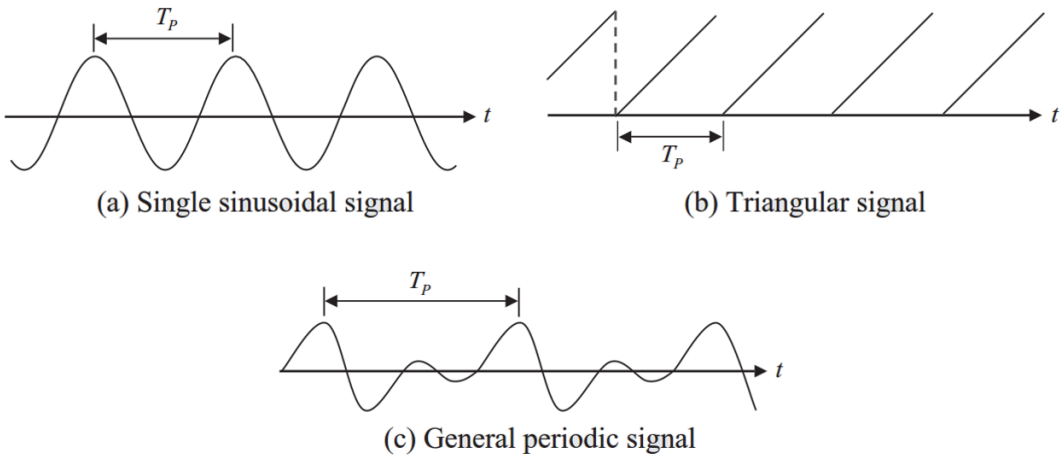

Figure 2.2: Examples of periodic signals [5].

Another example is a triangular signal (or sawtooth wave), as shown in Figure 2.2(b). This signal has an abrupt change (or discontinuity) every T_P seconds. A more general periodic signal is shown in Figure 2.2(c) where an arbitrarily shaped waveform repeats with period T_P . In each case the mathematical definition of periodicity implies that the behavior of the wave is unchanged for all time. This is expressed as:

$$x(t) = x(t + nT_p) \quad n = \pm 1, \pm 2, \pm 3, ... \tag{2.1.1}$$

For cases (a) and (b) in Figure 2.2, explicit mathematical descriptions of the wave are easy to write, but the mathematical expression for the case (c) is not obvious. The signal (c) may be obtained by measuring some physical phenomenon, such as the output of an accelerometer. In this case, it may be more useful to consider the signal as being made up of simpler components. One approach to this is transforming the signal into the *frequency domain* where the details of periodicities of the signal are clearly revealed. In the frequency domain, the signal is decomposed into an infinite (or a finite) number of frequency components. The periodic signals appear as discrete components in this frequency domain, and are described by a Fourier series which is discussed in Chapter 3

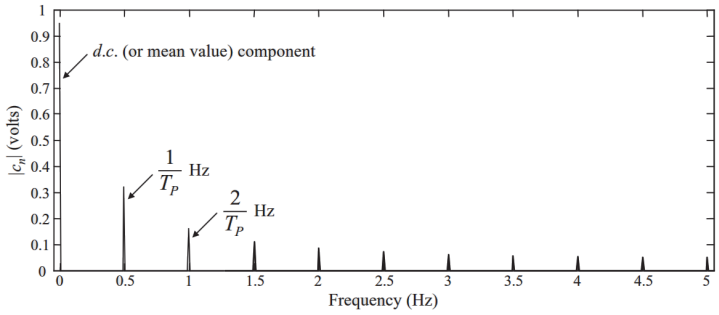

Figure 2.3: Frequency domain representation of the amplitudes of the triangular wave with a period of $T_p = 2$ (s) [5].

As an example, the frequency domain representation of the amplitudes of the triangular wave (Figure 2.2(b)) with a period of $T_P = 2$ seconds is shown in Figure 2.3. The components in the frequency domain consist of the fundamental frequency $1/T_P$ and its harmonics

$2/T_P$, $3/T_P$, and all the other frequency components that are "harmonically related".[5]. It is noted that most periodic signals in practical situations are not "truly" periodic, but are quasi-periodic. The term quasi-periodic is discussed in the next section.

Stationary Quasi-Periodic Signals

The name quasi-periodic seems self-explanatory, i.e. it looks periodic but in fact it is not if observed closely. It shall be seen in Chapter 3 that suitably selected sine and cosine waves may be added together to represent the full signal. Also, even for apparently simple situations the sum of sines and cosines results in a wave which never repeats itself exactly. As an example, consider a wave consisting of two sine components as below:

$$x(t) = A_1 sin(2\pi p_1 t + \theta_1) + A_2 sin(2\pi p_2 t + \theta_2) \tag{2.1.2}$$

where A_1 and A_2 are amplitudes, p_1 and p_2 are the frequencies of each sine component, and θ_1 and θ_2 are called the phases. If the frequency ratio p_1/p_2 is a rational number, the signal $x(t)$ is periodic and repeats at every time interval of the smallest common period of both $1/p_1$ and $1/p_2$. However, if the ratio p_1/p_2 is irrational (as an example, the ratio $p_1/p_2 = 2/\sqrt{2}$ is irrational), the signal $x(t)$ never repeats. It can be argued that the sum of two or more sinusoidal components is periodic only if the ratios of all pairs of frequencies are found to be rational numbers (i.e. ratio of integers). A possible example of an almost periodic signal may be an acoustic signal created by tapping a slightly asymmetric wine glass. [5].

Transient Signals

Generally speaking, a transient signal has the property that $x(t) = 0$ when $t \to \pm\infty$. In vibration engineering, a common practical example is impact testing (with a hammer) to estimate the frequency response function of a structure. The measured input force signal and output acceleration signal from a simple cantilever beam experiment are shown in Figure 3.1 in Chapter 3. It should be noted that the modal characteristics of the beam allow the transient response to be modeled as the sum of decaying oscillations, allowing the estimation of the amplitudes, frequencies, damping and phases [5].

Random Signals

A random signal (also called stochastic) is an infinite indexed collection of random discrete samples defined over a common probability space, where the index parameter t is typically time. One simple example is gaussian white noise. It can take any values from $-\infty$ to ∞, but its behavior along a long time period, can be calculated as having a constant mean, and a constant standard deviation.

Cyclostationary Signals

The cyclostationary classification family accepts all signals with hidden periodicities, either of the additive type or multiplicative type; this includes periodic and random stationary signals as particular cases, as well as periodic modulations, repetitive transients, among

others [9]. However, in the literature, when a signal is referred as cyclostationary, it usually means it is a second-order cyclostationary signal. The various cyclostationary processes applied in the literature as they can detect the nature of first-order and second-order of cyclostationarity. Thus, mechanical signals produced by rotating or reciprocating machines are remarkably well modeled as cyclostationary processes [10].

In a few words, a cyclostationary signal is described by a probability density function which is periodically time-varying. In such cases, the signals are not strictly periodic, but "cyclostationary" (of second order), meaning that their second-order statistics such as autocovariance function are periodic [9]. This definition accepts periodic signal and stationary signals as two important particular cases, and more generally all nonstationary signals which are produced by a periodic mechanism such as amplitude or frequency modulations. Since most signals of interest in condition monitoring happen to be well described by their first two moments, the expected value and the autocorrelation function, it is helpful to use them in a formal definition of cyclostationarity. From now on, continuous time is considered t for simplicity.

Strictly speaking, an n^{th} order cyclostationary signal is one whose n^{th} order statistics are periodic or, in other words, one which produces a peak in its Fourier transform after passing through any non-linear transformation involving n^{th} power. The simplest example is a first-order cyclostationary signal $x(t)$, which is just a periodic signal $p(t)$ embedded in additive stationary noise $n(t)$, as follows: $x(t) = p(t) + n(t)$. Its first-order statistics, i.e. its mean value in the ensemble average sense, then reproduces the periodic component $p(t)$ unaltered, as expressed in Equation 2.1.3.

$$E[x(t)] = E[p(t) + n(t)] = E[p(t)] = m_p \tag{2.1.3}$$

Where the $E[x(t)]$ denominates the mean of the signal $x(t)$, which is equal to the mean of the deterministic signal m_p.

Similarly, a second-order cyclostationary signal is one whose autocorrelation function expressed in Equation 2.1.4 is a periodic function of time, where the condition $R_{xx}(t, \tau) = R_{xx}(t + T, \tau)$ is verified. Here, τ is the time-lag away from the mean signal position in time, and T is the constant period component of the signal.[11]

$$R_{xx}(t, \tau) = E\left[x(t - \frac{\tau}{2})x(t + \frac{\tau}{2})\right] = R_{xx}(t + T, \tau) \tag{2.1.4}$$

A simple example is provided by a white noise modulated by a periodic amplitude, as illustrated in Figure 2.4(a). It can be noted that, in spite of the periodic modulation, this is still a completely random signal. The autocorrelation function, by virtue of the second-order non-linearity it introduces, succeeds in revealing the hidden periodicity as shown in Figure 2.4(b).

For time-lag $\tau = 0$, it returns the instantaneous power of the signal which is seen to flow periodically as a function of time. For other values of the time-lag the autocorrelation function is zero because the carrier signal is white noise, but any dependence on τ (compatible with an autocorrelation function) will be possible in general depending on the color of the signal.
Higher-order types of cyclostationary signals are defined following similar lines as for first and second orders, although not reviewed here. Indeed, restriction to first and second orders of cyclostationarity appears good enough for many practical purposes. [12]

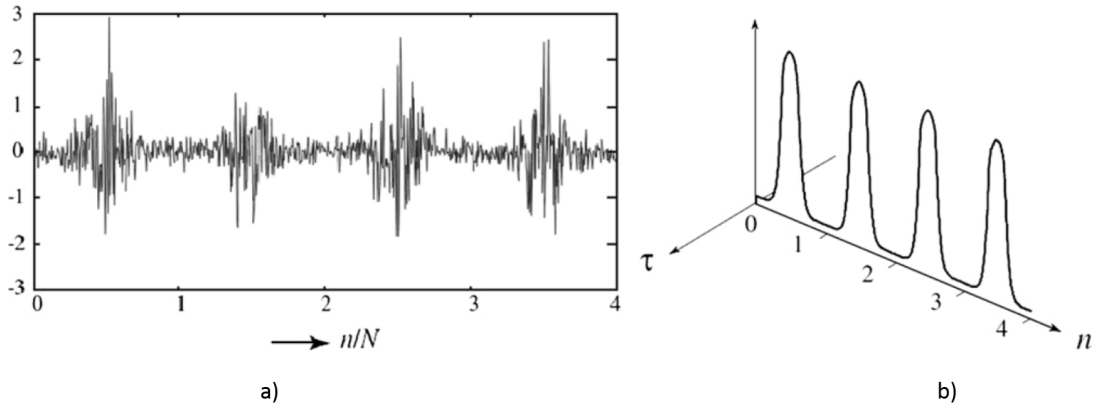

Figure 2.4: Example of amplitude modulated white noise [11] : (a) time signal over four periods of cyclic frequency; (b)two-dimensional autocorrelation function vs time (sample) n and time lag τ.

2.2 Common types of faults in a gearbox

Most machine components give rise to specific vibration signatures, that allow to separate, characterize and distinguish between healthy and faulty condition. In a rotating machine the vibrations are associated with elements, which involve rotation such as: shafts, gears, rolling element bearings, couplings, rotors etc. In gearboxes, the main components are rolling bearings and pairs of meshing gear. This work will focus on gears since they are one of the main components of a gearbox.

Considering that the vibrations tend to change as a function of operational conditions, like speed and load, the diagnosis of the condition of a gearbox is done by reading its vibration and/or acoustic signal, and compared it with a baseline signal obtained from the healthy state. In the laboratory it is done by changing one healthy component for another faulty, and in industrial environment means by comparing the evolving signal as operation time advances in days, weeks and years.

The correct isolation of these deterministic components for the obtained signals is then common practice and imperative, as they supply the information on the state of these components that provide the deterministic part of the signal. This chapter focuses on the diagnosis and prognosis of gearbox faults using vibroacoustic methods.

Gears produce a deterministic signal for each rotation. This happens because the gears are "forced" to mesh together, unlike the rolling bearing element that slips. Thus the impulsive nature of the rolling bearing element has an unpredictable behavior inherent to it, and the meshing gears has mandatory and determined behavior for each revolution.

This generates a first-order cyclostationary signal, for pairs meshing gears in general, and a second-order cyclostationary signal for bearing signals and worn gear signals. These are in fact the two distinct groups that are seen in the literature, where the bearing and worn gears are diagnosed by removing the deterministic part of the gearbox overall signal. The other signals are diagnosed with the more deterministic components.

With set number of impulses per revolution of the shaft, the baseline spectrum depends mainly on the geometry of the gears. To be more precise, for a one stage only gearbox, the number of teeth in the input gear of the gearbox, called the pinion, is the number of impulse per revolution that occur due to the meshing of these gears.

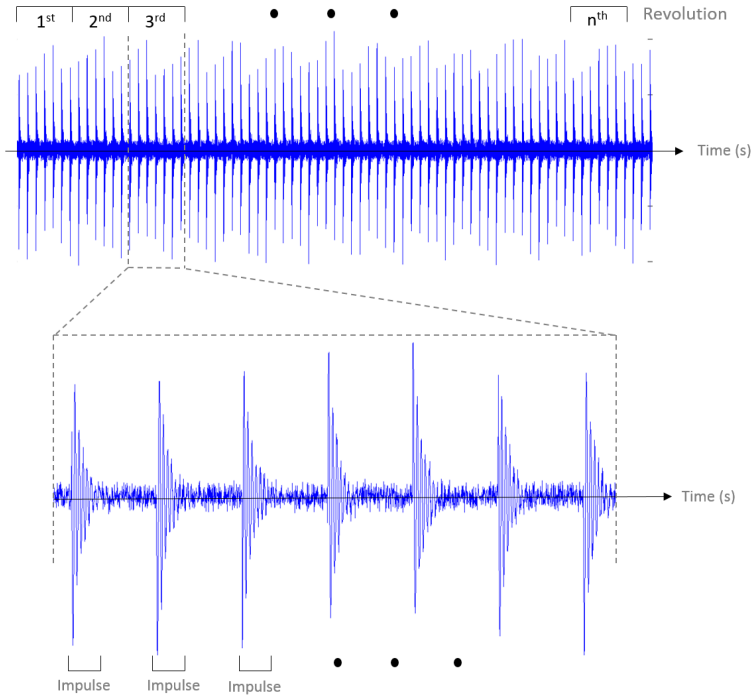

Figure 2.5: Typical time signal produced by gears meshing.

In a gearbox all those signals are mixed together, the measured signal x is the sum of d deterministic gearmesh and shaft rotation frequencies, of w fault impulses and of e_0 noise. All of them are modified by the transmission path h, and can be described by Equation 2.2.1.

$$x = (d + w + e_0) \times h \tag{2.2.1}$$

Usually the impulses are covered by the deterministic part, and for this reason the signal should be processed in order to detect faults that produce impulses. So gear faults do not have a set frequency for each type of faults, like the rolling element bearings. Instead, gears' spectra should always show the gear mesh and shaft frequencies, and their correspondent harmonics and sidebands. The fault detection of these deterministic signals is performed by examining the variations of these frequencies of interest.

In Figure 2.5 it is shown an example of a typical gearbox signal, where the impulse of the meshing gears is generated for each gear. Assuming a stationary signal, where the speed of the shaft remains approximately constant, each cycle of rotation is similar to one another, meaning it is deterministic nature, and a pattern arises from each set number of impulses that correspond to one revolution of the shaft. Thus with this, the expected spectrum of a pair of healthy gears meshing, will be as shown in Figure 2.6.

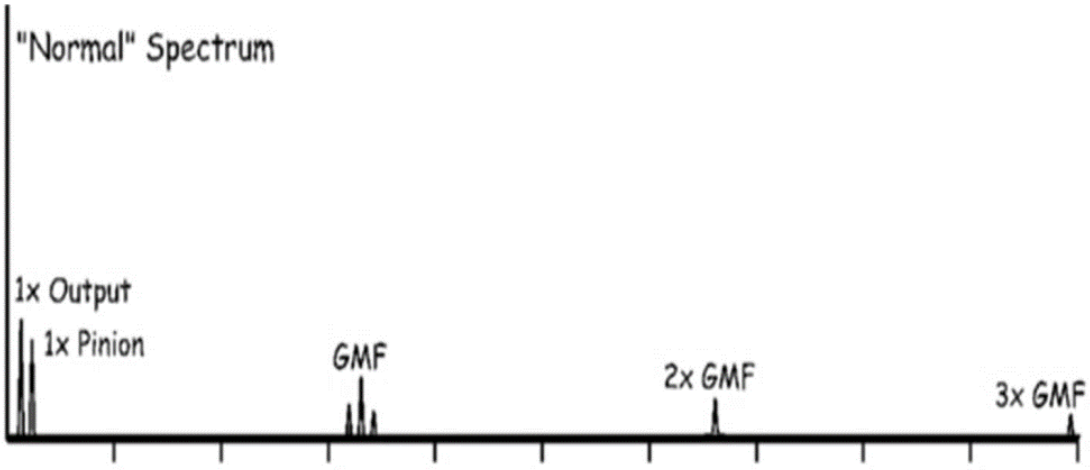

Figure 2.6: Expected Healthy Spectrum of a Gearbox [13].

2.2.1 Frequent Component Signals

Unbalance is the most common cause of excessive vibration, and it results from the fact that the center of gravity of a rotating member does not coincide with the center of rotation. [14] This causes the creation of a centrifugal force vector pointing radially out from the center of rotation and rotating at a speed equal to the speed of the rotating member itself, as described in Figure 2.7. The amplitude of this force can be described in Equation2.2.2

$$F_{bal} = Mew^2 \tag{2.2.2}$$

Where M is the unbalance mass, e is the distance between the center of rotation and the center of gravity, and w is the rotational speed. The generated centrifugal force results on the rotor actually rotating off its center, causing high vibration equivalent one order of the shaft rotation.

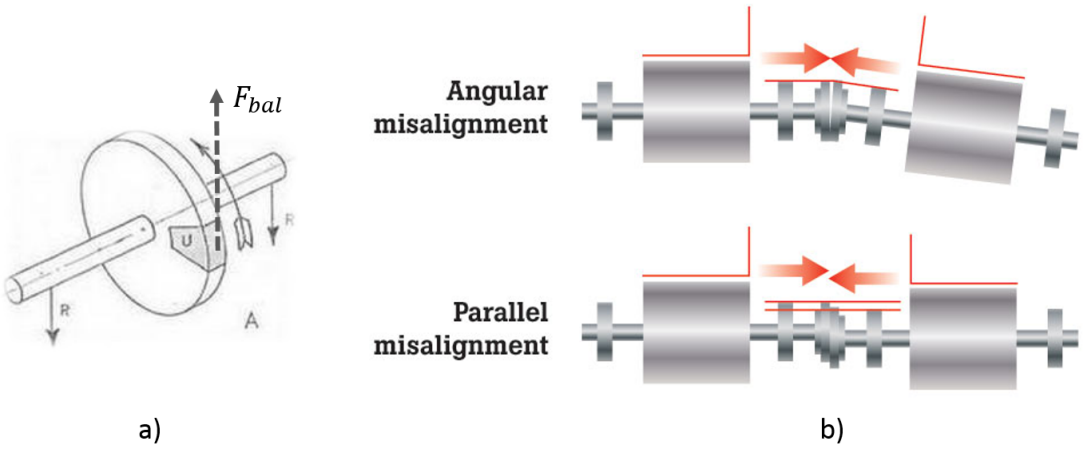

Figure 2.7: Frequent Gearbox Fault a) Unbalance b)Misalignment [15].

Shaft misalignment are also one of the common problems in gearbox structures. These cause additional loads and vibrations in the system, leading to early damages and energy loss [16].

Coupling misalignment is a condition where the shaft of the driver machine and the driven machine are not on the same centerline. The non-coaxial condition can be parallel misalignment or angular misalignment as depicted in Figure 2.7.

The more common condition is a combination of the two in both the horizontal and vertical direction. These type of faulty coupling is sometimes unsolvable, due to mating parts being produced by different manufacturers [17].

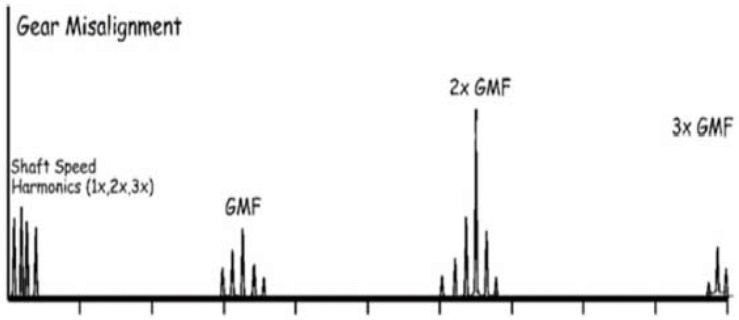

Figure 2.8: Shaft Misalignment [13].

The resulting spectrum has greater amplitudes for increasing unbalance, with increased harmonics and sidebands, and the $2^{nd}GMF$ typically larger than the GMF, represent in Figure 2.8.

Backlash is a clearance between the mating gear teeth, which causes loss of motion between the reducer input and the output shafts. It can be derived from many situations, like manufacturing errors or mounting tolerances. It introduces either a lot of impulse forces due to high clearances, or high stress due to a tight clearance.

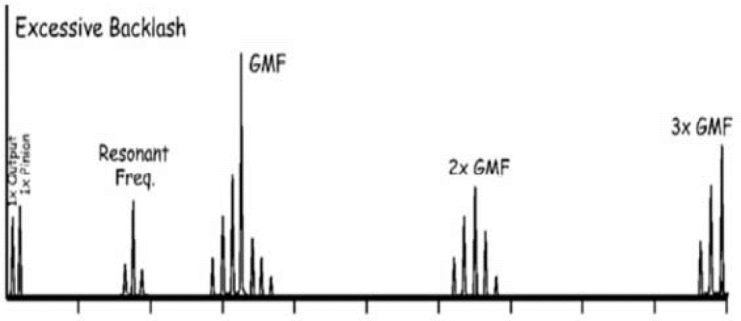

Figure 2.9: Gear with excessive Backlash [13].

Missing teeth faults can also be seen as an excessive backlash, through this definition, as the missing tooth itself is a clearance in the mating gears that generates high impulses, and thus excites the resonant frequencies of the structure. Figure2.9 shows a typical spectrum due to backlash.

Hunting Tooth theoretically occur when faults are present on both the gear and the pinion, and if there is a low number of revolutions until the same pair of teeth mesh again. Each gear has set number teeth, and the same teeth cycle on each shaft revolution. The same way, when the exact same pair of meshing gears mate together N revolutions later, the Hunting Tooth Frequency (HTF) is declared, and the frequency is the shaft speed divided by the said integer N.

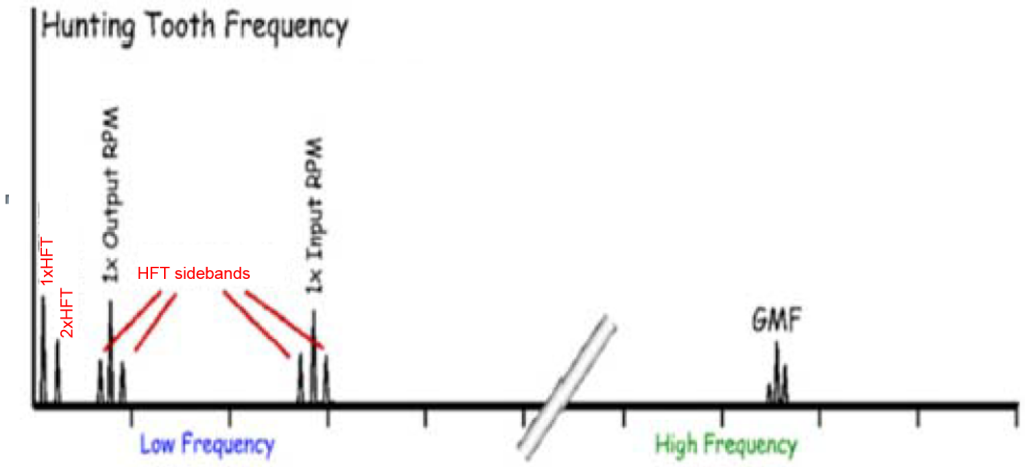

Figure 2.10: Hunting Tooth Gear Spectrum [13].

If there is a fault in both mating gears, or the ratio between them has a high integer, *HTF* arises due to the exact same gears meshing together frequently. However, it is a rare fault, as the engineers project the number of teeth of the gears to have the lowest common factor.

The signals of the gearbox studied in this dissertation are considered to be deterministic or cyclostationary.

2.3 Rolling Element Bearing Signals

Rolling element bearings are one of the most used elements in rotating machines, for supporting and locating of the shafts, and their failure is a common reason for a breakdown. Usually bearings fail due to: manufacturing errors, improper assembly, loading, lubrification, harsh environment or fatigue. A fault starts as a small pit or spall on the raceway or on a rolling element, this discontinuity grows and spreads with the time and if the bearing survives long enough it may be smoothly worn.

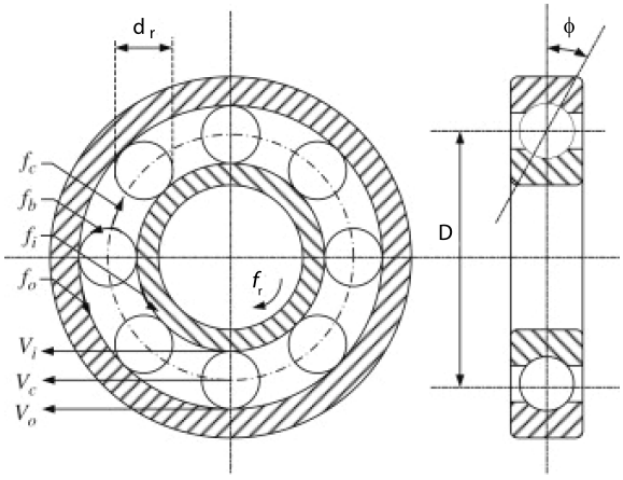

Figure 2.11: Rolling element bearings geometry [6].

Fault Characteristic Frequencies

The vibration signal produced by a healthy bearing is low in level and looks like random noise. When the fault starts to show up the vibration changes: every time that a rolling element strikes a local fault generates an impulse in a wide frequency range with a rate that depends on the location of the fault and on the bearing geometry. Those repetition rates are called bearing frequencies:

$$BPFO = \frac{nf_r}{2}\left(1 - \frac{d_r}{D}cos\phi\right) \tag{2.3.1}$$

$$BPFI = \frac{nf_r}{2}\left(1 + \frac{d_r}{D}cos\phi\right) \tag{2.3.2}$$

$$BSF = \frac{f_r D}{2d_r}\left[1 - (\frac{d_r}{D}cos\phi)^2\right] \tag{2.3.3}$$

$$FTF = \frac{f_r}{2}\left(1 - \frac{d_r}{D}cos\phi\right) \tag{2.3.4}$$

where n is the number of rolling elements, f_r is the shaft speed, d_r is the diameter of the rolling element, D is the pitch diameter and ϕ is the contact angle.

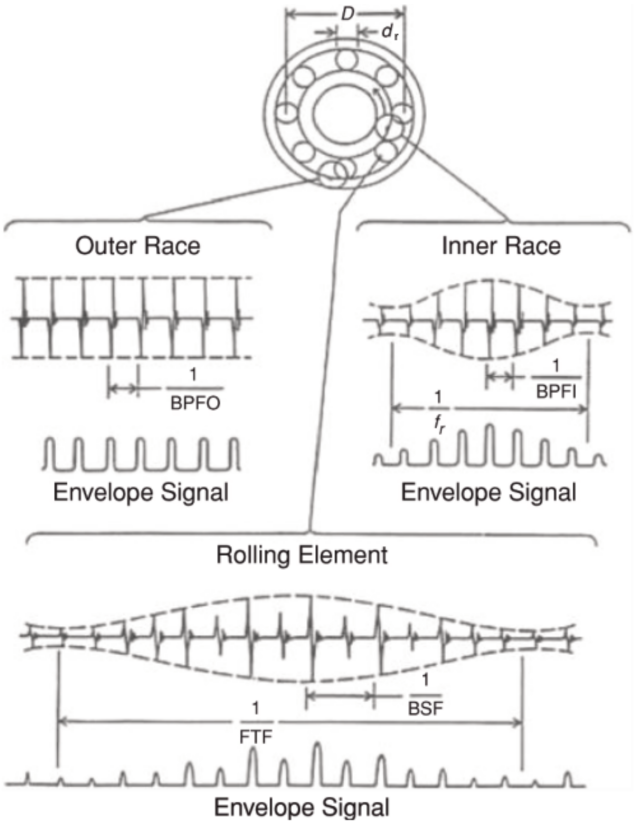

Figure 2.12: Typical time signal produced by localized faults on bearings [18].

The bearing frequencies are calculated assuming no slip, but in fact there is always some slip, because the angle ϕ varies with the position of each rolling bearing element, as well the ratio between local radial and axial load changes. For this reason each rolling element has a different actual rolling diameter, due to stress and imperfections, and is trying to

roll at different speed, but the cage limits the deviation causing some random slip. When the fault becomes smoothly worn it may not produce impulses anymore but could still be detected by the way it modulates other components.

Diagnosis of bearing defect involves then removing the shaft and gear meshing components that are usually predominant on the gearbox signal. This residual signal is supposed to have minimized the deterministic signal components, and thus enhancing the signal-to-noise ratio of the bearing fault. After obtaining the frequencies of interest for each bearing fault, at the selected speed, signal processing is used to confirm if any of those frequency components is present in the signal.

2.4 Gear Signals

Gears are used in machines to transmit power from one shaft to another by a variation of speed and torque. The majority of problems do not arise after several years of fatigue, but instead are caused during the manufacturing, when the quality is not satisfactory or the working conditions are not respected [6].

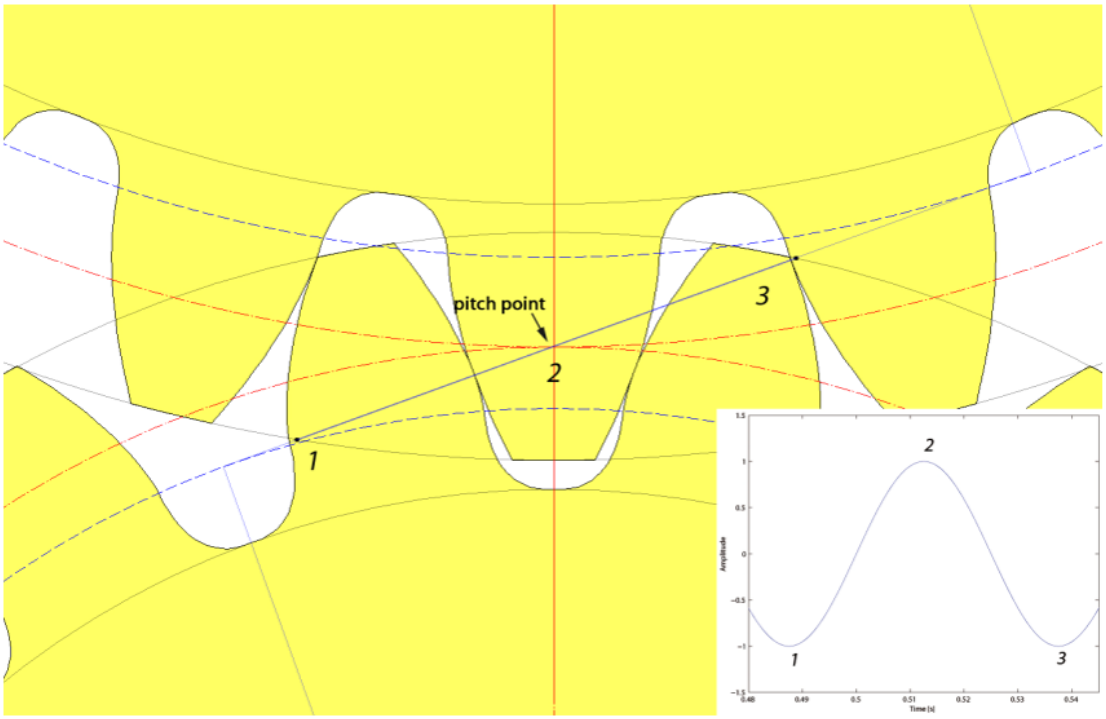

Figure 2.13: Gear Tooth Mesh and Load Fluctuation Produced [6].

On most gears, at a given instant, one tooth is in mesh, one is going into mesh and one tooth is going out of mesh. Considering the simple case of spur gears, they engage from the root on the top of the drive gear and from the top to the root of the driven one. In the time signal each cycle starts at the tooth transition point (1), that is the most negative point of the leading edge 2.13 and the gear are out of mesh on the most negative point of the lagging edge (3). The most positive point is when the two teeth are at the pitch line (2). Since this repeats each rotation in the same way the vibration produced is deterministic and periodic. In a ideal situation the gear's teeth have an infinite stiffness and perfect

profile so the signal produced is a sine wave with a frequency called Gear Mesh Frequency (GMF) that is equal to the number of teeth on the gear times the speed of the gear.

$$GMF = Z_1 * f_{r,1} = Z_2 * f_{r,2} \tag{2.4.1}$$

In reality teeth deform under the load, introducing a meshing error or transmission error, even when the tooth profile is perfect. Moreover there are always geometrical deviations from the ideal profile both wanted and unwanted. For example wanted deviations are due to 'tip relief ', where metal is removed from the tip of each tooth to avoid impact during the mesh. Those differences between the theoretical case manifest themselves as GMF and its harmonics. [6].

In a healthy condition the amplitude of the GMF and harmonics is quite low, there are also small sidebands spaced at f_r. When the faults start to arise the amplitude of GMF and sidebands around them can significantly increase. So high amplitudes of GMF often indicate a meshing problem.

2.4.1 Distributed Defects

Gear Wear occurs in every pair of mating gears, even if the loads are low and the gear profiles are ideal. Just through the metal-to-metal contact between meshing gears, material is slowly removed in the addendum and dedendum area, over a long period of time [17].

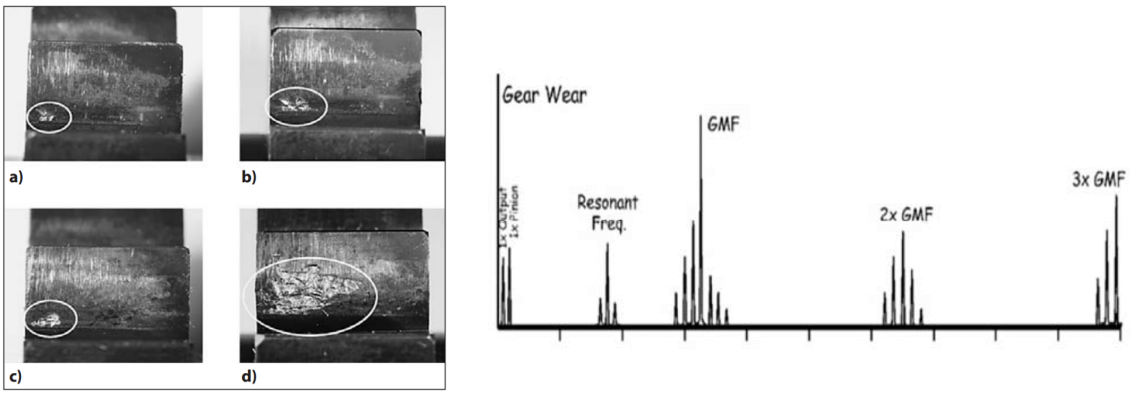

Figure 2.14: Progression of Gear Wear and typical Spectrum [13].

This simply normal wear can progress faster or slower due to various reasons, like inappropriate lubricant specification, high rotation speeds, or bad lubricant filter. With moderate wear a corroded pitch line begins to show as an unbroken line, and with excessive wear, the material removal progresses to the point where the involute profiles are destroyed.

Pitting is a surface fatigue failure, which occurs when the endurance limit of the material is exceeded. A failure of this nature depends on the surface contact stress and number of cycles. It can be seen as a type of wear of the gears, but under different and more extreme conditions, with less homogeneous removal of the material, and some specific patterns. One straightforward example is Initial Pitting, where the removal of material is distributed only on one side of the gears, the side they mesh. This is caused by the misalignment of the mating gears, which concentrates the load in this area.

Spalling is a type of destructive pitting, resulting to the extreme operational loads, that surpass the endurance limit for the material, removing chunks of material [17].

These distributed faults in gears are not divided in gearbox diagnosis. They all provide a similar result, in which the distributed fault behaves [19]. The common procedure for the diagnosis of these faults is by obtaining residual signal which should have the resonant frequencies excited by the faults. Figlus [20] diagnosed early cases of wear, pitting and spalling in gear teeth, by wavelet denoising and feature extraction.

Smith [21] proposed that cyclostationary signal analysis tools can detect changes in roughness of gear tooth surfaces, because it is thought they would affect the nature of amplitude modulation of the random vibrations produced from asperity contacts between the teeth when they slide against one another, this being a second-order cyclostationary (CS2) signal.

2.4.2 Localized Defects

Cracks, Broken and Chipped Tooth are common defects localized on the gears. Often resulting from excessive tooth loads or cyclic stressing, which in turn result in root stresses higher than the endurance limit of the material. In case of the cracks which propagates through the tooth, it can result in a chipped or even fully broken tooth.

Overload Breakage is an short-cycle break caused by an overload which exceeds the tensile strength of the gear material [17].

It is seen in the literature [22, 23, 24, 25] these cracks based faults generate an impulse on each gear revolution, that excite the structural resonant frequencies of the structure. These impulses are seen to be greater with the level of damage, from crack, to chipped to missing tooth.

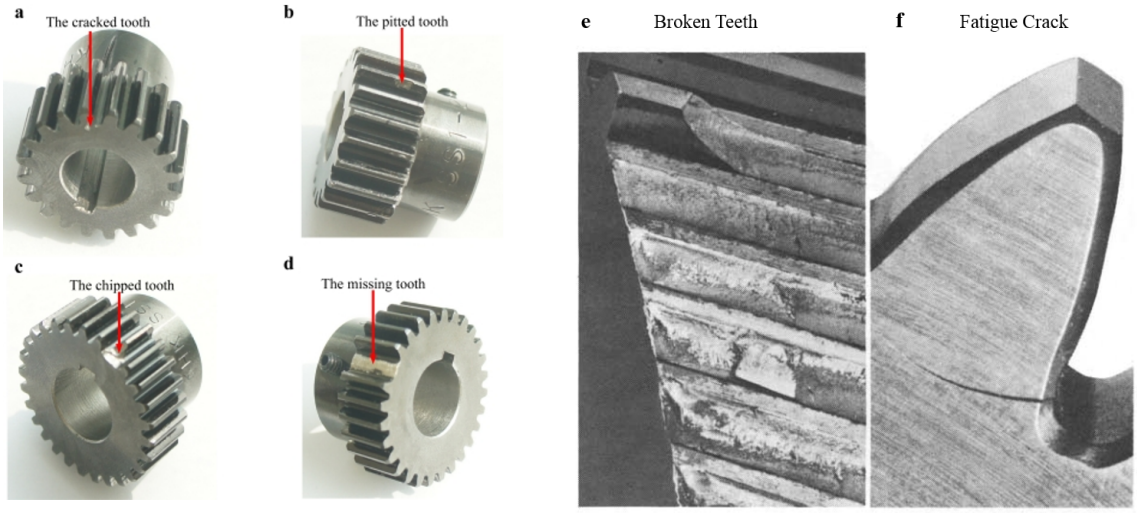

Figure 2.15: Crack related faults on gears [17].

Besides the overall levels of amplitude for these cases, usually it is possible to see the present impulses due to cracks in the time domain, particularly for the missing tooth.

There are, however, some cases where the chipped tooth results in lower averaged magnitudes. Figuretti experimental results on a SpectraQuest test rig [6], and Ghasemloonia experimental results on Yamaha test rig [26] studied three different levels of gear tooth damage, and noticed the chipped tooth fault had lower levels of amplitude than the healthy. For the missing tooth the impulsiveness spiked having greater amplitude levels than the other two.

Li [27] studied a worn gear and a gear with chipped tooth, and noted that both had higher amplitudes when compared to the healthy case, however some conditions lowered the chipped signal amplitudes to below that of the other two.

CHAPTER 3

Data Processing Techniques

As shown in the previous chapter the collected data should be treated with digital signal processing algorithms in such a way to enlighten the components that are useful for the diagnostic of the machine.

3.1 Signal Representation Methods

Several techniques have been developed with the purpose of condition monitoring. Usually they operate in time domain or in frequency domain. The gearbox diagnostic methods have been investigated for a long time and have recently been improving at a high rate pace [26].

Most of the methods are based on the calculation of the Time Synchronous Averaging (TSA) of each gear. The raw data and usually the tachometer signal are acquired, then the first step is normally applying the order tracking technique in order to avoid speed fluctuation. After that the TSA is calculated for each gear, the comparison of the TSA spectrum between a previous inspection and a new one can give information if there are some faults. Usually, though, the extraction of parameters (Kurtosis, FM0, FM4, etc.) is preferred because ideally they should be more stable and less affected by conditions change, like speed fluctuations. These parameters, also known as features, have the possibility of classification of the different conditions of the gearboxes. However, they depend greatly on the processing of the signal from which they are determined.

As seen in previous chapter, there are ways to represent the signals, and the first and foremost begins with the visualization in time domain or, in other words, the waveform.

3.1.1 Time Domain

The time domain methods try to analyze the amplitude and the phase information of the time signal. Often some statistical indicators are used to quantify the time signal such as the peak level, RMS and crest factor. This topic is further explained in Chapter 4.

Although it could be argued that not much information could be gained from inspecting the time domain, it is however a fundamental practice to examine the signal prior to any further analysis to ensure validity and gain some insight into the nature of the signal [24], as it allows the user to determine the presence of amplitude modulation, shaft components,

unbalance, transients or even higher frequency components, when analyzing portions of the time waveform.

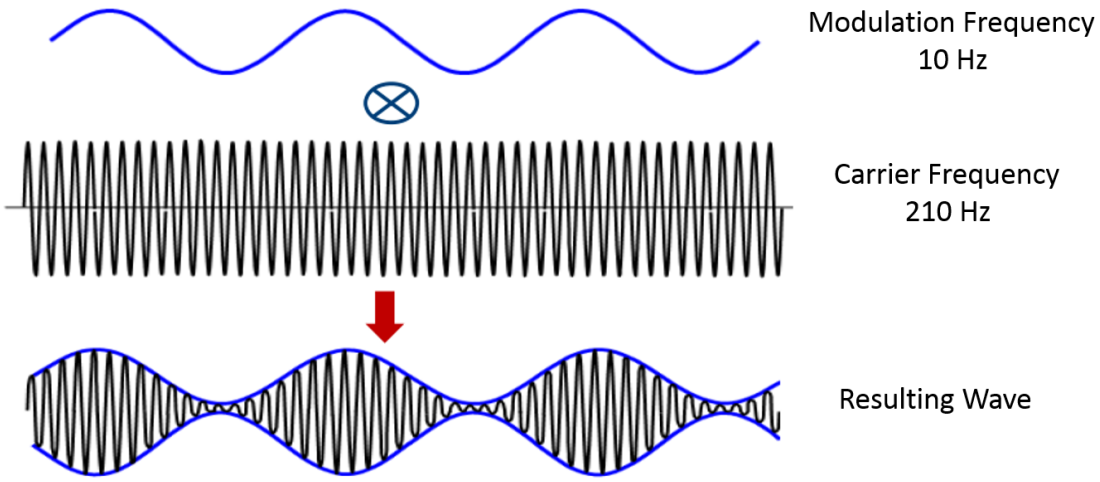

Figure 3.1: Modulation of a Carrier Wave.

One such case is when there are known transients inserted in the signal, it is possible to extract the filter parameters to obtain this transient frequency by determining the carrier frequency visually through the time-signal analysis. This method is further explained in this Chapter, on Section 3.3.

Considering a carrier wave as a pure sine wave, expressed in Equation 3.1.1, being modulated in amplitude by a lower frequency pure sine wave, expressed in Equation 3.1.2, the resulting wave follows the Equation 3.1.3, and the transformation is represented in Figure 3.1.

$$s_c(t) = A_c \; cos(w_c t) \tag{3.1.1}$$

$$s_m(t) = A_m \; cos(w_m t) \tag{3.1.2}$$

$$s(t) = [A_c + s_m(t)] \; cos(w_c t) = [A_c + A_m cos(w_m t)] \; cos(w_c t) \tag{3.1.3}$$

Usually the goal is to enhance these signals, as they are submerged in noise, and it can be said that all processing algorithms were implemented with this objective in mind. In reality, however, the signals do not behave like pure sine wave, but more like decaying transients which occur at certain intervals of time. This is called a damped impulse, as represented in Figure 3.2 and expressed in Equation 3.1.4.

The negative exponential corresponds to the modulating wave, and this signal theoretically repeats at a set frequency. It can be said with confidence that the decaying amplitude of the transient is much lower than the transient frequency itself, a lot of the time.

$$s(t) = A_m \; e^{\sigma \; t} \; sin[(w_c t + \theta)] \quad \sigma < 0 \tag{3.1.4}$$

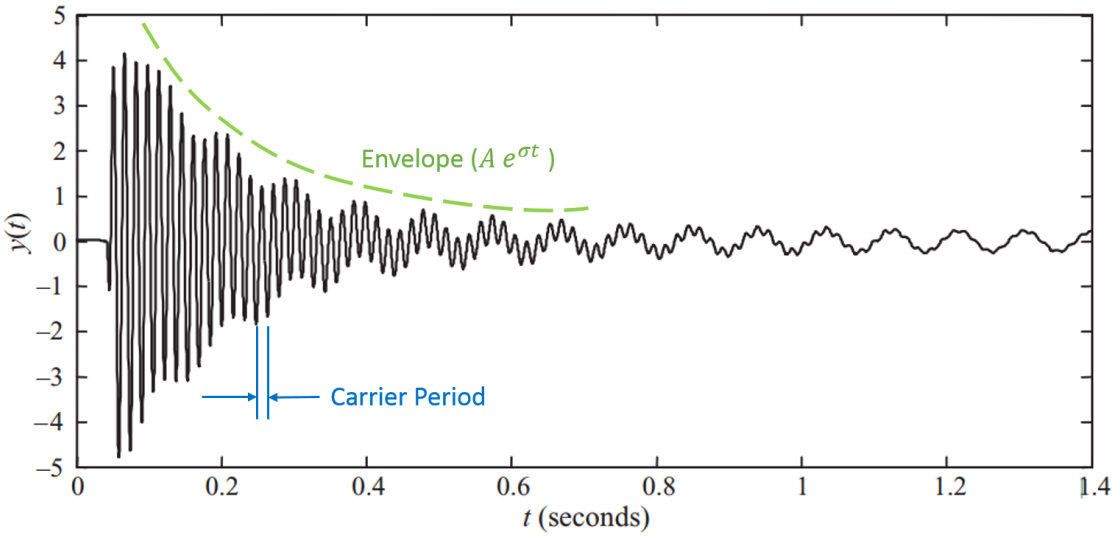

Figure 3.2: Transient impulse.

These transients are usually derived from the impulses gear teeth meshing and faults. However for the diagnosis of faults by evaluation of these transients and time waveform analysis is a complex and indirect process that requires a great level of expertise by the user.

3.1.2 Frequency Domain

Spectral analysis of functions, or time-series, is used for solving a wide variety of practical problems encountered by engineers and scientists. The most basic purpose of spectral analysis is to represent a time-series by a sum of weighted sinusoidal functions called spectral components; that is, the purpose is to decompose (analyze) a function into these spectral components. The weighting function in the decomposition is a density of spectral components. This spectral density is also called the *spectrum*. The reason for representing a function by its spectrum is that the spectrum can be an efficient, convenient way, and often revealing description of the function [28].

Any real signal can be broken down in a combination of sine waves. The spectrum is the representation of the present waves at each correspondent frequency, and their impact on the overall signal. In other words, the signal is a sum of pure sine wave, and each sine wave appears as a vertical line in the frequency domain. Its height is the amplitude and its position in the abscissa location is the corresponding frequency.

It is then a good and frequent way to visualize the nature of the signal, and the corresponding frequencies, as the time-domain signal is usually chaotic and, in practice, conclusions are hard to obtain just from the time signal.

As an example of the use of spectral representation of temporal waveforms in the field of signal processing, it can be considered the signal extraction of a gearbox with a faulty bearing, as shown in Figure 3.3. This signal is considered ideal and with no noise for easier understanding.

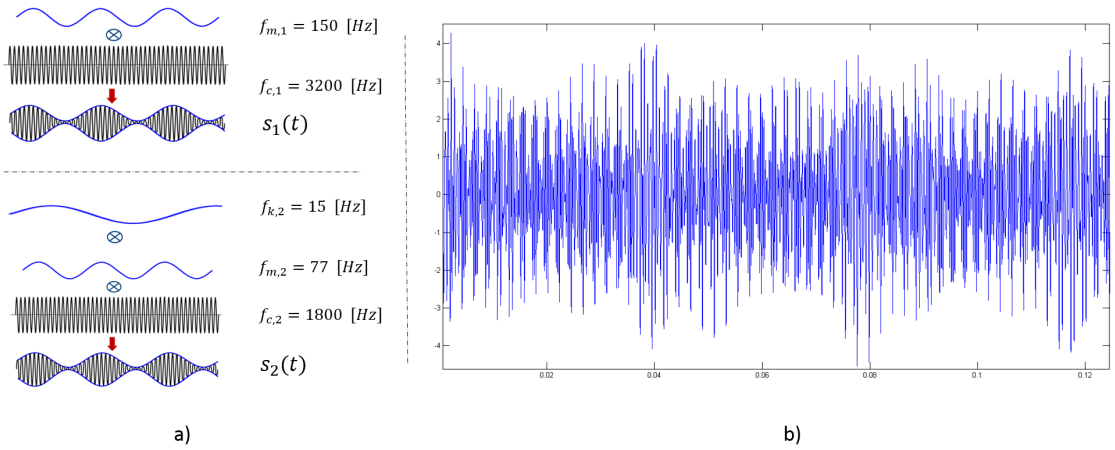

Figure 3.3: Time-Domain Signal of, a) Isolated Modulation of both signal 1 and 2, b) Sum of both signals in Time Domain.

Similarly to what is presented in Section 3.1.1, a carrier wave with frequency equal to $f_{c,1} = 3200$ Hz is modulated by a sine wave of frequency $f_{m,1} = 150$ Hz to generate signal $s_1(t)$, is simply added to a second simulated signal $s_2(t)$ whose carrier signal of frequency $f_{c,2} = 1800$ Hz is modulated twice by sine waves of frequencies $f_{c,2} = 77$ and $f_{k,2} = 15$ Hz, in this order. Figure 3.3 shows that the simulated signal that derives from these described pure sine waves. As it can be seen, not a lot of information can be extracted, as the scales of the inherent frequencies are in completely different orders.

Using spectrum comparison, or in other words, plotting the signature spectrum obtained, it is possible to observe the frequency components of the full signals. Figure 3.4 declares clearly the carrier frequencies as peaks, at 1800 and 3200 Hz. Any signal that is modulated produces sidebands, the smaller peaks around the carrier frequencies. These carry the information on modulation. It is easier to understand the inherent frequencies of a signal by spectral visualization than through the messy waveform signal. However, it should also be noted that the spectra obtained in real life and experimentation are not as clear as the one simulated in this example, and even the spectral analysis proves insufficient to determine the nature of the signal in most of the cases.

Fourier Transform

A vibration response can be defined by displacement, velocity or acceleration, and these quantities can be represented in both time and frequency domains. In the frequency domain, the waves have a magnitude and phase variable with the frequency. All the measured vibrations are always in analogue form, or simply, in the time domain and need to be transformed to the frequency domain. This is accomplished using a Fourier Transform to convert the signal $x(t)$ on variable time to $X(f)$ on the frequency domain.

Before applying the Fourier transform, the signal must be processed with a technique called windowing in order to minimize signal leakage effects. This method is equivalent to multiplying the signal sample by a window function of the same length, and is necessary as the Fourier Transform treats the discontinuities as varying frequencies which cause them to appear as sidebands in the spectrum. Windowing affects the ability to resolve closely spaced frequencies.[29]. In this dissertation, Hanning window was chosen and applied throughout the signal processing.

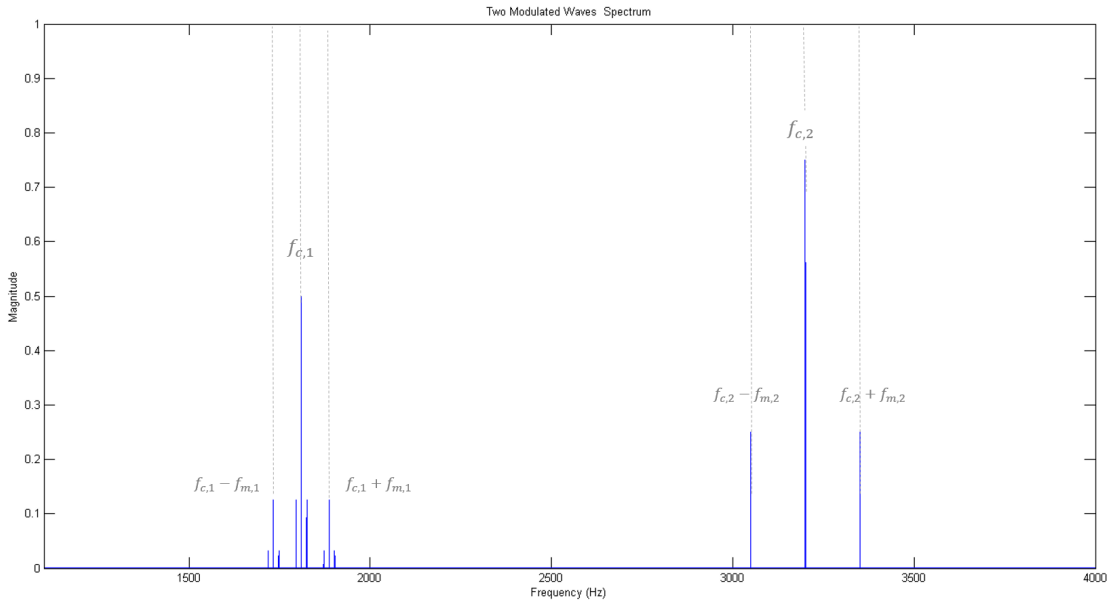

Figure 3.4: Spectrum of Simulated Signal.

Fourier Transform is widely used in signal processing as it describes what frequencies are present. If a signal $x(t)$ is a time domain function, then the frequency spectrum $X(f)$ of this signal using the Fourier transform is given by Equation 3.1.5.

$$X(f) = \int_{-\infty}^{\infty} x(t) e^{-j2\pi ft} dt \tag{3.1.5}$$

However, as the signals are sampled in time, the most used transform is the Fast Fourier Transform (FFT), as is an algorithm which realizes the Discrete Fourier Transform (DFT) in an efficient computational way by reducing the number of multiplications and additions involved. The DFT of a signal $x(n)$ is given by Equation3.1.6.

$$X(k) = \sum_{n=0}^{N-1} x(n) e^{-j\frac{2\pi}{N}nk}, \quad 0 \leq k \leq N-1 \tag{3.1.6}$$

Where N is the length of the signal, n is the discrete time.

3.1.3 Time-Frequency Domain

It is quite difficult to handle signals carrying nonstationary or transient components, using conceptualizations based on stationarity, as it is the case of frequency domain methods. The production of particular frequency may change in time, and these frequencies may not last enough to be detected by the Fourier Transform. Therefore, examining local behaviors in respect to time with precise frequency information is a useful way to gain insight to the nonstationarities that are inserted in the signal.

A time-frequency representation uses a 2-axis coordinate system to plot the frequency and time giving the magnitude as color. There are several techniques performing this representation, which show potential to detect and diagnose bearing problems in complex

rotating machines, where the SNR is very low and in the presence of several frequency components. [29]

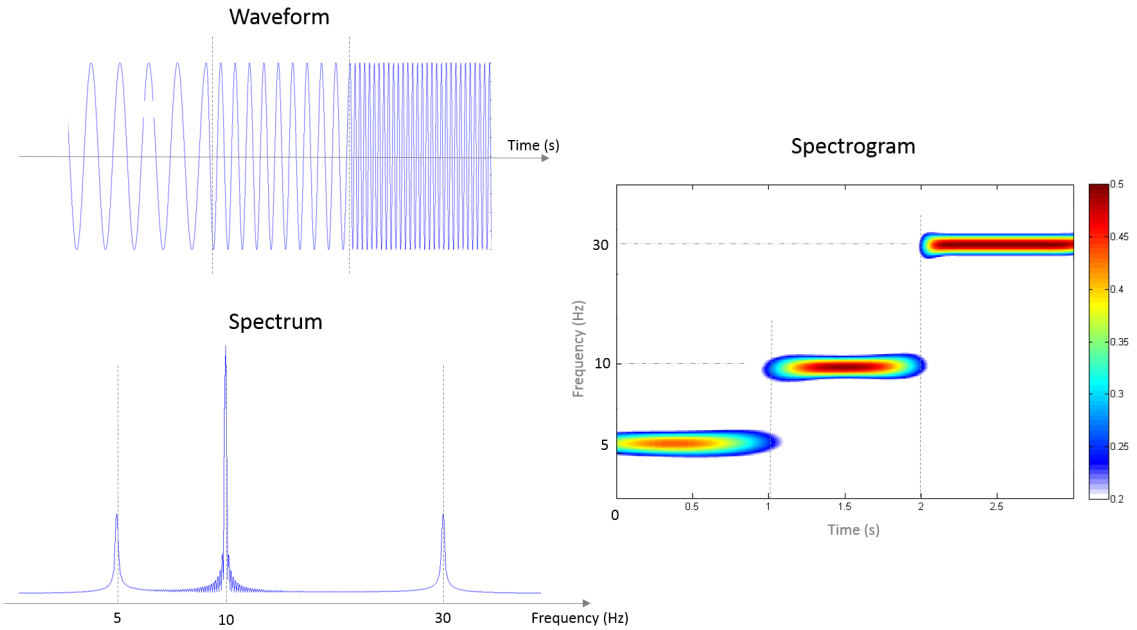

Figure 3.5: Waveform, Spectrum and Spectrogram using Short Time Fourier Transform.

This time-frequency representation are also called Spectrogram, and as a given example, Figure 3.5 shows the Waveform, Spectrum and Spectrogram of a signal with increasing frequency in time. The Spectrum results in the 3 frequency components that are seen in all the time signal, but it does not declare information as when those frequencies were present. The Spectrogram returns this information, as it can be noted where the 3 different frequencies are present in time.

Short Fourier Transform (STFT)

The Short Time Fourier Transform (STFT), also know as the Windowed Fourier Transform or spectrogram, is a development that extends standard Fourier Transform techniques to handle non-stationary data. Fourier Transforms are applied to short windows of data. These windows are moved along the data and may overlap.

With this the Fourier spectrum is obtained as a function of time. The STFT is given by Equation3.1.7.

$$SF(f,\tau) = \int_{-\infty}^{\infty} x(t)w(t-\tau)e^{-j2\pi ft}dt \tag{3.1.7}$$

Where w is the window function that is translated through time by τ.

Wavelet Transform

The Wavelet Transform is an alternative to the Short Fourier Transform, when used to visualize the Time-Frequency signal response. The formula for the Wavelet Transform is shown in Equation 3.1.8, where the $\psi*$ is the complex conjugate of the mother wavelet,

which is translated by b and dilated by factor a. This is in fact a convolution, and considered as a set of impulse response of filters. The shape of the mother wavelet influences the wavelet analysis, and for all the cases in this dissertation the Morlet Mother Wavelet was used [30].

$$W(a,b) = \frac{1}{\sqrt{a}} \int_{-\infty}^{+\infty} x(t)\psi^*(\frac{t-b}{a})dt \tag{3.1.8}$$

Due to this, Wavelet analysis gives better time localization at high frequencies. It provides information about speed fluctuations, transient events, verification of information obtained from time and frequency domain data, signal modulation, as it represents the evolution of the spectrum with time.

3.1.4 Angular Domain

When the vibration produced by rotating machines are analyzed it is often desired to have the axes represented in term of *Orders*, that are multiples of the rotation speed, instead of absolute frequencies (Hz). This technique allows firstly to see how the intensity of different harmonics changes over a big speed range, secondly to avoid smearing of discrete components due to the speed fluctuation [31] . Even with the machine running at constant nominal speed there are always some random speed variation.

If the speed of the signal can vary as function of time the number of samples is different for each revolution, this manifests as smearing and leakage in the frequency domain because the frequency component will not be stationary on one spectral line. To avoid this problem the signal is re-sampled at constant angle, but varying time, in this way there are the same number of sample in each revolution. This is what the angular resampling performs, turning the data from the time domain to the angular domain.

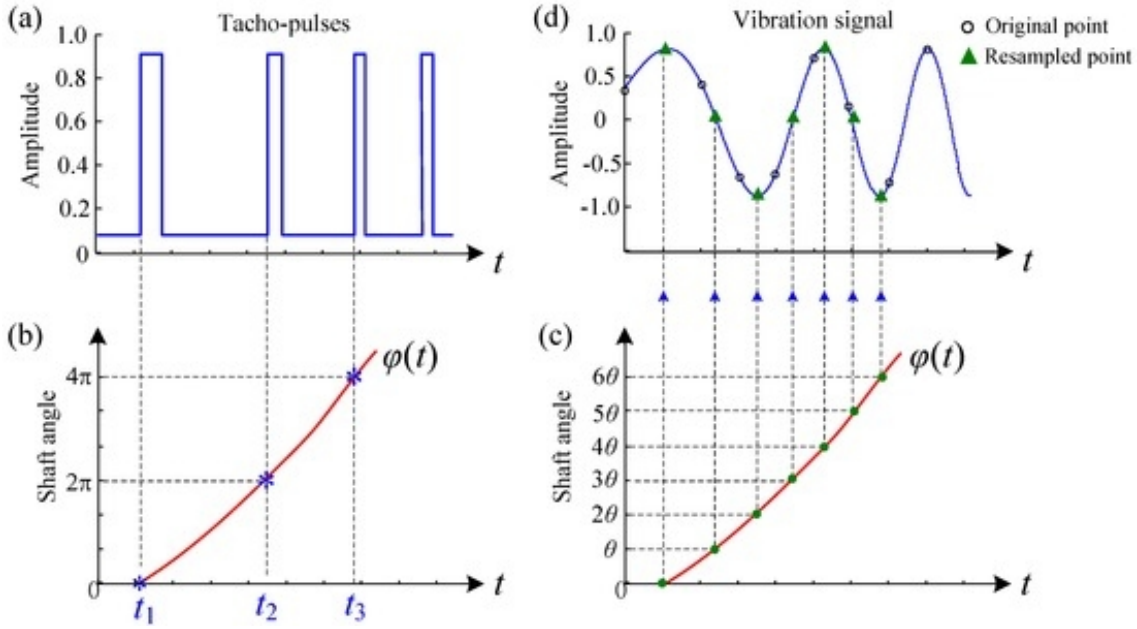

Figure 3.6: Angular Resampling Transformation [32].

Figure 3.6 represents how the transformation from constant time intervals to constant angular intervals is achieved.

3.2 Signal Processing Methods

Their main purpose is to change the signal in order to remove its undesirable part, known as noise, and to enhance the signal components of interest. This is a fundamental difference from the different domain representations of the signal, where this source signal is not altered, rather the signal is represented in different ways with the objective of understanding the nature of the signal, and possibly classify the inserted faults.

It is common practice to use both. First the different ways of representation of the signals to understand which signal processing methods should be used and applied to enhance the signal to noise ratio, followed again by the representation of the signal to correctly classify and confirm the hypothesis that was given before the method processing.

3.2.1 Cepstrum

Cepstrum analysis is a topic of a relatively small amount of research activity in the field of machine fault detection. Cepstrum magnitude spectrum is the FT magnitude spectrum of the log-magnitude FT of the signal. This method is used to detect the side-bands associated with time varying components or to quantify harmonics. Cepstrum was originally proposed for application of gear and bearing faults but does not indicate the type of problem with the machine. The lack of research papers in this field applied to gears indicates that the method is likely advised against them, however it is extensively applied to bearing fault diagnosis, as the removal of the discrete components of the shaft and gears is proved to be robust [33]. This method is mostly used in bearing signals rather than in gears.

3.2.2 Time Synchronous Averaging (TSA)

This technique is most commonly referred to as TSA in the gear and bearing fault detection field, but is sometimes referred to as synchronous signal averaging technique, synchronous averaging, or time domain averaging. As a denoising method, the TSA technique is very commonly applied. Bechhoefer [34] purposely applied TSA to gearbox analysis with the objective of evaluating performance of different algorithms and the signal noise reduction. To filter out asynchronous vibration and noise, speed or tachometer information is combined with angular re-sampling to an integer number of samples per revolution of the gear or bearing critical period using an interpolation method, such as spline interpolation.

This angular re-sampling is performed as a first step to deal with slight variances in the machine rotational speed, and to deal with the samples not being acquired at exactly the same angle positions. The method then averages the vibration over many revolutions of the gear or bearing critical period. This reduces asynchronous vibration components and zero-mean noise is expected to approach zero, as the number of averaged revolutions gets very large .

Time synchronous averaging is a signal processing technique that extracts periodic waveforms from noisy data. The TSA is well suited for gearbox analysis, where it allows the vibration signature of the gear under analysis to be separated from other gears and noise sources in the gearbox that are not synchronous with that gear. Additionally, variations in shaft speed can be corrected, such that the spreading of spectral energy into an adjacent gear mesh bin.

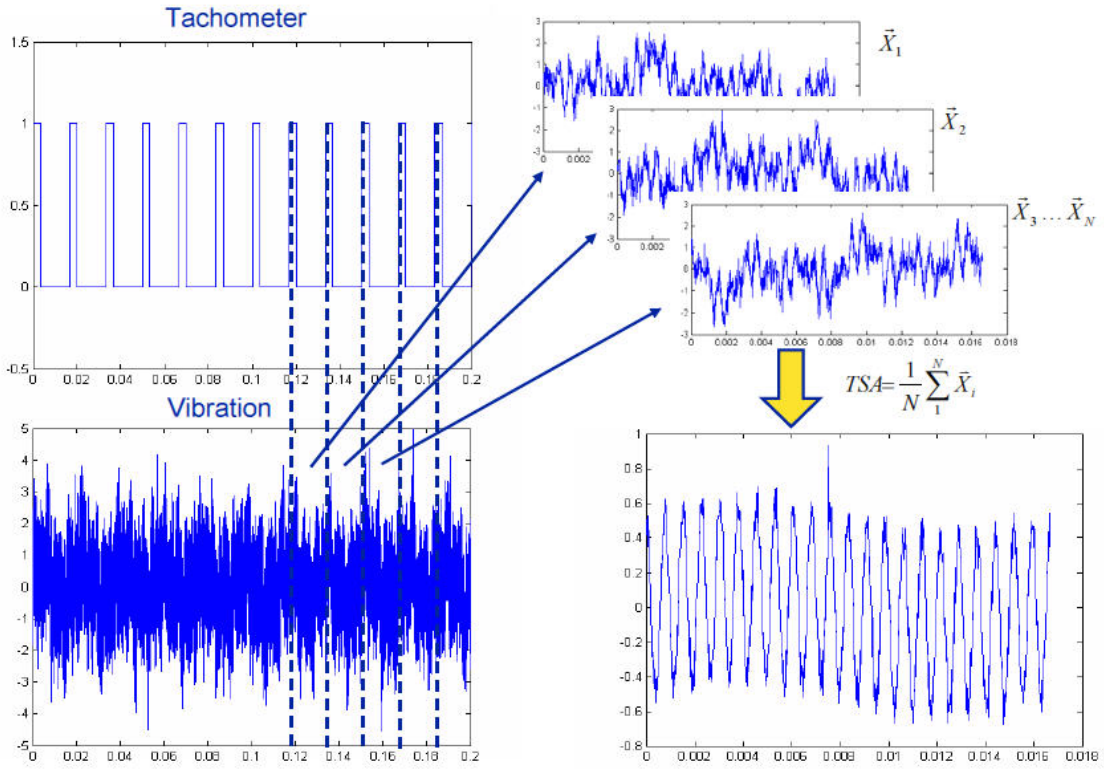

Figure 3.7: Time Synchronous Averaging of the signal [35].

A major drawback of TSA is the significant loss of information contained in the distribution or auto-correlation function, which contains important information related to fault detection. Despite this loss of information, the method is widely applied as a pre-processing step and as a rough estimate approximately 40% of gear and bearing fault detection papers implement this method [36].

3.3 Envelope Analysis

Each time a localized defect in a gear makes contact, while under load, with the surface of another gear, an impulse of vibration is generated. This impulse will have an extremely short duration compared to the interval between impulses and due to this, its energy will be distributed across a very wide frequency range. As a consequence to that, various resonances of the gearbox and the surrounding structure will be excited by those impacts.

The spectrum of the raw signal often contains little diagnostic information about the faults. With envelope analysis, the signal is band-pass filtered in a high frequency band in which the fault impulses are amplified by structural resonances. After that it is amplitude demodulated to form the envelope signal whose spectrum contains the desired diagnostic information.

One of the biggest difficulties with envelope analysis is how to determine the best frequency band to envelope [29]. In this text, this band is chosen around the maximum Cyclic Spectral Correlation Density which returns the clearest deterministic frequencies of the gearbox. The procedure is shown in Figure 3.8

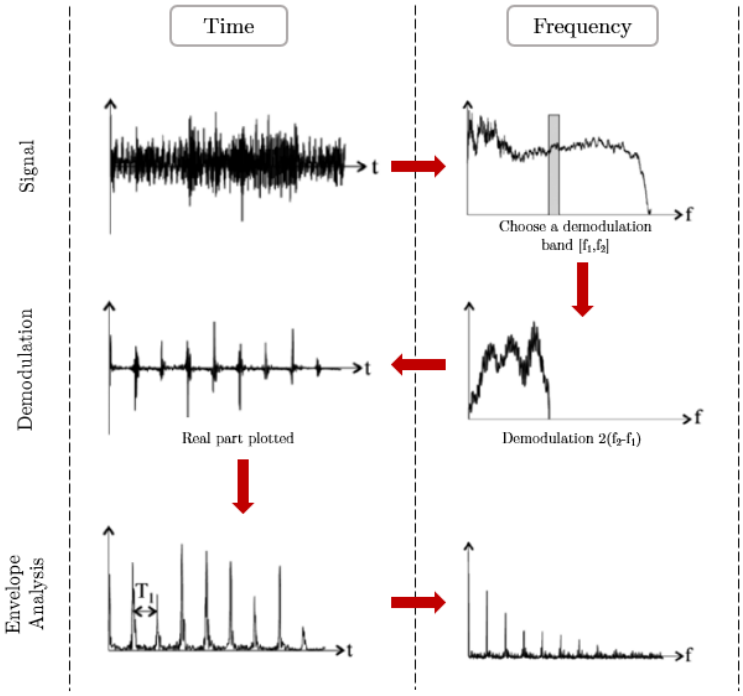

Figure 3.8: Envelope Analysis Procedure [18]

3.4 Filter Selection Techniques

3.4.1 Spectral Kurtosis

Spectral Kurtosis (SK) was proposed for fault detection on rotating machine vibration data by J. Antoni and R.B. Randall [37]. SK is a method in which a band-pass filter is selected to identify the band that has the maximum Kurtosis of the resulting filtered signal. The idea is to calculate the kurtosis at each frequency band in order to discover the presence of hidden non-stationarities. In [38] the author defines the SK as the fourth order normalized cumulant. He suggests using the SK as a detection tool that precisely points out in which frequency band.

3.4.2 Kurtogram

The concept of kurtogram is the display of the SK as a function of frequency and of spectral resolution, so the filter selection can be extracted from it. The maximum then provides the optimal parameters from which a band-pass filter can be designed, for instance as a prelude to envelope analysis [38]. The idea of the kurtogram is to create a robust detection filter with an imposed band-pass structure with only two parameters to be identified. The objective of this technique is to find the central frequency f_c which tunes the filter where the SK is maximum, or in other words, where the signal to noise ratio is the highest, and the bandwidth B_f of the filter which achieves the best compromise between filters that are too wide, which would alter the signal to noise ratio, and filters that are too narrow with a very long impulse response that would alter the impulse like nature of the filtered signal.[29]

The basis behind this approach is that a band-pass filter has good chance of selecting the frequency band where the signal to noise ratio is maximum. This could achieve detection of

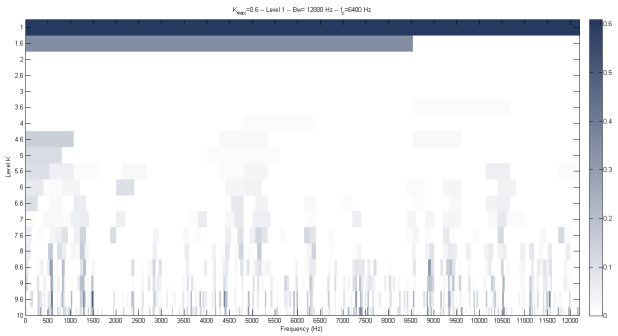

Figure 3.9: Fast Kurtogram.

the one case with the strongest impulsiveness in cases with multi-sources. It is indispensable to apply a band-pass filter before carrying out envelope demodulation. In addition to this, forcing a pre-defined structure on the filter makes it independent of the assumed validity of the model. The computation of the full kurtogram covering all combinations of center frequency and bandwidth is very costly and so a number of more efficient alternatives have been proposed. The most detailed one was the so called Fast Kurtogram based on a series of digital filters rather than the STFT. In the most basic version, the frequency range is progressively split into bands that are one-half the width of the previous stage or scale, also known as binary tree.

Although it allows an automated filter selection, by the inputs it selects, the Kurtogram is not consistent enough. As an example, the signal shown already in this Chapter, in Figure 3.3, plus added random gaussian noise. The carrier frequencies are known to be 3200 Hz and 1800 Hz, and thus the filtered signal around one of the bands filters out the information on the signal correspondent to the other. The Fast Kurtogram, in Figure 3.9, returns a maximum at the the full band spectrum. This "filter" is equivalent to the demodulation alone. The end result would still be a noisy signal with both components.
In short, the Kurtogram returns the filter for the biggest resulting kurtosis, but not necessarily for the filter that would increase the kurtosis of the specific component of interest.

3.4.3 Wavelet Analysis

The wavelet transform spectrum has been used for fault detection of gears and bearings in many papers dating back a few decades. The wavelet transform is the leading time-frequency signal analysis method, and is commonly applied in the analysis of non-stationary signals. It has been proven to be a very effective diagnostic tool and a brief summary of some of the papers is provided. Liu [24] found that gear cracked tooth flaws resulted in increased spectrum peaks at the characteristic frequency. The authors proposed averaging the Wavelet Transform sections across a frequency range, and taking the DFT of this averaged signal [36].

Compared to the STFT, whose time-frequency resolution is constant, the wavelet transform depends on the frequency of the signal. The wavelet transform is commonly applied as a filter to emphasize the fault signal, as the wavelet in denoising allows the "energy" of the signal in relatively small number of big coefficients [39].

Mcdonald implemented the discrete wavelet transform with Meyer wavelet and used a single decomposition signal as the output, hence just using the method as a basic filter design tool. Features of this filtered signal were used in fault classification of ball bearings

with a support vector machine [36].

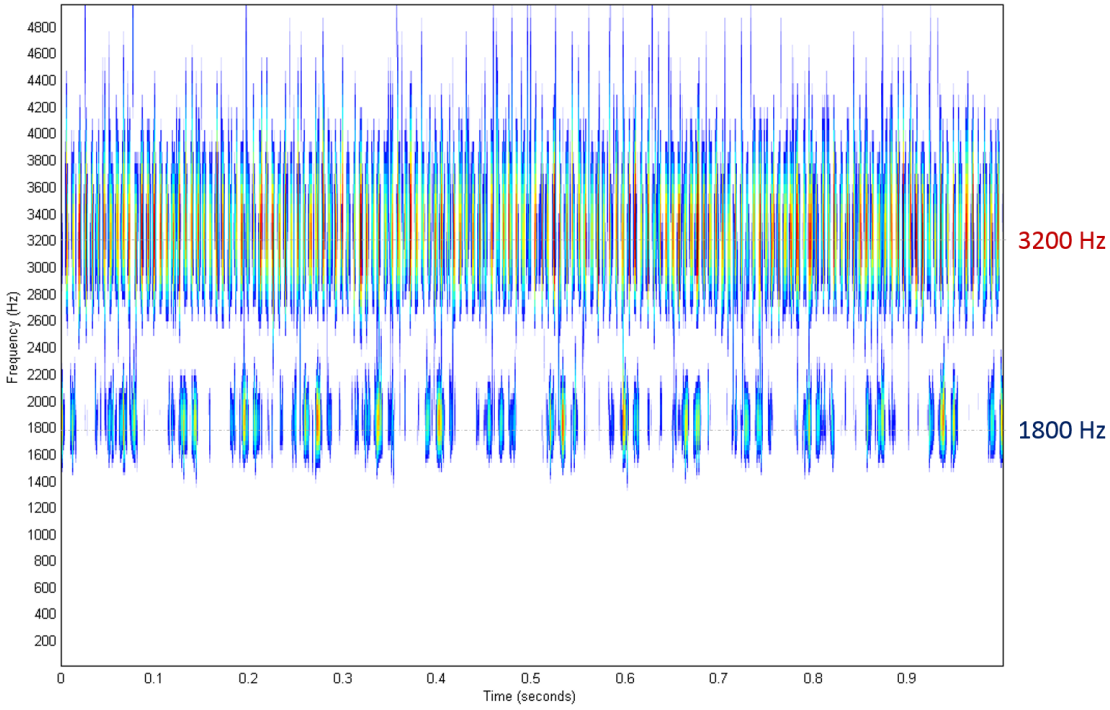

Figure 3.10: Wavelet Analysis of Generated Signal with noise.

Providing again the same signal given in Figure 3.3 plus white noise, with simulated components, one generates a carrier frequency of 3200 Hz, and the other generates a carrier frequency of 1800 Hz. The Wavelet Analysis in Figure 3.10 clearly shows both frequency bands. Knowing the 1800 Hz component has actually two levels of modulation, makes the signal show less intensive colors than the other in that band. The 1800 Hz is akin to the FTF of a bearing, and the other to a gear fault. In case the desired analysis would be for the gears, the filter center frequency would be selected at 3200 Hz band.
The advantage of the Wavelet Analysis, besides providing the information of which frequencies are present in the signal as a function of time, is that it allows greater resolution, less leakeage and more noise reduction than the STFT.

3.4.4 Cyclostationary Analysis

In recent years there has been an increasing interest in applying cyclostationary analysis to the diagnostics of machine vibration signals. This is because some machine signals, while being almost periodic, are not exactly phase-locked to shaft speeds, and thus even after compensation for speed fluctuation cannot be extracted by synchronous averaging. The benefits offered by the cyclostationary formalism in Condition Monitoring have been explored for more than one decade; research in this domain has resulted in the proposal of a quite general methodology and processing tools to analyze mechanical signatures of machines. Antoni *et al.* [10] exposed that a common approach in Condition Monitoring is to first decompose the signal into its periodic and random parts in order to separate out contributions from different physical origins, and that the Cyclostationary Analysis by the *Cyclic Spectral Correlation* (CSC) efficiently differentiates first-order cyclostationarity from (pure) higher-order cyclostationarity, respectively.

Cyclostationary Analysis is also another spectrum method applied to fault detection of gears and bearings, and it takes advantage of the stochastic process nature of the vibration signal. A signal is cyclostationary of degree N if its N^{th} moment is periodic about any period. In different words, a cyclostationary signal is described by a probability density function which is periodically time-varying.

Then the first-order of cyclostationarity can be defined as a function whose expected value is a T-periodic function, whose any two points in time meet the equivalence at the T-time distance:

$$Ex(t) = m_x(t) = m_x(t+T) \tag{3.4.1}$$

This definition of first-order of cyclostationarity models well the gear signals.

Similarly the second-order of cyclostationarity is a function whose autocorrelation, described by Equation 3.4.2 is a T-periodic meets the condition described by Equation 3.4.3.

$$R_{xx}(t,\tau) = \lim_{T\to\infty} \frac{1}{T} \int_{-T/2}^{T/2} x\ (t-\frac{\tau}{2})\ (t+\frac{\tau}{2}) dt \tag{3.4.2}$$

$$Ex(t)x(t-\tau) = R_{xx}(t,\tau) = R_{xx}(t+T,\tau) \tag{3.4.3}$$

The powerful statistical descriptor of the second-order of cyclostationary can be determined by the Cyclic Spectral Correlation, in Equation 3.4.4.

$$S_{xx}(\alpha, f) = \lim_{W\to\infty} \int_{\mathbb{R}} \int_{-W/2}^{W/2} R_{xx}(t,\tau) e^{-j2\pi(f\tau+\alpha t)} dt d\tau \tag{3.4.4}$$

which may be equivalently defined as the limit in Equation 3.4.5

$$S_{xx}(\alpha, f) = \lim_{W\to\infty} E[X_W(f) X_W(f-\alpha)] \tag{3.4.5}$$

where $X_W(f)$ stands for the Fourier transform of signal $x(t)$ over a time interval of width W. Frequency f physical meaning is correspondent to the time-lag τ, indicating the frequency of the carrier signal. Frequency α corresponds to time t, indicating the frequency of the modulation, also described as cyclic frequency. So it can be inferred that the CSC shows the correlation levels at which each carrier frequency f is modulated by the cyclic frequency α.

Randall [9, 12] and Antoni [7, 18, 11] have worked extensively on this method, for both gear and bearing faults. Besides the high level of expertise that is demonstrated by their findings over the years, they've achieved a successful application in detecting the faults. The most interesting part of the method is the selection of the correct filter for a determined cyclic fault frequency, and thus shows great potential to be used in parallel with the Envelope Analysis.

Application of this method typically results in either a one-dimensional fault indicator or a three-dimensional plot for human diagnostics. [36]. The last one is applied in a way to obtain the filter parameters for the raw signals.

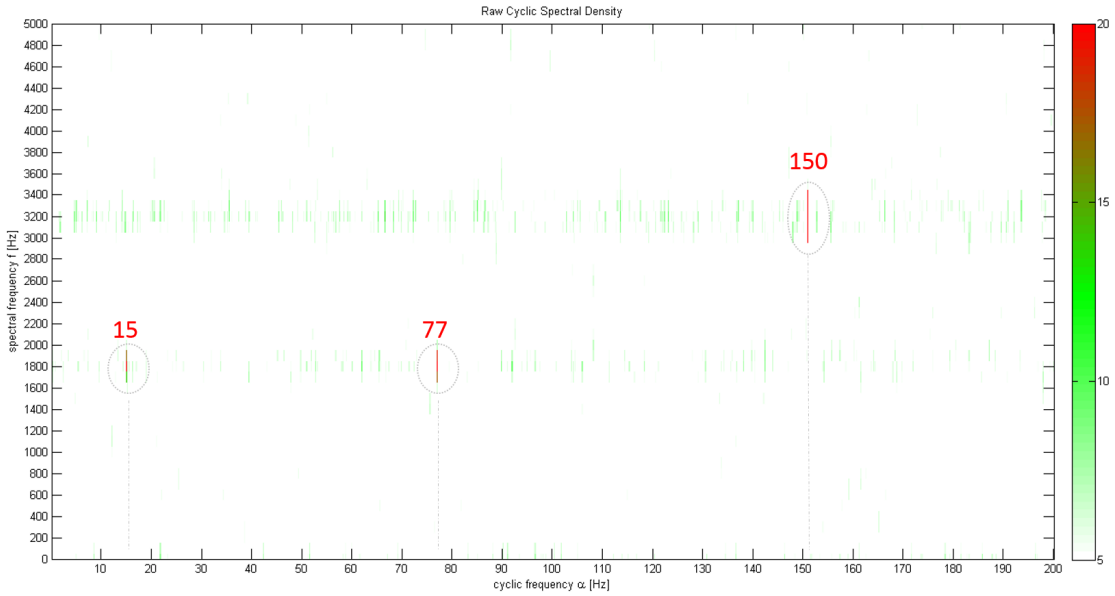

Figure 3.11: Cyclic Analysis with Spectral Correlation

The Cyclostationary Analysis of the signal of Figure3.3, with added noise, is determined as an example of the method. The CSC returns 3 points where the coefficients are maximum, that correspond to the 3200 Hz ($f_s = 3200$) and 1800 Hz band of frequency. Like the Wavelet Transform, it returned the two bands, but it can be seen in Figure3.11 that the range of the band is more tight and precise. The greatest advantage would be that the method provides information of how many modulations exist for each component, and allows an automatized selection of the filter parameter by selecting a maximum on the cyclic frequency (α) line correspondent to the fault frequency of interest.

CSC is a recent method that is gaining interest in the industry, but until now seems to not cope well with some signal processing methods, like the TSA. Zhu et al. [40] investigated the effectiveness of cyclostationarity from the first order to the third order, that is, spectrum of time-synchronous average, cyclic spectrum and cyclic bispectrum, in gearbox condition monitoring. The author stated that TSA is in fact the first-order cyclostationarity, and by performing TSA the randomness information in this second-order cyclostationarity is lost, and thus the CSC becomes redundant after the TSA.

3.5 Fault Indication

The goal of fault indication is to detect faults in the vibration data and depending on the method, indicate the type of fault as well. In general, most fault indication methods can be grouped into:

1. **Feature Extraction** [41, 42, 43, 44]. These approaches typically indicate the fault type and fault level but require extensive data knowledge of the machine under fault conditions and typically requires detailed training for each individual machine. It is common to use a method to reduce the dimensionality, which allows the classification of machine condition by themselves. The most common are Fisher Discriminant Analysis (FDA), Independent (ICA) and Principal Component Analysis (PCA).

2. **Human Factor** [45, 24, 31, 46]. When authors provide no clear fault indication variable it is expected that fault detection and diagnosis is performed by human analysis of the results (e.g. by examination of a wavelet scalogram).

3. **Threshold** [47, 34, 23] Methods which perform fault indication by comparison of an indicator (typically Kurtosis or RMS of a filtered signal) are assumed to be implemented online by a threshold alarm. These approaches are very practical for industrial condition-monitoring applications, as the alarm threshold can be easily adjusted by on-site engineers. These approaches often do not indicate the type of fault, just that a fault is present.

The novel method presented in this dissertation applies these 3 different methods. The correct selection of the band-pass filter is semi-automated for the studied signals, but other mechanisms may behave differently, so the filter selection is done by the CSC that provides the knowledge of the carrier frequencies for each modulation frequency. Afterwards, the features selection is also studied briefly by Human factor, and the ones that show promise of classification are selected. And finally, the selected features are fed to as input to the Principal Component Analysis, which allows the reduction of the dimensional space to 3 or 2 dimensions.

CHAPTER 4

Condition Diagnosis

Features are used for the fault detection and fault classification, as explained in Chapter 3. In this chapter, the applied features are explained, as well as how they are used for fault detection.

Also called Condition Indicators (CI), features are usually statistical parameters that provide some information on the nature of the time-signal. These time domain statistics are usually applied to obtain the amplitude levels of the vibration signal after Envelope Analysis. The vibration amplitudes in the narrow band is theoretically affected by the fault in that band of frequencies, and thus the feature levels change as well, detecting the fault. Case the features remain unaffected, it is assumed that no fault that excites that frequency band is present in the structure.

4.1 Classification Features

It is common to normalize the moments, that are higher than the second order, by removing the mean and dividing by the standard deviation raised to the order of the moment. The higher moments are sensitive to impulsiveness in the signal which make moments such as the Skewness and Kurtosis, respectively third and fourth moments, so relevant to the diagnosis analysis.

Due to the large variations, direct comparison of signatures is difficult, and thus statistical features provide a reduced data set for the application of pattern recognition and tracking technique. Ideally, these features are more stable and well behaved than the raw signature data itself. Besides the most common ones, like Standard Deviation, Kurtosis, Crest Factor, among others, which are all time domain statistics, more complex features are presented from the literature.

Bartelmus [47] showed that faulty components are more susceptible to load, and he applied a feature which consists of the sum of the first 10 harmonics of the gear mesh amplitude. The feature showed a linear decline when plotted against the gearbox speed, proving to be a good classifier of the condition of the gearbox. Lebold [48] also enumerates and exposes other common features not used in this thesis.

Standard Deviation and Percentiles

Both are a measure to quantify the amount of variation or dispersion of a set of data values commonly used in statistics. Variance refers to the second moment of the probability density function, and it provides information on the spread of the signal. The standard deviation (σ) is the squared root of the variance. The Percentiles specify the amount of dispersion in a specific interval, with P_{75} and P_{25} referring to the number of points above 75% and below 25% of the mean, correspondingly.

$$\sigma = \sqrt{\frac{1}{n-1}\sum_{i=1}^{n}(x_i - \bar{x})^2} \tag{4.1.1}$$
$$P_{75} = P(x \geq x_{0.75})$$

Skewness

The third moment, skewness (S), provides information on the symmetry of the probability density function.

$$Sk = \frac{N\sum_{i=1}^{N}(x_i - \bar{x})^3}{\sigma^3} \tag{4.1.2}$$

If the S is negative, the probability function is left inclined, and vice-versa if S is positive. The higher the absolute of the skewness is, the more asymmetric the function is, or in another, more inclined.

Kurtosis

It is the fourth order moment normalized by the square of variance of a signal and gives a measure of the spikiness or impulsiveness of the signal.

$$K = \frac{N\sum_{i=1}^{N}(x_i - \bar{x})^4}{(\sum_{i=1}^{N}(x_i - \bar{x})^2)^2} \tag{4.1.3}$$

Kurtosis (K) describes the shape of the function, and its value is equal to 3 for gaussian distribution, and being very high for impulse signals. The literature suggests that for a perfectly healthy and uniform mating gears, Kurtosis is expected to be 3, and a faulty gearbox would increase its Kurtosis with the level of the damage..

Peak to Peak

It is the range between the maximum and minimum value in the signal.

$$PP = max(x) - min(x) \tag{4.1.4}$$

This is akin to determine the maximum amplitude, as the vibration signals are simetric by nature. Thus the higher the amplitude, it can be assumed that the level of the fault impulsive nature increases. It is a simple feature with some proven application.

Root Mean Square

It signifies the energy content within a signal with respect to time. The root mean squared (RMS) is defined as the square root of the mean of the sum of the squares of signal samples and is given by

$$RMS = \sqrt{\frac{1}{N}[\sum_{i=1}^{N}(x_i)^2]} \tag{4.1.5}$$

Where, x is the original time signal, sampled at N points, where i is the sample index.

Crest Factor

Defined as the ratio of the peak value divided by the RMS value, it gives the shape of the waveform. [49]

$$CF = \frac{Peakvalue}{RMS} \tag{4.1.6}$$

Zero Order Figure of Merit (FM0)

It is an indicator of major faults in a gear mesh. Changes in the meshing pattern can be noticed by comparing the maximum peak-to-peak amplitude of the signal to the sum of the amplitudes of the mesh frequencies and their harmonics. It is given as

$$FM0 = \frac{PP}{\sum_{N=0}^{H} P_N} \tag{4.1.7}$$

Where PP is the maximum peak-to-peak amplitude of the signal, P_N is the amplitude of the harmonic, and N is the total number of harmonics in the frequency spectrum to be taken into consideration.

Fourth Order Figure of Merit (FM4)

FM4 was developed to detect changes in the vibration pattern resulting from damage on a limited number of gear teeth. [50] FM4 is calculated by applying the fourth normalized statistical moment to the difference signal as given in the equation.

$$FM4 = \frac{N\sum_{i=1}^{N}(d_i - \bar{d})^4}{(\sum_{i=1}^{N}(d_i - \bar{d})^2)^2} \tag{4.1.8}$$

M6A & M8A

Proposed by Martin [51] to detect surface damage on machinery components, they are the 6th and 8th statistical moments of the signal, as opposed to the 4th statistical moment, as the Kurtosis or FM4. It is expected to be more sensitive to peaks.

$$M6A = \frac{N^2 \sum_{i=1}^{N}(x_i - \bar{x})^6}{(\sum_{i=1}^{N}(x_i - \bar{x})^2)^3}$$
$$M8A = \frac{N^3 \sum_{i=1}^{N}(x_i - \bar{x})^8}{(\sum_{i=1}^{N}(x_i - \bar{x})^2)^4} \tag{4.1.9}$$

These are suggested to be applied to the difference signal [48], for a stronger classification system.

ENA4

NA4 was developed to detect the onset of damage and to continue to react to this damage as it spreads and increases in magnitude. ENA4 is an enhanced version of NA4, and was expected to be more robust when progressive damage occurs. It is determined as the normalization of the fourth statistical moment divided by the signal variance for a healthy gearbox.

$$ENA4 = \frac{\frac{1}{N}\sum_{i=1}^{N}(x_i - \bar{x})}{(\tilde{M}_2)^2} \tag{4.1.10}$$

where $\tilde{M}_2$ is the variance of the signal for a healthy gearbox. Lebold [48] suggests that if it is applied to the TSA residual, it provides better classification.

Entropy

The entropy is a quantitative measure of system disorder. It is proposed to obtain higher values for signal with more random content, like gear wear, or broken tooth. The parameters of Entropy studied in this thesis are the Logarithmic Entropy(Ent_{log}) and the Shannon Entropy ($Ent_{shannon}$).

$$Ent_{log} = \sum_{k=1}^{n} log(x_k^2) \tag{4.1.11}$$

$$Ent_{shannon} = -\sum_{k=1}^{n} x^2 \; log(x_k^2) \tag{4.1.12}$$

Harmonics

Not exactly one feature, but more of a family of features which derived from the spectra, as opposed to the time domain statistics that were previously shown. The objective is usually to obtain the amplitude level of frequency bands that are assumed to be declarative of the fault nature. Taking the example of unbalance, that greatly increseas the shaft rotation frequency amplitude, Kumar [14] obtained this amplitude in 3 axes (horizontal, vertical and axial) and concluded that both 3 values increase with unbalance, for various speeds. Bartelmus2009 [47] showed the variation of the sum of the 10 first harmonics of the GMF can detect if there is any damage in a planetary gearbox.

3 Harmonics Gear Mesh Distribution (3 GMF)

Created to detect specifically the chipped tooth fault, due to the impulse signal being weakly damped, as suggested by FMTC [52]. It is the sum of the amplitudes of the Gear Mesh Frequency and its first 2 harmonics.

$$3GMF = \sum_{k=1}^{3} A(k * GMF_1) \tag{4.1.13}$$

where $A(k * GMF_1)$ is the amplitude of the spectral peaks at $k * GMF$.

Sideband Power Factor (SBPF)

Initially suggest in [53], it can be described as the sum of the Gear Mesh Frequency (GMF) and the 2nd GMF, plus the sidebands around them, from 1 until 5.

$$\begin{aligned} SBPF = PSA(GMF) + \sum_{i=-5}^{5} PSA(SB_i) + \\ PSA(2GMF) + \sum_{i=-5}^{5} PSA(SB_i) \end{aligned} \tag{4.1.14}$$

Where PSA is the power spectrum amplitude that can be integrated from the Fourier Transform of the signal.

4.2 Feature Analysis

For a reliant classification system of the gear faults, it is important to assess the robustness of the features.

4.2.1 Single Features

First it is needed to see if each individual feature provides some level of classification. In other words, if the features intersect or not at different speeds. Figure 4.1 provides an example of two features, one that shows promise of a good classification and the other with bad classification. These classifications were actually determined from one observation of 30 seconds. The feature on the left (SBPF) does not allow classification, as the features for the healthy case intersects with the faulty one. On the other hand, the feature on the right (CF) possibly allows classification, as the feature for each the faults have different levels and remain relatively constant, thus not intersecting and possibly allowing a threshold classification.

It should be noted that each speed has only one sample value. This does not provide statistical confidence for a correct classification. In order to prove this, it is necessary to see if the extracted features correspond reliably with a greater number of observations. For this, the 30 seconds measurement was truncated and divided into 10 blocks of 3 seconds each. The same was applied to the other two measurements that also had 30 seconds of time sampling. In the end, instead of determining each feature for only one measurement

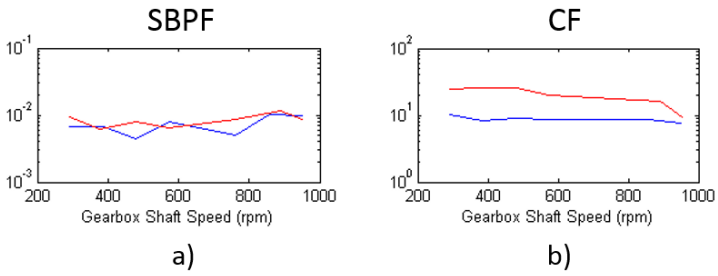

Figure 4.1: Two Features Classifying Faulty case (red) from Healthy case (blue). a) Sideband Power Factor with bad classification, and b) Crest Factor with good classification.

of 30 seconds, it was determined each feature for 30 observations of three seconds each. This provides an understanding of how the features behave, and if they return the same values for similar signals, albeit different. The features proven to have low volatility, are assumed to be robust and selected for the system classification.

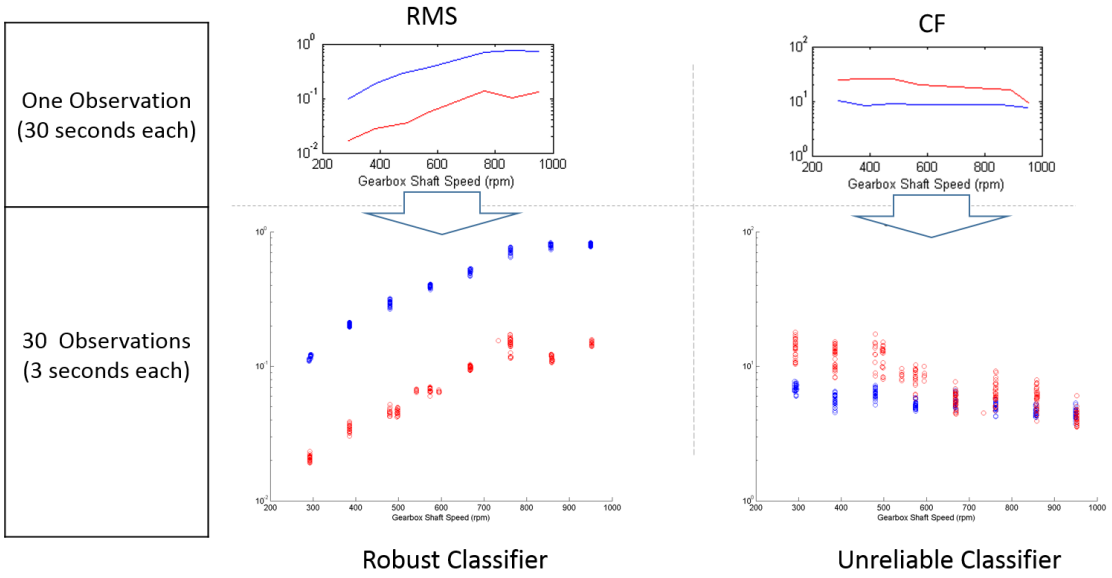

Figure 4.2: Two Features Classifying Faulty case (red) from Healthy case (blue) . a) Root Mean Square with Robust classification, and b) Crest Factor with Unreliable classification.

Figure 4.2 shows that the feature previously thought to be a good classifier is unreliable, as it is proven to be erratic. The other feature shows that with a greater number of samples, the feature behaves consistently and is selected as a robust feature.

4.2.2 Principal Component Analysis (PCA)

To classify all the states, and to obtain more definitive conclusions towards developing a diagnostic tool, it is important to present a complete picture between the faulty gears and healthy gear states which can be easily comprehended from one or two key plots. This is established through the use Principal Component Analysis (PCA) based clustering [25].

Assuming m number of features are selected, PCA allows the data dimension reduction, by searching for the lowest linear transformation in the m-dimension space. It can do this by calculating the eigenvectors from the covariance matrix of the features.

Defining a $m \times n$ X matrix, where m rows are each feature, and n columns are each measurement, the covariance matrix is defined as Equation

$$S_x \equiv \frac{1}{n-1} X X^T \tag{4.2.1}$$

As S_x is a square symmetric matrix $m \times m$, it can be diagonalized by choosing a new orthogonal coordinate system, given by its eigenvectors; corresponding eigenvalues will then be located on the diagonal. In this new coordinate system, the covariance matrix is diagonal.

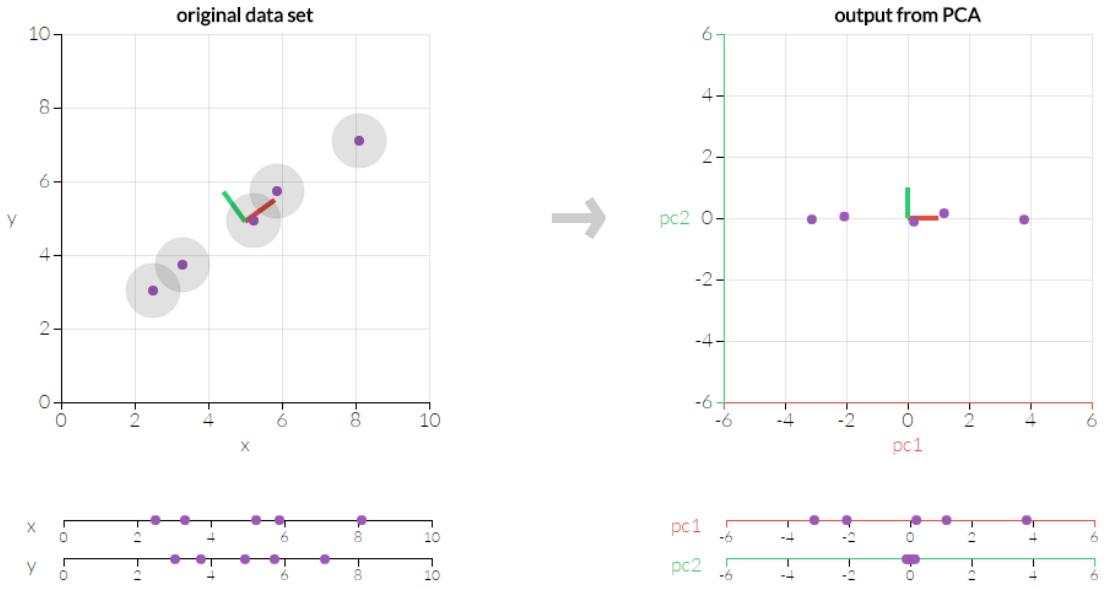

Figure 4.3: Principal Component Analysis example of dimension reduction [1].

The correlation between points is now zero, and the variance of any projection will be given by a weighted average of the eigenvalues. Consequently, the maximum possible variance will be achieved if we simply take the projection on the first coordinate axis. It follows that the direction of the first principal component is given by the first eigenvector of the covariance matrix. The second eigenvector corresponds to the second principal component, so on. This process, in fact, just selected a vector that maximizes the variance of the dataset, and the following orthogonal vectors to it that maximize the remaining variance.

This process assumes that there is a combination of axes in the m dimensional space that captures the most information about the data. Similarly, it also assumes there in that combination, there are axes that can be dismissed because of the low variability they provide. In this way, features space is reduced to a lower dimension (usually no more than 3) to the few that are more meaningful.

In Figure 4.3 is given an example of the result of PCA. The vector that maximizes the variance is obtained for the 2 features (2 dimensions) is obtained, and this vector is the so called fundamental (or first) principal component (PC_1). The projection of the full data onto PC_1 axis captures the behavior of the data, while the orthogonal second principal

component PC_2 is deemed redundant and is neglected.

Attention is needed when handling PCA, as sometimes the PC_2 and PC_3 may provide a better classification of the results.

4.2.3 Adopted Procedure

The method present on this dissertation is the correct application of the Demodulation and Envelope Analysis by selecting the correct band-pass filter from the Cyclic Spectral Correlation Analysis. The filter parameters are taken after knowing the carrier frequencies that are modulated by the frequencies of interest, such as the GMF. Then Features are calculated on the demodulated signal and selected based on their performance. Finally the Principal Component Analysis is applied to provide a solid method of fault classification.

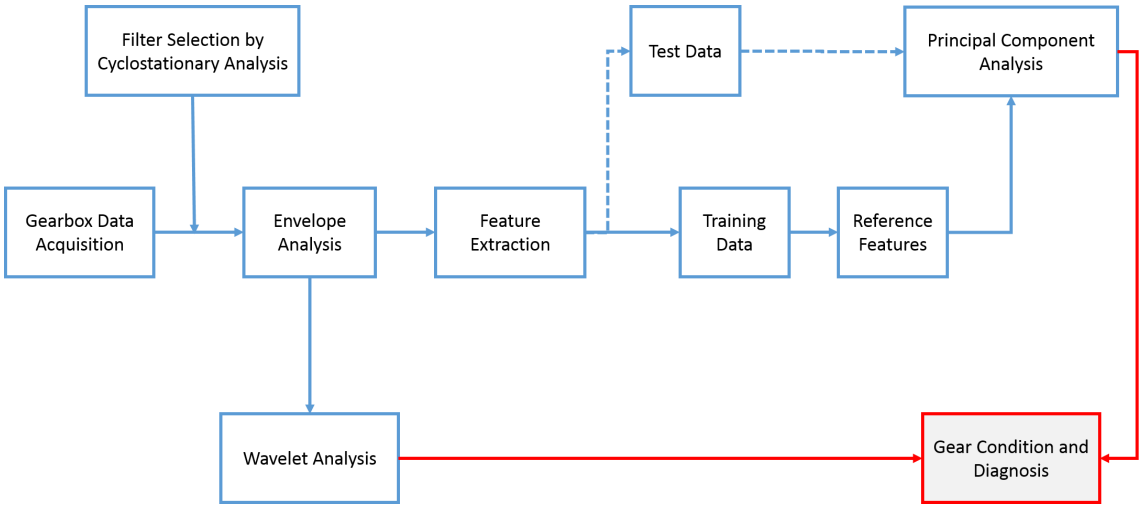

Figure 4.4: Adopted Procedure.

CHAPTER 5

Experimental Tests and Results

The results presented in this section were obtained from one test rig at the facilities where this Dissertation was developed, at Siemens SISW, a world-leading provider of product life cycle management and manufacturing operations management software, located in Leuven Belgium. All testing was conducted in a Machine Fault Simulator (MFS), shown in Figure 5.1 manufactured by SpectraQuest (SQ), a company whose main core is mechanical structures built specifically for the study of mechanical and electrical damage, in case of motors. The results are divided into two sets of measurements, one for the vibration signals from the accelerometer applied at the center of the gearbox, and another for acoustical signals obtained from the microphone located also at the center of the gearbox.

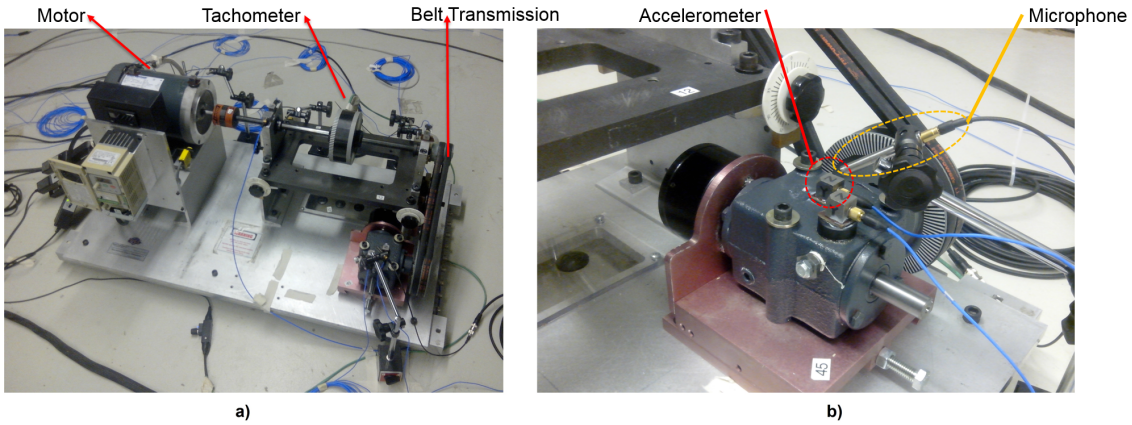

Figure 5.1: SpectraQuest's Machine Fault Simulator (MFS) test rig from Siemens

The MFS allows the simulation of machinery faults for diagnostic purposes. For gear faults, it is delivered with two gearboxes, a new one and a worn one. The worn gearbox is representative of an old gearbox that has been extensively use. Only the new one is studied here, although measurements were taken for both.

The gearboxes are 1-stage with perpendicular shafts. The two bevel gears have 27 and 18 teeth respectively. The input bevel gear, also called the pinion, is the one with the ingrained faults. Each time a pinion was exchanged, the test rig ran for eight different speeds. After the data acquisition with healthy gears, the pinion with the missing tooth was exchanged in the gearbox, and the procedure was repeated. The same took place with the pinion with the chipped tooth.

5.1 Experimental Setup

The measurements were taken with two accelerometers and one microphone above the gearbox. The complete setup diagram is shown in Figure 5.2. The motor has a driver which controls the speed of the motor output shaft. This is where the input of speed is selected. It is important to notice that the actual speed is always smaller than the selected speed, due to mechanical loads and other system errors.

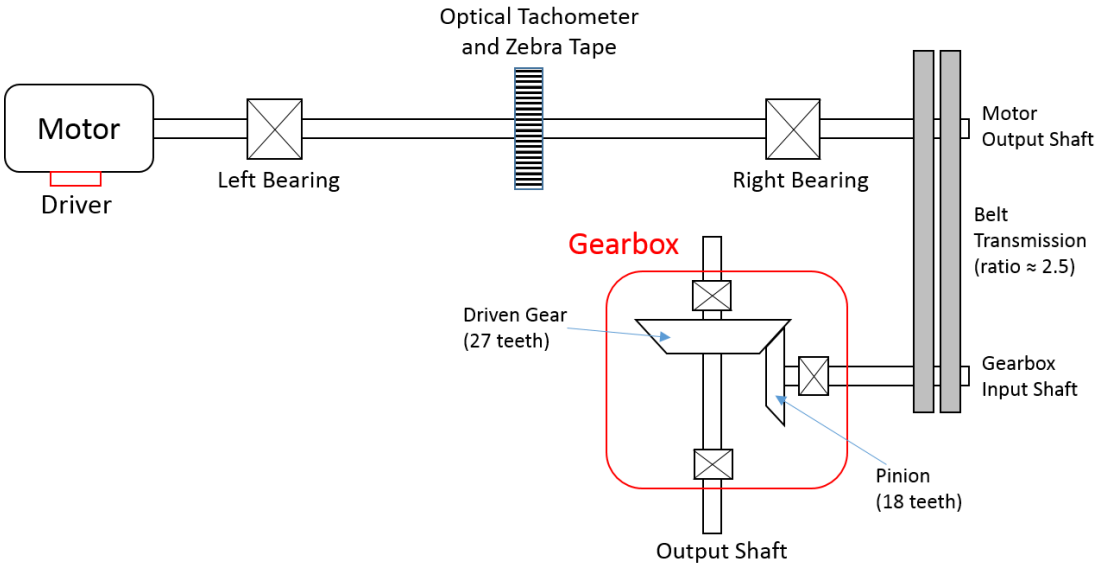

Figure 5.2: Experimental Setup Diagram.

The Gearbox faults are divided into three levels of damage imposed on the pinion : Healthy (H); Chipped Tooth (CT); Missing Tooth (MT). Figure 5.3 shows these 3 pinions, each corresponding to one level of damage.

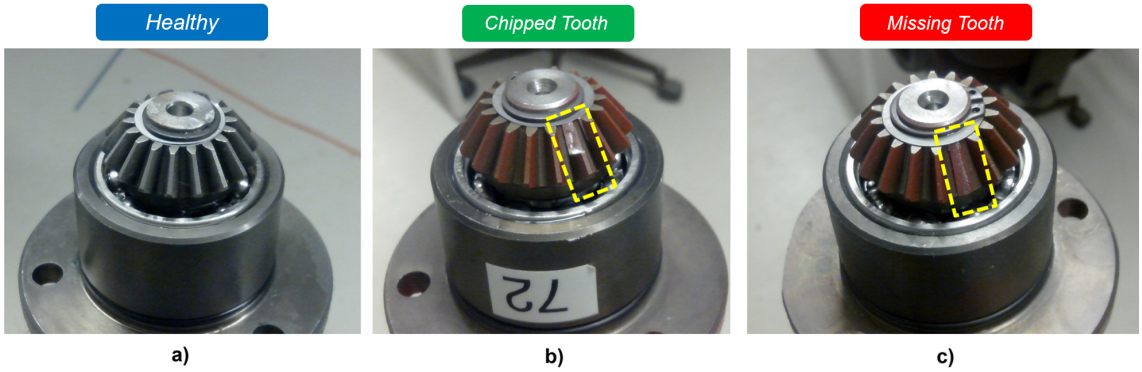

Figure 5.3: Three pinions for the experimental test: a) healthy ; b) chipped tooth ; c) missing tooth.

In order to declare a fault, usually features, or Condition Indicators (CI), are used. These are based on the frequencies of interest for gearboxes. The common frequencies for gears corresponding to the geometry of the gearbox of this paper are presented in Table 5.1

To understand the benefits of the different processing techniques, vibration signals were acquired and analyzed for different speeds in the machine fault simulator of SpectraQuest.

The analyzed speeds are enumerated in Table 5.1, along with the frequencies of interest.

Table 5.1: **Frequencies of Interest for Different Speeds**

Motor Speed	780	1020	1260	1500	1740	1980	2220	2460	RPM
Input shaft frequency (f_r)	5.2	6.8	8.4	10	11.6	13.2	14.8	16.4	Hz
Gear Mesh Frequency (GMF)	86	115	144	172	201	229	265	293	Hz
Hunting Tooth Frequency (HTF)	1.7	2.3	2.8	3.3	3.8	4.4	4.9	5.5	Hz

5.2 Gearbox Raw Vibration Signals

To have a preliminar notion of the signals, the common practice is to visualize both the spectrum of the raw signal and in the time-domain.

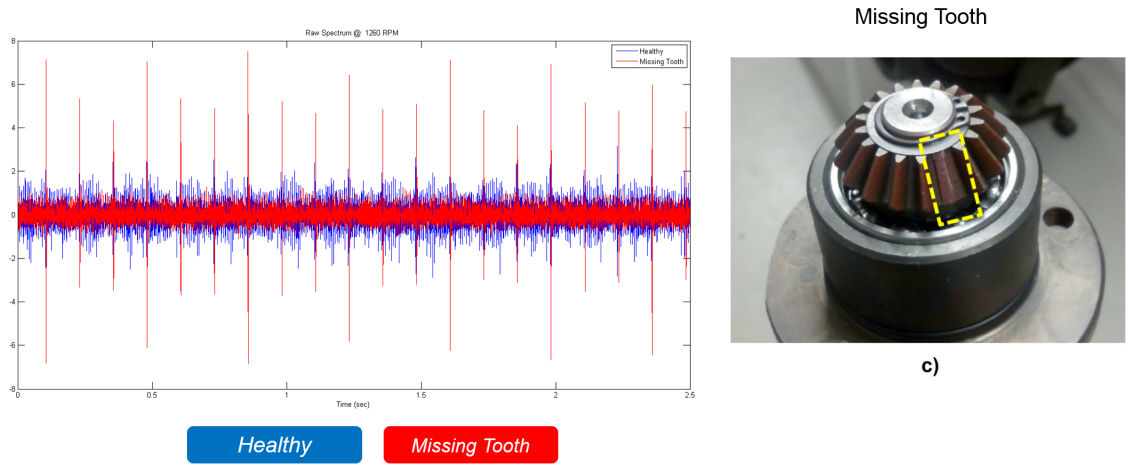

Figure 5.4: Comparison of gearbox accelerometers raw time signals of Missing tooth (red) and Healthy(blue).

A comparison between the missing tooth fault signal and the healthy gearbox signal can be seen in Figure 5.4. Here it can be seen that the missing tooth clearly generates periodic transients, correspondent to the high impulses of the missing tooth itself. The other transients due to the normal meshing of the teeth decrease a small amount in amplitude when compared to the same transients of the healthy gearbox signal.

Even though the impulse due to the missing tooth is evident in the signal, no clear evidence of the impulses due to the meshing of the gears is distinguishable in the signal. This possibly suggests some combination of faults is included in the overall system, and that the Spectral Analysis or any application of other methods to the raw signals will turn in an incorrect classification, as the GMF and its harmonics should prove to be under the noise. Some level of signal processing should be applied in order to increase the signal-to-noise ratio.

Figure 5.5 compares the chipped tooth faulty signal, in green, against the healthy gearbox signal, in blue. The raw signal shows that the amplitude of the raw signal due to the Chipped Tooth is clearly lower than the Healthy case, similar to what Figuretti [6] obtained.

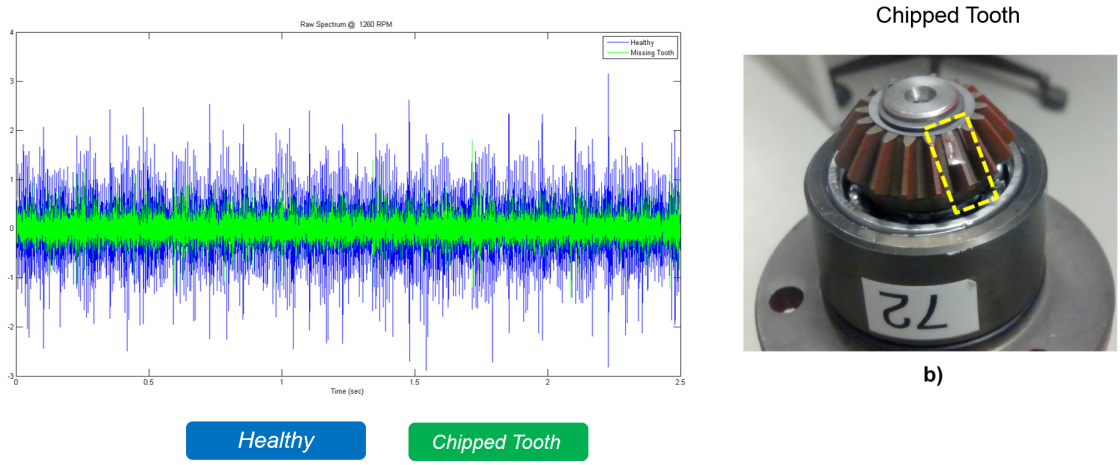

Figure 5.5: Comparison of gearbox accelerometers raw time signals of Chipped tooth (green) and Healthy(blue).

This may be explained by the extra clearance provided by the extracted volume on the chipped tooth, which causes damping in the impulses. The literature suggests that because there is still a tooth, although incomplete, the tooth still meshes correctly, and thus no clear impulses alike the ones seen in the missing tooth case are generated. On the other hand, the meshing of the gears is not so tight or constricted as the healthy case, which allows for a smoother run. Another reason can be that the mounting process of the faulty gear do not have the exact belt tension, as this one is made manually [27].

Despite this unexpected advantage of smooth meshing and lower noise levels, this type of fault inserts a fragility point that could develop into a missing tooth, and its classification and maintenance is strongly advised.

The resulting signals follow the trend described extensively in the literature, but caution is advised, as there are cases where the nature of the signals follows other patterns due to these faults . Sharma [54] showed that, at constant speed, the vibration signals increase and then decrease, as a crack propagates in one of the meshing gears. Another experiment in Ames Research Center,at NASA [55], performed a long-run test, where the pinion was confirmed to be completely damaged by the end of the experiment. Here, the TSA was performed every 30 minutes, and the results show that the amplitude of the TSA signals tended to increase over time, until a certain level of damage, and then it decreased.

This gives an explanation as to why, with a high level of expertise of condition monitoring and a lot of experience and knowledge of the monitored machinery, one condition analyst could correctly detect these two faults from the vibration signals.

5.2.1 Spectrum

The Spectral Analysis for all three cases show that the pattern seen in the time-domain is maintained throughout all of the measurements, for all the speeds.

Figure 5.6 shows the spectra for the three cases at the selected input gear rotation speed of 10 Hz (600 rpm). The second line is the zoom on the low frequency band of the spectra

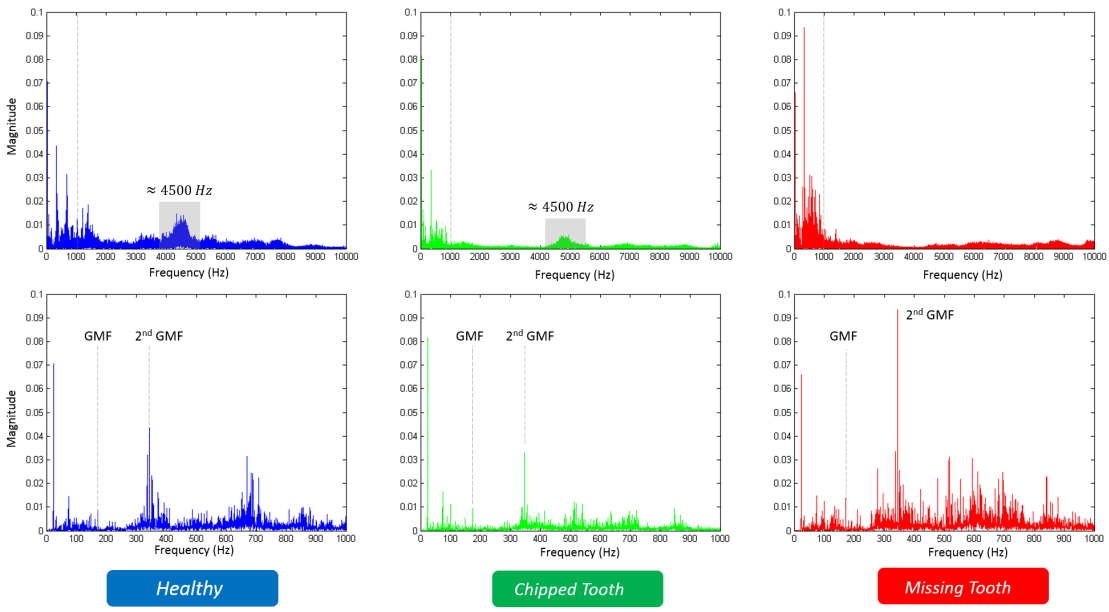

Figure 5.6: Spectra of Raw Vibration Signals for a shaft speed of 1500 RPM.

of the first line. The first column corresponds to the healthy gearbox (blue), the second column to the chipped tooth (green) and the last to the missing tooth (red) gearbox. All the measurements show the same pattern.

As was expected, the spectrum shows a high level of noise, and the GMF is not clear from the spectral analysis of the raw vibration signals. By knowing the geometry of the gearbox, the GMF and its harmonics are determined and declared on the plot. The second harmonic of the Gear Mesh Frequency (2nd GMF) can be seen to have a higher amplitude and greater sidebands than the 1st and 3rd GMF. This may suggest misalignment.

It is also noticed that the chipped tooth vibration levels are smaller when compared to the other two cases. This was to be expected, as the vibration levels in the time domain were, in fact, smaller for the chipped tooth. SpectraQuest [56] published a technical report where this phenomenon took place, in a similar test rig, and came to the conclusion that the vibration signals would decrease in the presence of a chipped tooth, and more so if the chipped tooth had a load applied to it. For the Missing tooth signal, it has been extensively seen that the vibration levels have higher amplitudes than the other two cases [48, 24].
For the selection of the filter parameters through the spectral analysis, the missing tooth spectrum does not expose a band of frequencies that may be of interest. For this case, the bandpass filter should be applied through trial and error, until the missing tooth impulses show enhancement. For the chipped tooth and healthy case, both spectra show an excitation around the 4500 Hz frequency band, that suggests filtering around these frequencies to obtain a clearer signal. This will be shown to be the correct assumption in the following sections.

5.2.2 Wavelet Analysis

The next performed analysis is in the time-frequency domain, the Wavelet Analysis. It allows one to see which frequencies are present in different time intervals. Because the

coefficients that are returned from the Wavelet Transform are described as the frequencies which have the greatest amplitudes, and adding the smearing inherent to the method, the specific frequencies that are constant may be lost. Even so, this provides a better understanding of the frequencies present, as the Fourier Transform determines an weighted coefficient of the frequencies averaged through the whole time-series.

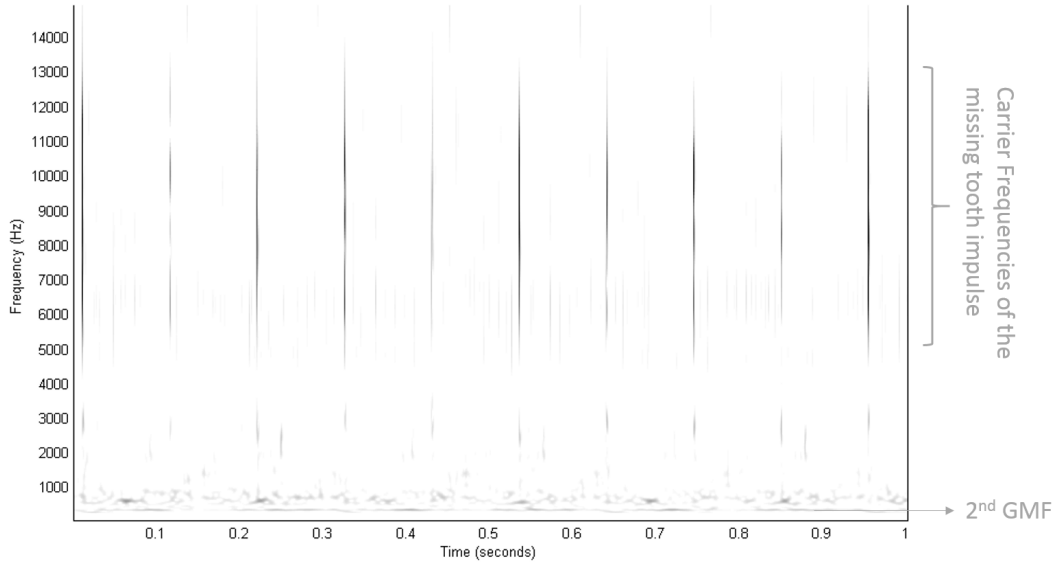

Figure 5.7: Wavelet Analysis of gearbox with Missing Tooth at input speed of 600 RPM (10 Hz).

The measurement at input shaft speed of 10 Hz is selected for a simpler understanding of the nature of signals. Figure 5.7 shows the Wavelet Analysis for the gearbox with the Missing Tooth. Here it can be seen that there are 10 equally spaced vertical lines in one second, confirming the correct 10 Hz shaft speed at the input of the gearbox. These correspond to the transient impulses of the missing tooth. The coefficients are demonstrated as a darker gradient, so the darkest section of the impulses correspond to the frequencies that carry the energy of the impulse. Because the impulses generate more impulse energy than the meshing gear and other impulses, these end up not being visible in the Wavelet Analysis. Along side this first result, the 2^{nd}GMF is also visible as the horizontal line in the bottom. Despite its lower coefficients, the 2^{nd}GMF is constant throughout the signal, and that is why it results in a peak in the frequency-domain through the Fourier Transform.

From this analysis it is assumed that the correct bandpass filter, for the enhancement of the missing tooth impulsive component of the signal, should have a center frequency of 8500 Hz, and a bandwidth of 3200 Hz. Again, from the frequency-domain analysis alone, these frequencies could not be seen, because since the transients happen in a very short time interval, the Fourier Transform nullified their contribution by averaging them through all the time interval.

Figure 5.8 shows the Wavelet Analysis for the other two cases (healthy and chipped), also at shaft frequency of 10 Hz. Both signals are similar to each other, and the chipped case has a lower amplitude level than the healthy one. The most prominent frequency band is around the 4500 Hz for both, correspondent to the meshing gear transients. The frequency-domain of these signals had already showed an excitation band in these frequencies, as seen in Figure5.6. The 2^{nd}GMF is also seen here as the horizontal line at the bottom of the

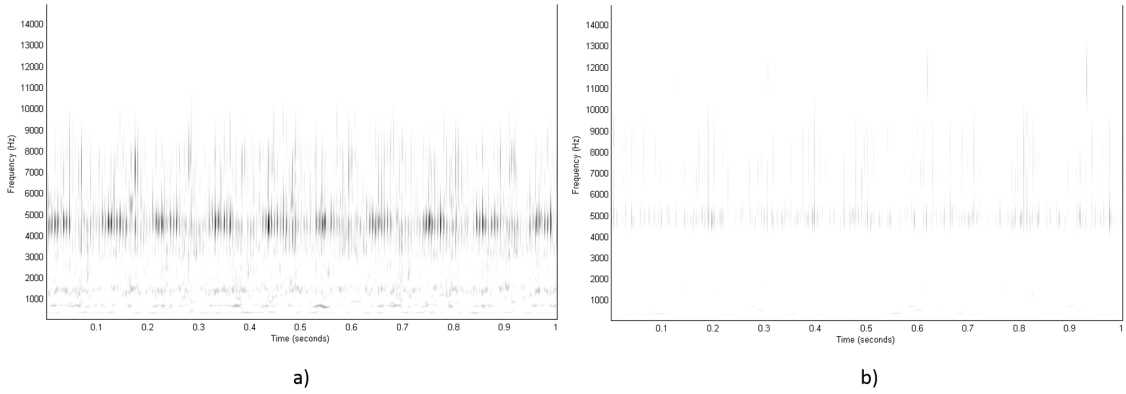

Figure 5.8: Wavelet Analysis of gearbox at input speed of 600 RPM (10 Hz) for the: a) Healthy gearbox; b)Chipped Tooth gearbox.

frequency band of the healthy case. The chipped tooth would also show the 2^{nd}GMF component if the Wavelet analysis range was smaller. However, to be able to make a proper comparison between the three different cases, the same coefficient range is selected. Again, here, the Wavelet Analysis clarifies which frequencies are present through time, and allows an explanation of the spectrum, a better understanding of the nature of the signals, and solid bandpass filter selection. The bandpass filter should be centered around 4500 Hz, and have a bandwidth of 1200 Hz for the chipped and healthy cases.

5.2.3 Cyclostationary Analysis

Cyclic Spectral Correlation (CSC) allows one to easily determine the structural mode frequencies that carry the deterministic modulation frequencies.

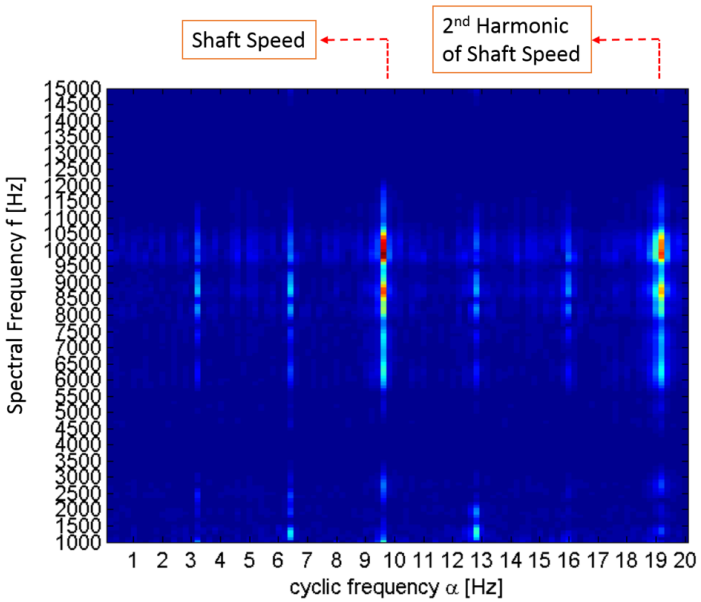

Figure 5.9: Cyclic Spectral Correlation of gearbox with Missing Tooth at input speed of 600 RPM (10 Hz).

The cyclostationary analysis shown in Figure 5.9 corresponds to the case of the gearbox

with the Missing Tooth, and the cyclostationary analysis shows similar carrier frequencies with a cyclic frequency equal to that of the shaft, for almost all the speeds. This allows the conclusion that the missing tooth impulses excite these natural frequencies, along this range.

Knowing that the input shaft speed of the gearbox is approximately 10 Hz, it can be seen that there are two peaks at the spectral frequency of 10 kHz and 9 kHz. The correct bandpass filter can be easily inferred to encompass these two carrier frequencies that are modulated by the respective shaft frequency $\alpha = 10$ Hz.

The same analysis, when applied to the other two cases (healthy and chipped), shows that both have carrier frequencies at around 4500 Hz. This information is actually provided by the Wavelet Analysis, from the previous section. They also provide with the carrier frequencies for the bandpass filter. However, the frequencies in the Wavelet Analysis were more disperse, and harder to provide with the proper parameters for the filtering, particularly for the Missing Tooth case.

This is because the Wavelet Analysis declares only the frequencies of highest amplitude levels and when they happen in the time signal. The CSC is actually a measure of how much the signal is auto-correlated at different time-lags, and returns the Spectrum of each autocorrelation at a set lag.

Filter Selection

With these different Analysis it can be concluded which filter parameters should be chosen to enhance the signals.

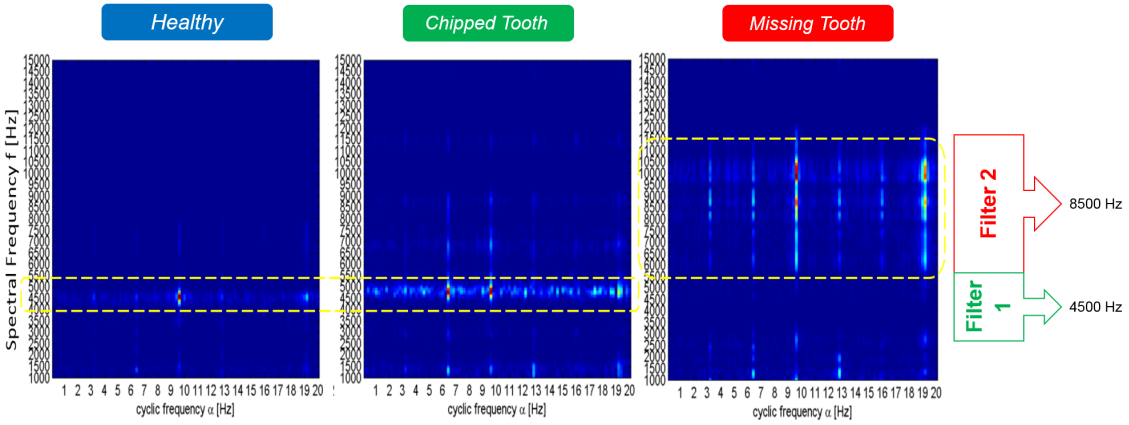

Figure 5.10: Cyclic Spectral Correlation the 3 level of damage at input speed of 600 RPM (10 Hz).

From the CSC shown in Figure 5.10 the first Filter of interest should be centered around the 4500 Hz band frequencies, with a bandwidth of 1200 Hz. This filter should capture the signal component due to the meshing gears on the chipped and healthy case, while minimizing the power of the missing tooth signal. With this Filter 1 it should be expected that the impulses of the meshing gears become cleaner, and the missing tooth signal to decrease in amplitude.

The second filter of interest should capture the frequencies that carry the missing tooth impulses, which are around 8500 Hz. It is also noticeable that the bandwidth of the frequencies should be wider than Filter 1, as it appears to have more than one carrier

Table 5.2: Filter Parameters.

Filter Selection (Hz)	Healthy and Chipped	Missing	Acoustic
Center Frequency	4500	8500	1500
Band Width	1200	3200	800
Filter #	1	2	3

frequency of interest. So to capture these frequencies of 10 kHz, 8.5 kHz and 7.5 kHz, the chosen bandwidth is 3200 Hz. Filtering the signal by this Filter 2, the opposite result of Filter 1 is expected. The missing tooth impulses should become more prominent especially when compared to the healthy and chipped cases, which become more indistinguishable now after this Filtering.

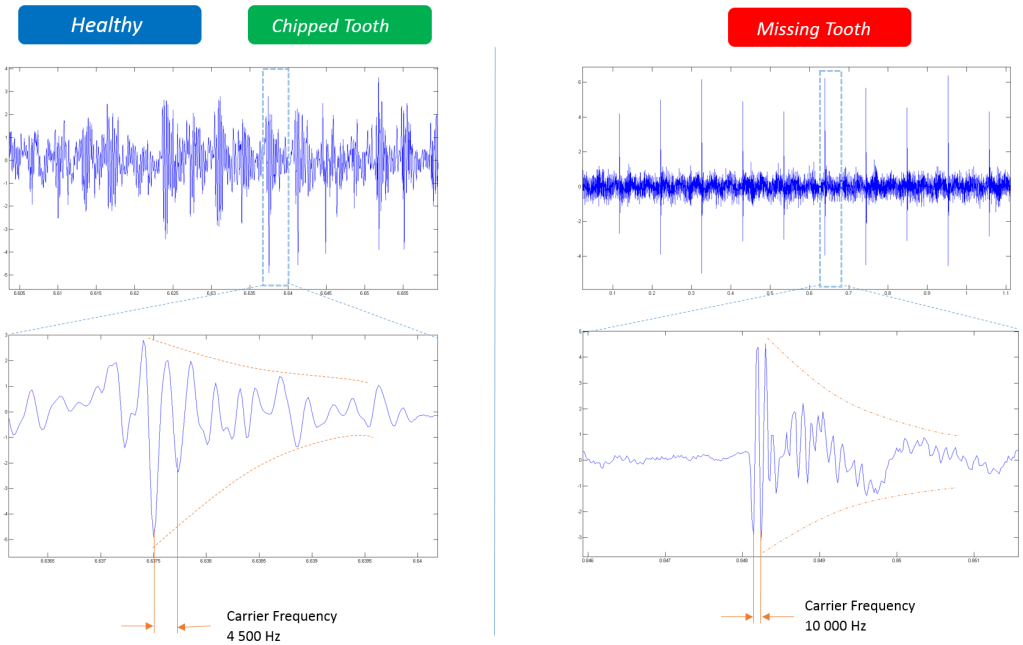

Figure 5.11: Cyclic Spectral Correlation the 3 level of damage at input speed of 600 RPM (10 Hz).

This filter selection can be further justified by looking at the time signal, shown in Figure 5.11. When searching the signals for the transient impulses, it can be seen that the period between two peaks of the carrier wave of the impulse corresponds to ≈ 4500 Hz for both the chipped and healthy case, and ≈ 10000 Hz for the missing tooth case. There are other frequencies that carry the impulses, but these either not as prominent as the ones declared, or are hard to isolate.

The analysis provided until now suggests the selected Filters exposed in Table 5.2. In Section 5.3 the results provided for Filter 1, for all three cases (healthy, chipped and missing tooth) are discussed, and in Section 5.4 for Filter 2 performed also on all three cases.

5.2.4 Hunting Tooth Diagnosis

The Cyclostationary Analysis suggested that another level of modulation is present, as there is a pattern with lower amplitudes at $\frac{1}{2}$ and $\frac{2}{3}$ of the indicated shaft rotation speed.

This demonstrated another advantage of the CSC; the clear insurgence of frequencies with lower amplitudes at $\frac{1}{3}$ and $\frac{2}{3}$ of the indicated shaft rotation speed, reveals a possible misalignment or a Hunting Tooth related problem.

Misalignment is quickly disproved, as frequencies usually result in harmonics half of the shaft rotation speed. After confirming the number of teeth in the pinion to be 18 and the teeth in the driven gear to be 27, the Hunting Tooth Frequency (HTF) presence was tested, resorting to Equation 5.2.1

$$HTF = \frac{N_a T_{pinion}}{T_{gear} T_{pinion}} f_r \tag{5.2.1}$$

Let $N_a = 9$ be the greatest common factor between the meshing gears, and T_{gear}, T_{pinion} be the number of teeth of the meshing gear and the pinion, respectively. Expression 5.2.1 determines the HTF. The frequencies correspondent to the HTF at all studied speeds have been already provided in Table 5.1, and are present in all the measurements with no exception. This proved that the Hunting Tooth Frequency is present.

5.3 Vibration Signal Filtered at 4500 Hz

All three cases had the same filter applied to them in order to compare them under the same conditions. The results were then analyzed, under this process for 2 main reasons:

1. For a solid differentiation between signals, they must be compared maintaing the same proprieties, or in other words, with the same filtering or any other signal process that may need to be applied
2. For the assumption that is not always possible to select different frequency bands, since one at least is always determined and applied to all the signals....

In this first section Filter 1 was applied to all signals and the results are discussed.

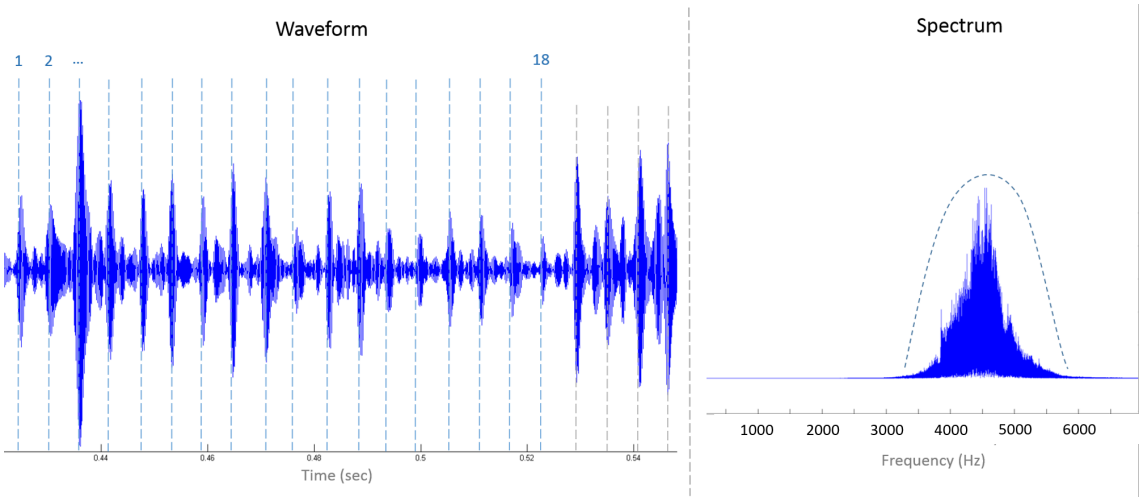

Figure 5.12: Waveform and Spectrum for the filtered healthy signal around 4500 band of frequencies (Filter 1)without signal demodulation

The time-domain and the frequency-domain signal from the Healthy gearbox at shaft rotation of 10 Hz is represented in Figure 5.12, after the filtering.

The time-signal is confirmed to be clearer, as the impulses of the meshing gears are enhanced. There are 18 prominent impulses in each period of 0.1 seconds, pertaining thus one revolution of the pinion with 18 teeth at a frequency of $1/0.1 = 10Hz$. This selection proves that the carrier frequencies of the impulses were indeed around the 4500 Hz band. On the other hand, the spectrum only has information on the frequencies of the bandpass, as shown in Figure 5.12. This is undesirable, as the frequencies of interest all lie on the low band of frequencies.

Demodulation of the signal by the Hilbert Envelope or the Squared Envelope is necessary, as no more information can be extracted with no demodulation to the signal. This provides the basis as to why the Envelope is necessary, and why all the filtered signals in the literature were demodulated.

As such, all the signals shown will be filtered at the selected bandpass Filter, and then demodulated by the the Hilbert Transform. This signal processing method is the so called Envelope Analysis method that was explained in Chapter 3.

Time Signal

As previously done, the time-domain signals are studied. The resulting signal obtained after filtering and demodulation is called the Envelope. Figure 5.13 shows the Envelope for the Healthy case at $f_r = 10Hz$.

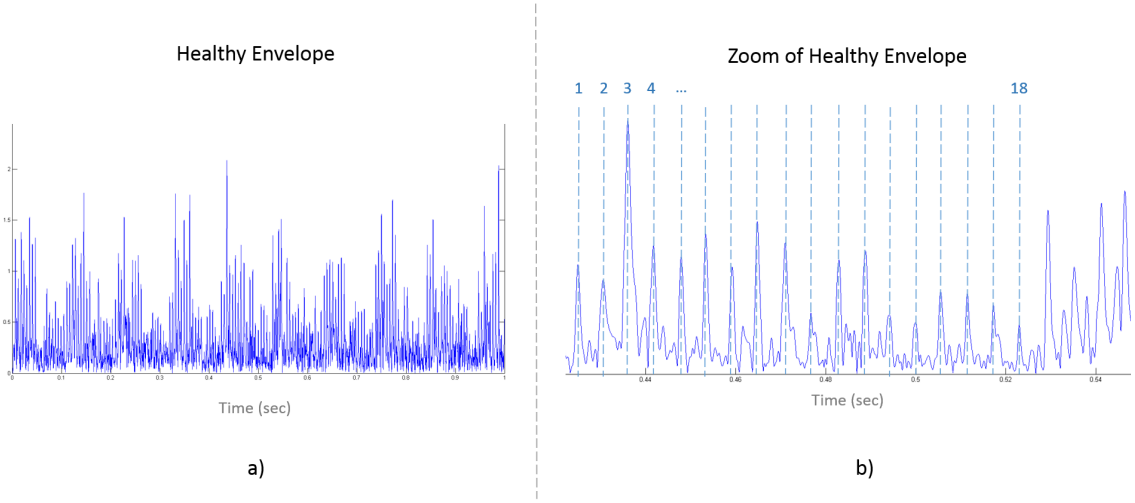

Figure 5.13: Envelope Signal of Healthy filtered around 4500 band of frequencies (Filter 1) with demodulation: a) One second sample; b) one rotation sample, equivalent to 18 impulses.

The Envelope became positive, as it is a derivation of the process, and the impulse signals were enhanced and the carrier signals minimized. Each individual impulse in each tooth of the pinion can be seen from the applied zoom.

The same happens with the Chipped and Missing tooth Envelope, whose signals can be seen in Figure 5.14. At the same time, the overall amplitude of the missing tooth Envelope is smaller than the chipped Envelope, which in turn is smaller than the healthy Envelope. This seems a good start for classification of the faults, as a feature based on the amplitude of the signals may be able to provide the faults diagnosis.

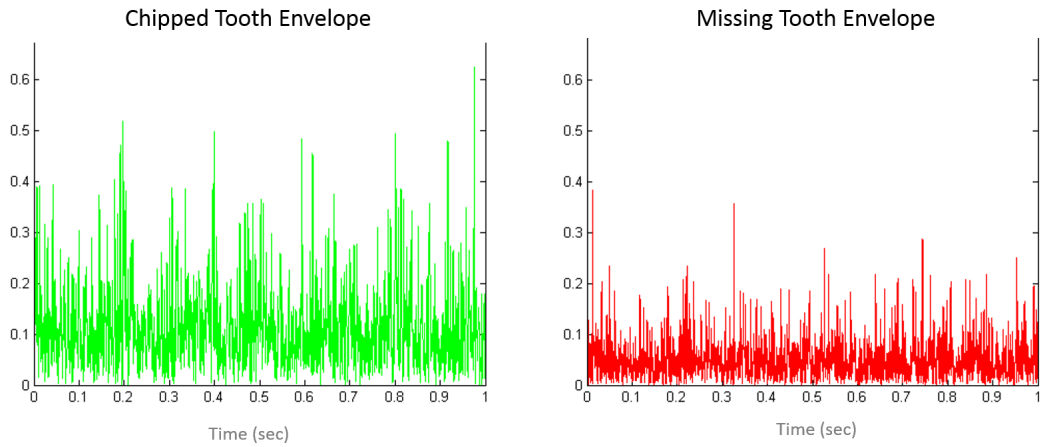

Figure 5.14: Envelope Signal of Chipped and Missing Tooth filtered around 4500 Hz band of frequencies (Filter 1) with demodulation.

The missing tooth Envelope is more random when compared to its raw signal. This was predicted, as it was seen before that most of the impulsive energy of the signal comes from the missing tooth impulses, and these are filtered out by Filter 1.

Spectral Analysis

The Spectral Analysis on the Envelopes proves to be much cleaner than the raw signals spectrum. Figure 5.15 shows the result for the healthy case. The most prominent peaks are the gearbox deterministic frequencies of interest, the shaft rotation speed, the GMF, its correspondent harmonic and sidebands.

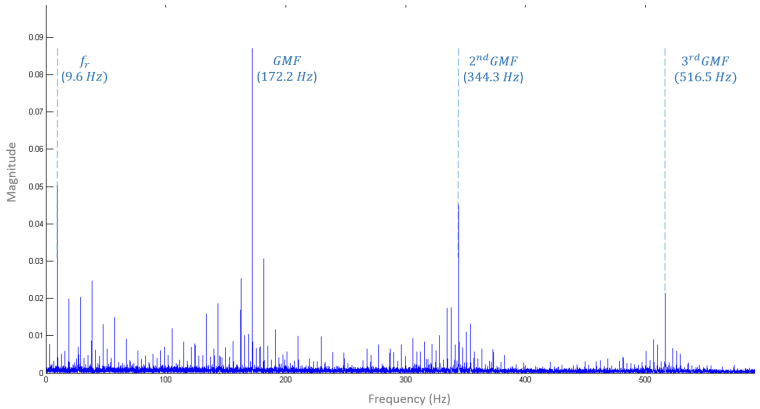

Figure 5.15: Envelope Spectrum of Healthy filtered around 4500 band of frequencies (Filter 1) with demodulation.

This holds true also for the chipped tooth gearbox spectrum, that is shown in Figure 5.16, and as predicted, the peaks are smaller than those of the healthy case. In fact, they are small enough that, in case the two were to plotted one against the other, the Chipped Spectrum would be too small to be recognized. In order to achieve a proper comparison, the spectra were separated in different figures with different scaling.

The same happens with the Missing Tooth spectrum, where the peak values are too small

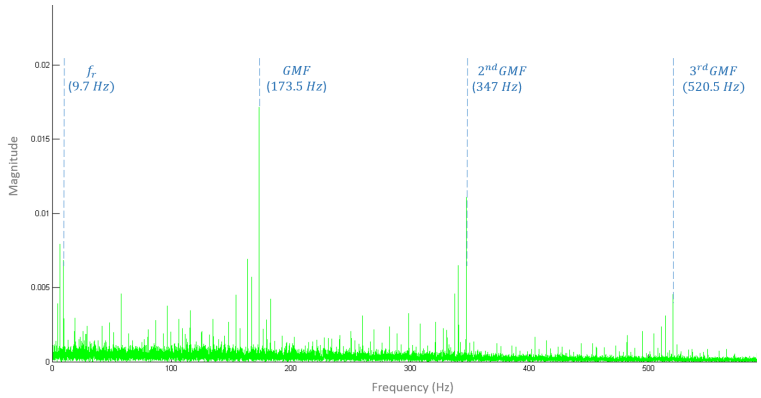

Figure 5.16: Envelope Spectrum of Chipped Tooth filtered around 4500 band of frequencies (Filter 1) with demodulation.

to compare with the other two. It is noticeable that the Magnitude in Figure 5.17, for the Missing Tooth spectrum, is multiplied by 10^{-3}. The spectrum also appears to be more random than the other, as expected, with a noticeable peak at the 2^{nd} GMF.

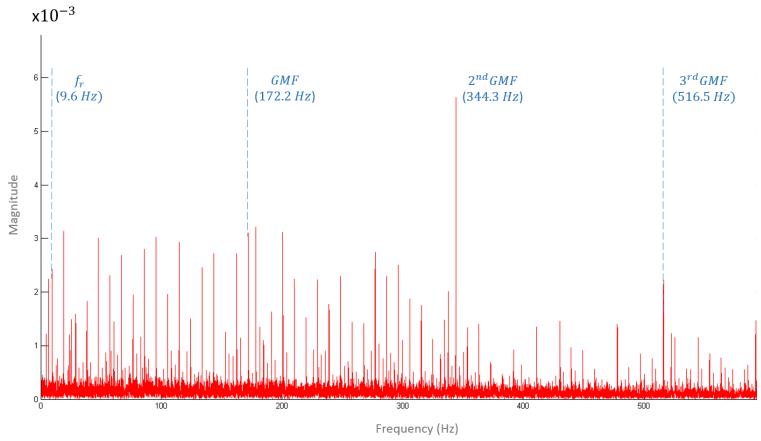

Figure 5.17: Envelope Spectrum of Missing Tooth filtered around 4500 band of frequencies (Filter 1) with demodulation.

The peak values for the different frequencies of interest appears to hold classification criteria, and those values, for the shaft rotation speed of 10 Hz, are shown in Table 5.3.

Wavelet Analysis

The Envelope's nature is easier to understand with the Wavelet Analysis. It provides the same information as both the time-domain analysis and the Spectral Analysis, as it allows the visualization of the Spectrum as a function of time.

The time-frequency domain for the healthy case is shown in Figure 5.18. The GMF and 2^{nd} GMF component are clear, and the meshing gear impulses appear as horizontal lines modulated by the shaft rotational speed. In fact, each area of higher value in time (can also be seen as the points are darker) corresponds each to one rotation, pertaining 10 in one second, as seen in the figure. This is interpreted also as the area where the applied

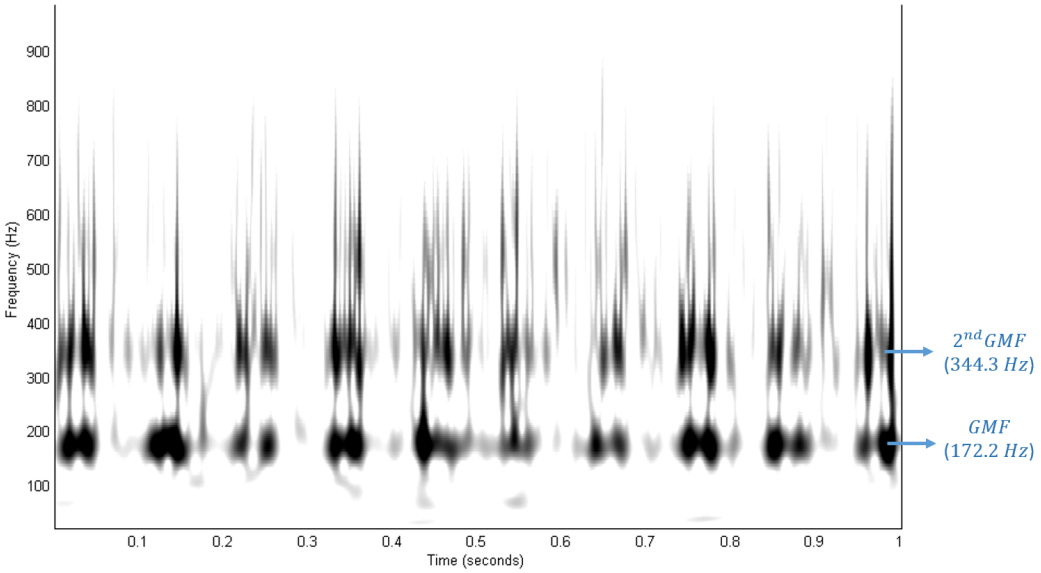

Figure 5.18: Wavelet Analysis of Envelope of Healthy filtered around 4500 band of frequencies (Filter 1) with demodulation.

Table 5.3: Magnitude of Frequencies of Interest for the three cases.

Magnitude (x10^{-3})	Healthy	Chipped	Missing
Shaft Rotation (9.7 Hz)	50	6.8	2.4
GMF (172.5 Hz)	87	17.6	3.1
2nd GMF (345 Hz)	45	11	5.6

impulses are greater, on each rotation. Following the reasoning of misalignment from the 2^{nd}GMF peak already seen in spectrum of the raw signal of Figure 5.6, it is then reaffirmed that the input shaft of the gear is indeed misaligned. In case of no misalignment, the literature suggests that the shaft modulation would not be so prominent.

The chipped case results in a similar output as the healthy case, with the only difference being the overall lower values.

For the missing tooth case, the wavelet appears chaotic and somewhat random, with 2^{nd}GMF being barely noticeable. This expected Wavelet Analysis is shown in Figure 5.19.

Time Synchronous Averaging

The TSA is only the averaged portion of the original signal, so it has to be repeated as many times as needed to form the entire synchronous signal. Its length will be a multiple of T_m. Hence, the original signal has to be truncated in order to adapt its length before any operations. The original signal must start at $t = t_0$ and end at $t = NT_m$ to ensure the synchronization with the calculated synchronous part $s(t)$. The non-synchronous part $r(t)$ is then obtained by subtracting the synchronous part from the initial signal. So far, it was supposed that the instantaneous rotational speed is strictly constant. It means that the mechanism period chosen is well defined and constant in the time domain. As a matter of

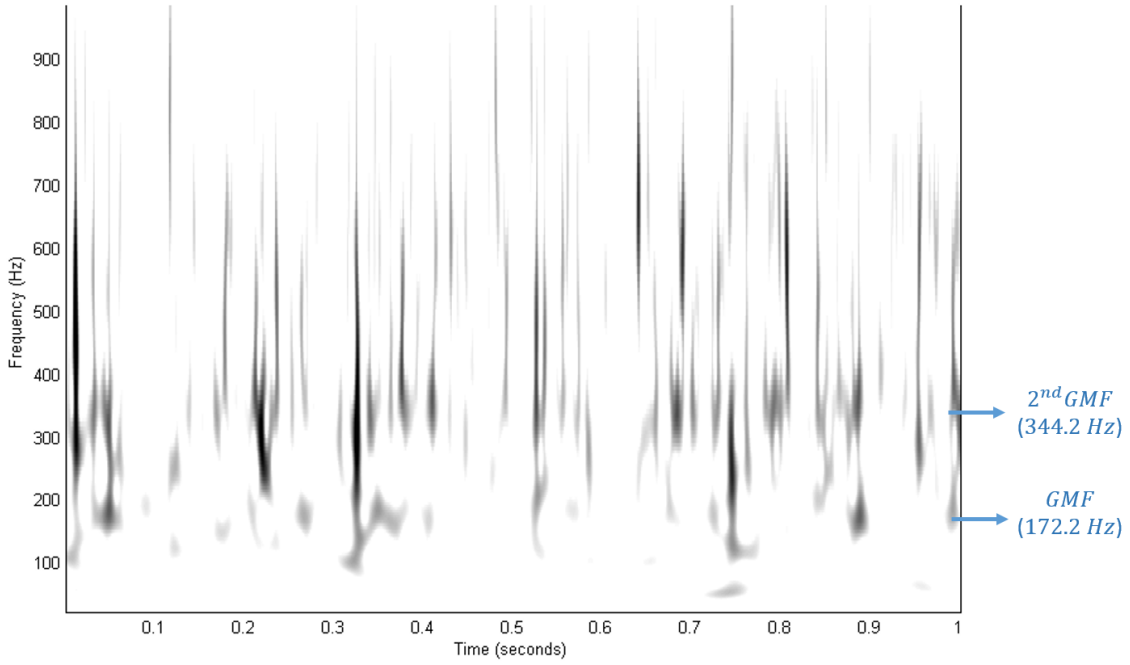

Figure 5.19: Wavelet Analysis of Envelope of Missing Tooth filtered around 4500 band of frequencies (Filter 1) with demodulation.

fact, the rotational speed is rarely constant because of mechanism uncertainties such as the clearances, unbalances or the geometries' imperfections. In such cases, time synchronous average will lead to an erroneous estimation of the synchronous signal since the portions to be averaged should not have the same length [57].

An algorithm was implemented to correct the length of the truncated signals, in order to approximate the truncated length to one revolution period as much as possible. This is applied because the tachometer speed that is used to define the shaft frequency of the gearbox does not measure this shaft, but rather the output shaft of the motor.

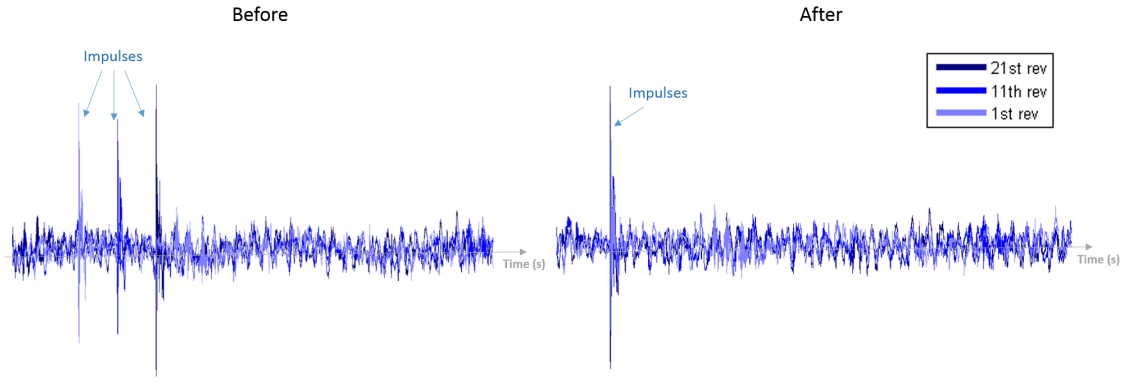

Figure 5.20: Impulse deviation phenomenon and correction for TSA, applied to the missing tooth.

As there is one belt transmission between the motor shaft and the gearbox shaft, this was assumed as the component that causes the most speed fluctuation. Figure 5.20 shows the Envelope of the missing tooth, before and after the correction, for the time-domain signals

of the 1^{st}, 11^{th} and 21^{st} revolutions. When the signal is divided based on the approximated shaft speed, the signal truncation is shown to select the incorrect length of the signal for one revolution. As a result, the signal before the correction shows the impulse deviation in the revolution count.

By maximizing the correlation between each revolution "truncated" signal, the correct length for one revolution is determined, and the signal is now truncated correctly for the averaging. As an example, Figure 5.20 shows the missing tooth impulses are all synchronized.

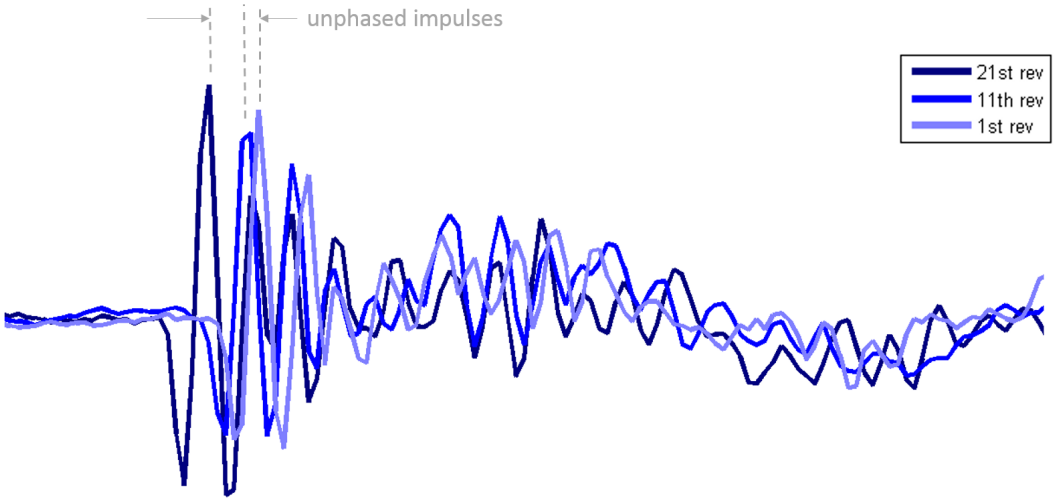

Figure 5.21: Unphased impulse after TSA correction.

Even after this correction, though the signals are synchronous with one another, the signals are not phase-locked with one another. This is proven to happen in all TSA processes, as there are always speed fluctuations, errors and other phenomena that cannot be controlled and predicted. However, the certainty that the signal is phase-locked and with the correct tachometer speed on the shaft, these effects should be minimized. From this method however, it is concluded that the algorithm alters the signal to a length that does not derive from the speed, but from the autocorrelation process, and as a final result the impulses in Figure 5.21 are not phase-locked with each another. Thus resulting in a noisier signal than the one with no TSA applied to it, as represented in Figure 5.22. The TSA results also in smaller amplitudes, due to the averaging out of positive and negative unphased values.

It is concluded that the TSA introduces undesirable noise to the signal, in this case because the tachometer was mounted on an inappropriate location, near the motor shaft, and not the gearbox shaft. Its application is strongly suggested, as it provides good results, if only a correct speed measurement of the gearbox is obtained. This complies with the literature, where the TSA is only applied with good results when there is a correct tachometer mounted on it. There is some literature where the application of TSA was applied based on the GMF, with no tachometer signal, but with no clear results.

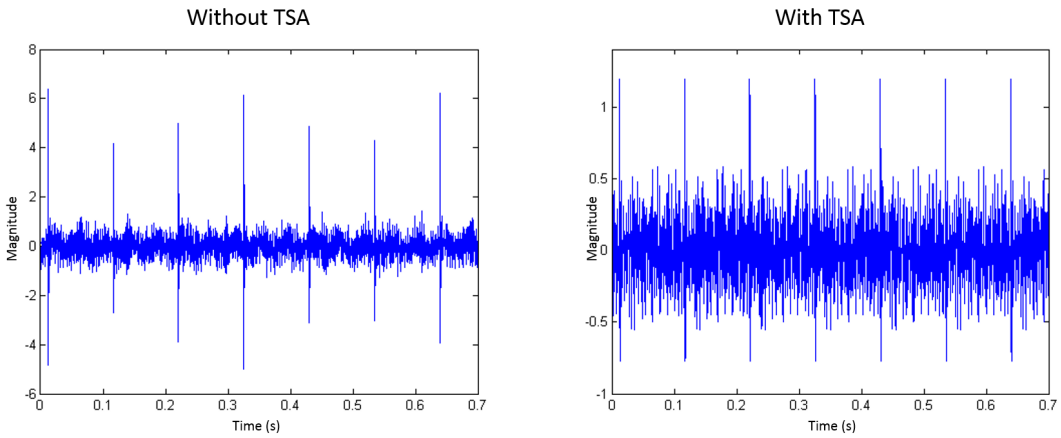

Figure 5.22: Comparison between the missing tooth signal with no TSA, and with TSA.

5.4 Vibration Signal Filtered at 8500 Hz

Filter 2 was developed for the diagnosis of the missing tooth fault. According to the theory, it should not allow the diagnosis of chipped tooth fault against the healthy gearbox, but should be able to better detect the missing tooth than Filter 1.

Time Signal

The Envelope Analysis using Filter 2 provides a great separation of the missing tooth from the other two cases. Figure 5.23 shows the time-domain signals of the three cases, all at the same scale. The first thing noticeable is how much the missing tooth envelope is completely different from the others.

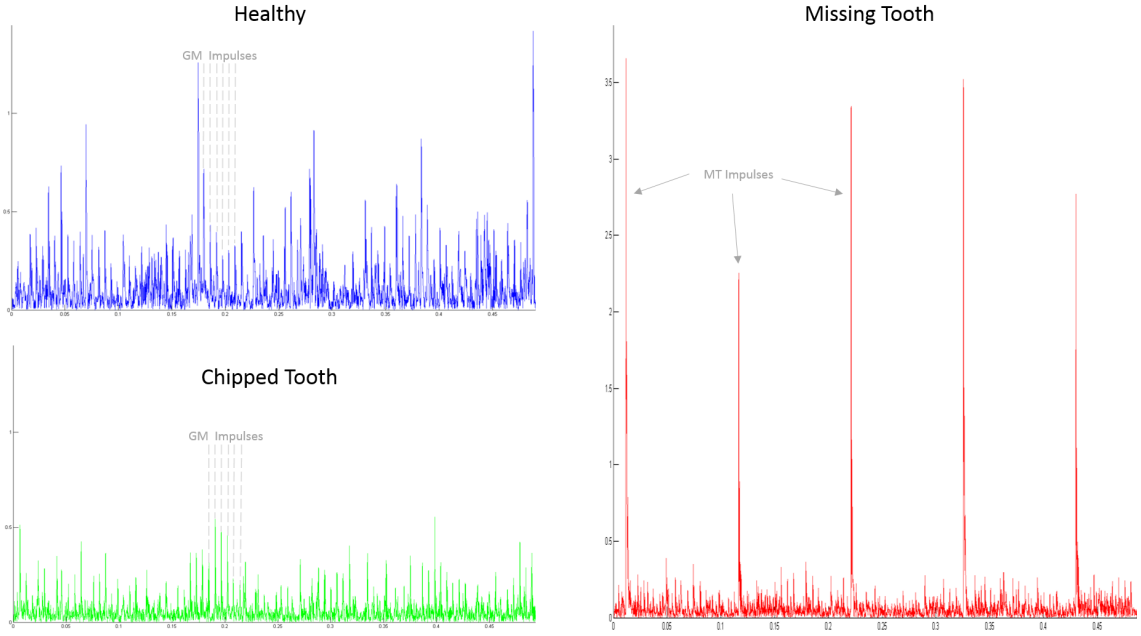

Figure 5.23: Envelope Signal of Healthy, Chipped and Missing Tooth signals filtered around 8500 band of frequencies (Filter 2) with demodulation.

Reaffirming the filter selection, it can be said that the carrier frequency that transports

the missing tooth impulses alone, this filter maximizes these impulses, and minimizes all other frequencies.

Once more, it can be seen that the chipped tooth envelope is similar to the healthy one, with lower amplitudes. These two cases appear with such low amplitudes, because the meshing gear impulses (GM Impulses) are filtered out.

The filter appears good enough to detect the missing tooth fault just from the time domain signal of the envelope, with a simple threshold.

Spectral Analysis

The Spectral Analysis returns a curious conclusion. As expected, the Chipped Tooth and Healthy Envelope are similar, with both showing peaks at GMF and 2^{nd}GMF.

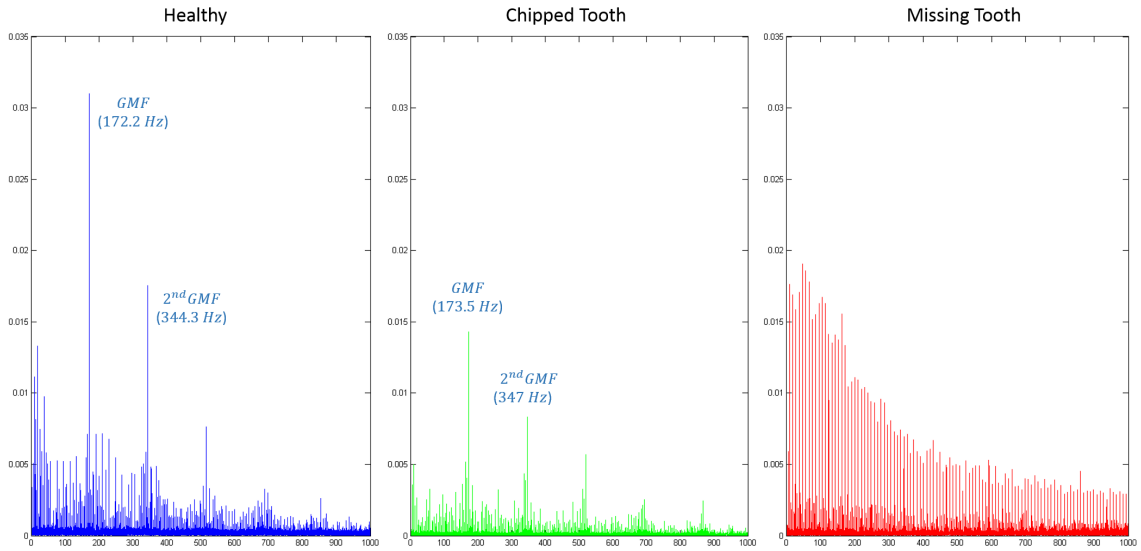

Figure 5.24: Envelope Spectrum of Healthy, Chipped and Missing tooth filtered around the 8500 band of frequencies (Filter 2) with demodulation.

The interesting part is the missing tooth envelope spectrum. It appears that its energy is distributed throughout the frequency range, decreasing exponentially, and appearing even smaller than the healthy envelope spectrum.

The result is a spectrum with the largest peak at the shaft rotation frequency, and its harmonics. Upon closer analysis, it can be seen this result is a combination of effects due to the high amplitudes of the missing tooth impulses for each revolution and of the meshing gear impulses 18 times per revolution, where the GMF is indeed present, but is not a phenomenon of the signal, but rather 18^{th} harmonic of the shaft speed.

From Figure 5.25 it is seen that every peak that appeared on the Spectrum of the Missing Tooth are all harmonics of the shaft rotation frequency, f_r. The GMF in this case is just the shaft rotation frequency multiplied by one. This allows leakage of f_r into the other harmonics.
Apart from the f_r, its harmonics, and its sidebands, which are the hunting tooth frequency (HTF), the spectrum is properly clean in all other frequencies.

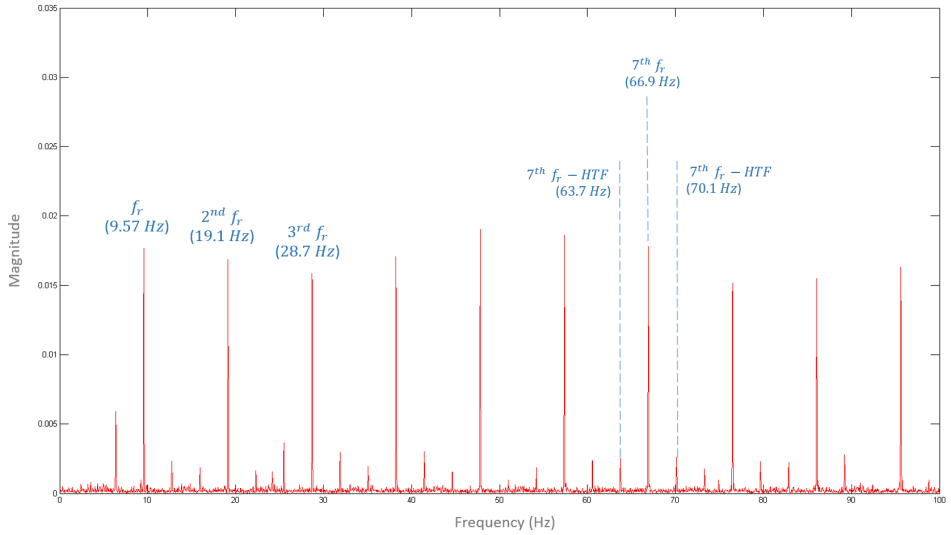

Figure 5.25: Zoom around the shaft rotation frequency of the Missing Tooth Envelope Spectrum for Filter 2.

Angular Resampling

The Chipped and the Healthy case show no relevant transformation from the time-frequency domain signals of Filter 1, showed in the last section, except for the lower values.

The one that shows a different signal is the missing tooth case. The impulsive transients of each rotation are dramatically visible, with decreasing along the spectral frequency axis. These vertical lines, which correspond to the impulses, appear continuous, but are known to be discrete by the study of the Spectral Analysis.

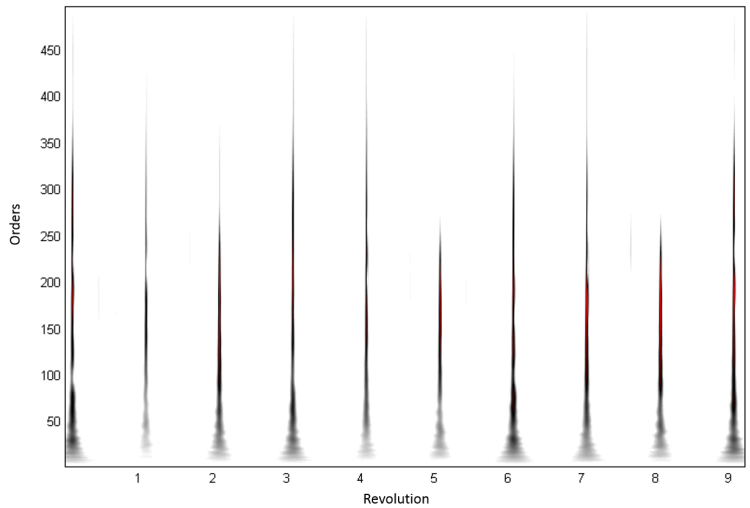

Figure 5.26: Order Tracked Envelope of Missing Tooth.

Applying the Angular Resampling on the signals for this filter allows the visualization of the signal at each different gear revolution. As the signal are represented in the angular domain, the x-axis represents the degrees (or radians), and the y-axis the order, or in other

words, the multiples of the shaft frequency.

In similar manner 2π is equal to 360^o, it is also equal to 1 revolution of the shaft. By this method, the signal can be order tracked and the location of each impulse can be determined.

Figure 5.26 shows the Wavelet Analysis in the angular domain of the missing tooth for 9 revolutions of the shaft. Each missing tooth impulse can be clearly detected, occuring at the same angle position, where the tooth is physically missing on the pinion.

If a reference on the shaft is applied, and ordered signals are plotted on top of the pinion profile, this notion becomes clearer.

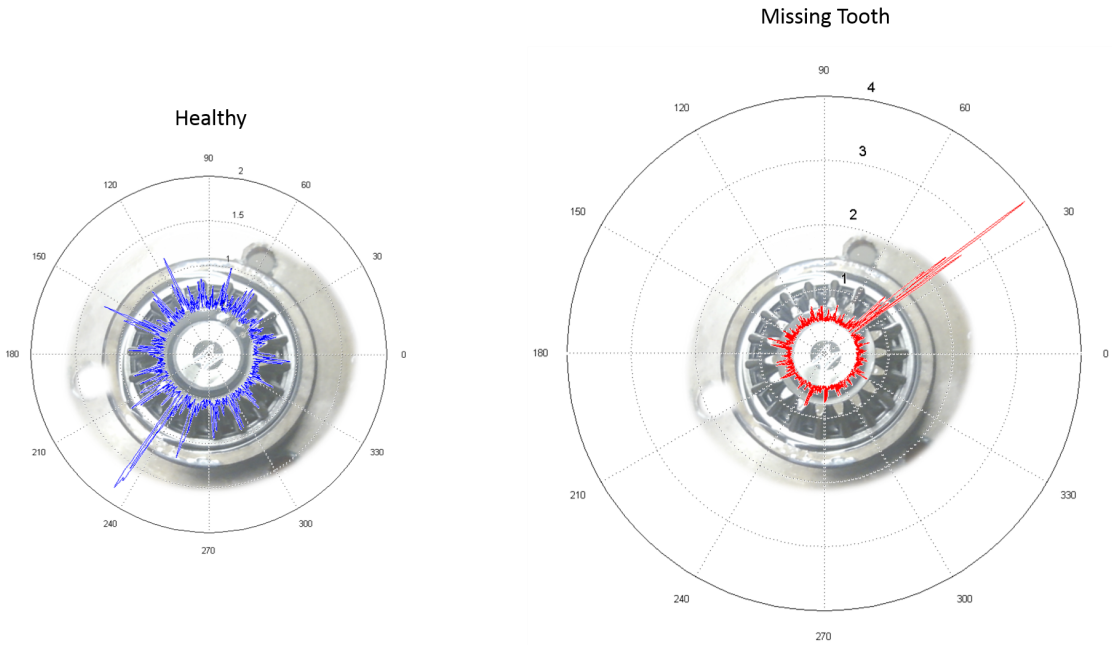

Figure 5.27: Order Tracked of the healthy pinion and missing tooth pinion.

Figure 5.27 shows the signal for two revolutions of the pinion shaft, for the missing tooth. Here it is seen that the impulses of the meshing gears on the healthy gearbox are coincident. The idea here is that by thresholding and analyzing this polar coordinate plot, when a missing tooth appears, the corresponding tooth translates to a prominent peak, as also seen in the figure.

Having this into account, the analysis can be extended to the other components. For example, in case a missing tooth is generated in the driven gear, as opposed to the pinion, the respective impulse should occur at a different order period.

This diagnosis is simulated as shown in Figure 5.28, where the pinion impulse occurs in each revolution, and two missing tooth impulses on driven gear would translate to three shaft revolutions, transcribing a period equal to gear ratio of $27/18 = 1.5$.

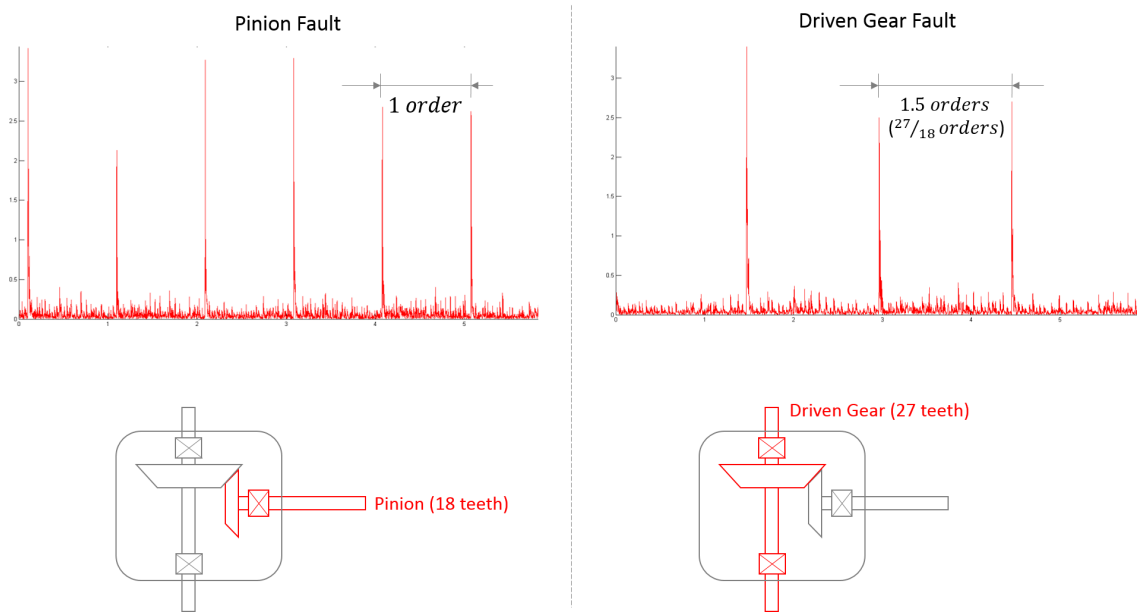

Figure 5.28: Order tracked of faulty pinion (left) and of faulty driven gear (right), with different periods.

5.5 Gearbox Raw Acoustic Signal

The same procedure is applied to the microphone acoustical signals, as they are expected to work in a similar way.

The CSC is applied, and the band of frequencies that carry the signal obtained. As the previously shown cases, this also obtained a constant band of excited frequencies around the 1500 Hz range. Thus the Acoustical Filter is selected with a center frequency of 1500 Hz and a bandwidth of 800 Hz. This small bandwidth is justified as a way to avoid filtering around the low range of frequencies, as it could contain undesirable modulation waves.

Unlike the vibration signals, the impulses and characteristics carrier frequencies are not clear of the raw acoustical signals, even though the components can be clearly heard, at the small speed at least. The correct filter should be selected for the removal of the unwanted noise due to the other components.

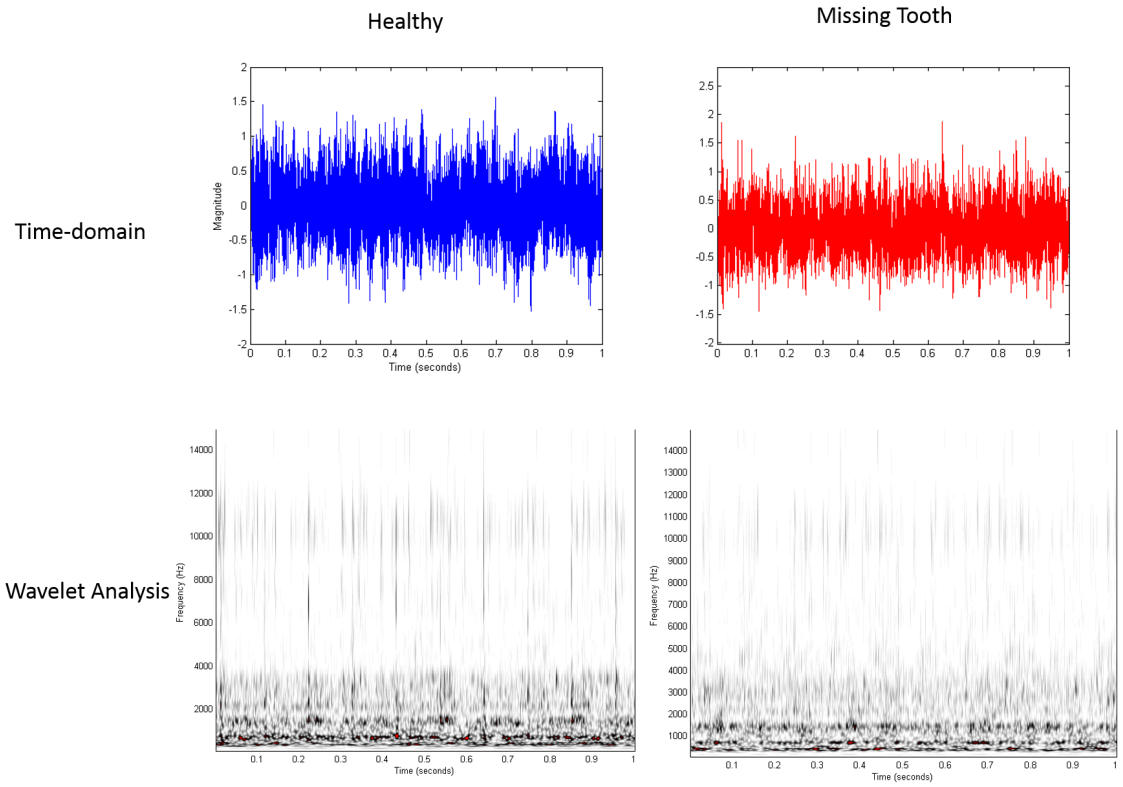

Figure 5.29: Raw Acoustic Signals of the Healthy gearbox (left) and Missing tooth case (right).

5.6 Acoustic Signal Filtered at 1500 Hz

By the CSC, it is seen that the maximum auto-correlation values happen around the 1500 Hz band. So, for the automated method, the band selection for the filter is centered around 1500 Hz, with a bandwidth of 800 Hz.

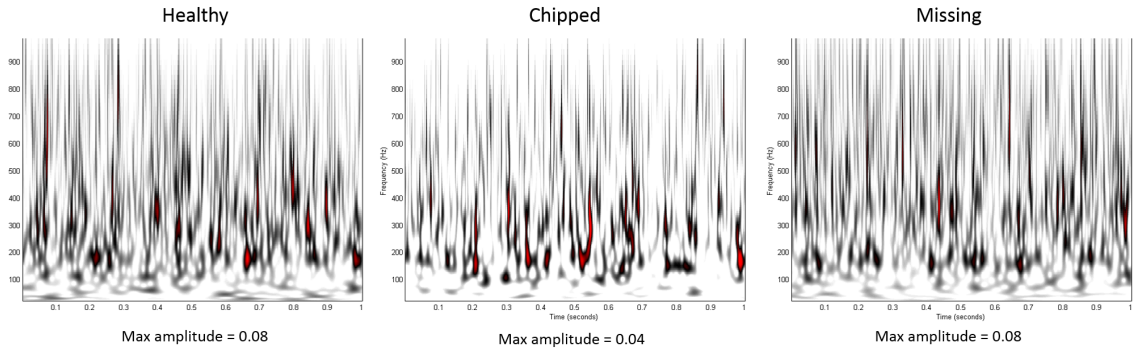

Figure 5.30: Wavelet Analysis of the Acoustical filtered signal around 1500 Hz band.

Figure 5.30 shows the Wavelet Analysis. All the signals show a similar behavior for the three cases. There is a maximum at the GMF for all spectra, with the maximum value being the only difference. The maximum for both the healthy and missing tooth case are equivalent, but the chipped is half the value of those two.

As the filter does not capture the missing tooth carrier frequencies, with the meshing gears frequencies being the only frequencies of interest captured by the filter. This is why the

chipped behaves different from the others, with the lower amplitudes, as it was the case with the vibration signals.

5.7 Acoustic Signal Filtered at 8500 Hz

Filtering the missing tooth carrier frequencies are tried next. Even though the maximum value of CSC occurs only at 1500 Hz, for the three cases, it is seen that there is in fact an autocorrelation factor at around the 8500 Hz band of frequencies for the time-lag correspondent to the shaft frequency, for the missing tooth alone, although small. A possible cause for this may be due to the nature of acoustic signals, where the lower-frequency content of the signals have better penetration, and the higher band of the spectrum have lower propagation, and thus the high frequency content may be submerged by the low frequency components[58].

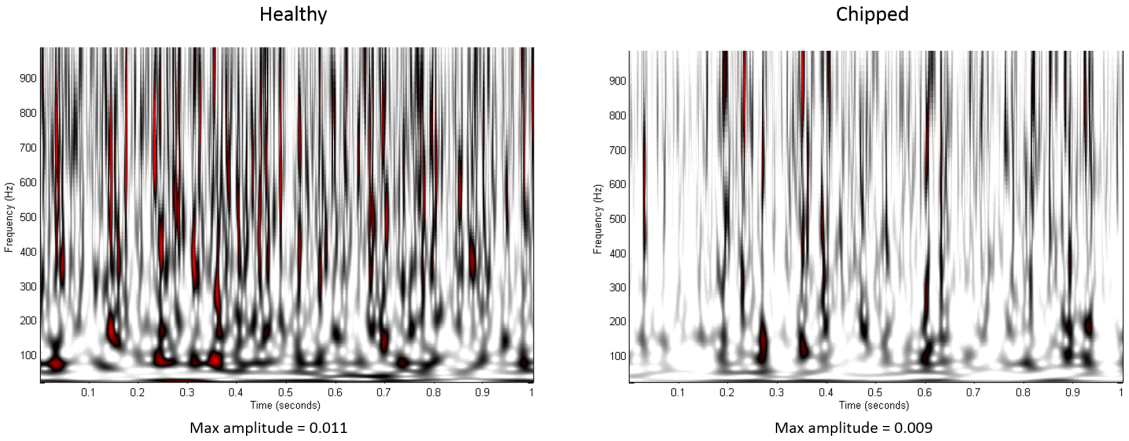

Figure 5.31: Wavelet Analysis of the Acoustical filtered signal around 8500 Hz band, for healthy and chipped case.

With this filter, the healthy and chipped case show approximately the same behavior, and same level of amplitudes. Figure 5.31 shows that the Wavelet Analysis returns mainly the gear meshing components of the structure. Comparing with the raw, the filtered values are extremely attenuated. This agrees with the vibration signals, as this filter was selected to obtain the missing tooth impulses alone, and minimize the healthy and chipped case.

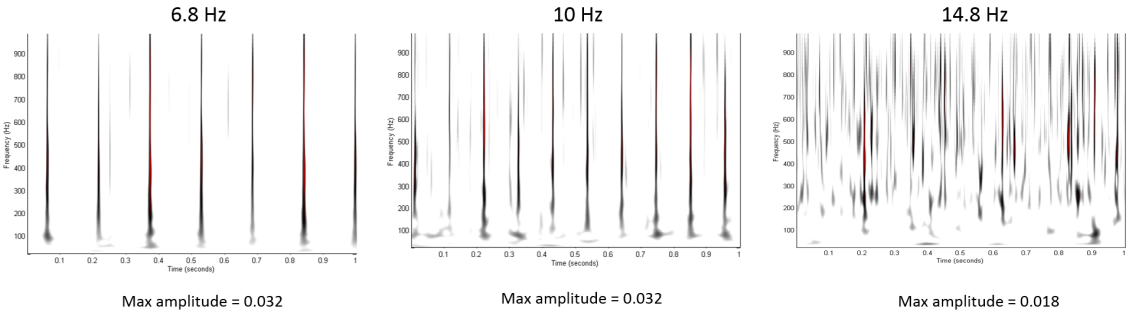

Figure 5.32: Wavelet Analysis of the Acoustical filtered signal around 8500 Hz band, for the missing tooth.

The Wavelet Analysis of the missing tooth acoustical signal, as well as the time domain,

shows that this band-pass filter evidences the missing tooth impulses that were hidden in the signal before filtering. Figure 5.32 shows the clear impulses of the missing tooth after filtering, at different shaft speeds. It is also noted as the speed increases, the impulses due to the missing tooth become less clear, and the signal becomes similar to the healthy gearbox signal, with the gear meshing components becoming more influential, and the overall amplitude level decreasing. The same phenomenon that was observed in the vibration signals is also detected by the acoustic signals.

5.8 Features Extraction

The final objective of this dissertation is to design a semi-automated classification system for the diagnosis of gearbox faults. The features that could allow detection of these faults must be tested, selected and extracted. After the Feature extraction, the application of a numerical method that allows the visualization of all the selected features was performed. The PCA was chosen, as it allows dimension reduction from the space of multiple features to 1, 2, or 3 dimensions, also known as principal components.

5.8.1 Filter Influence

Between the raw data and the filtered data for the four bandpass filters, the features which show the least amount of variability and intersection were chosen.

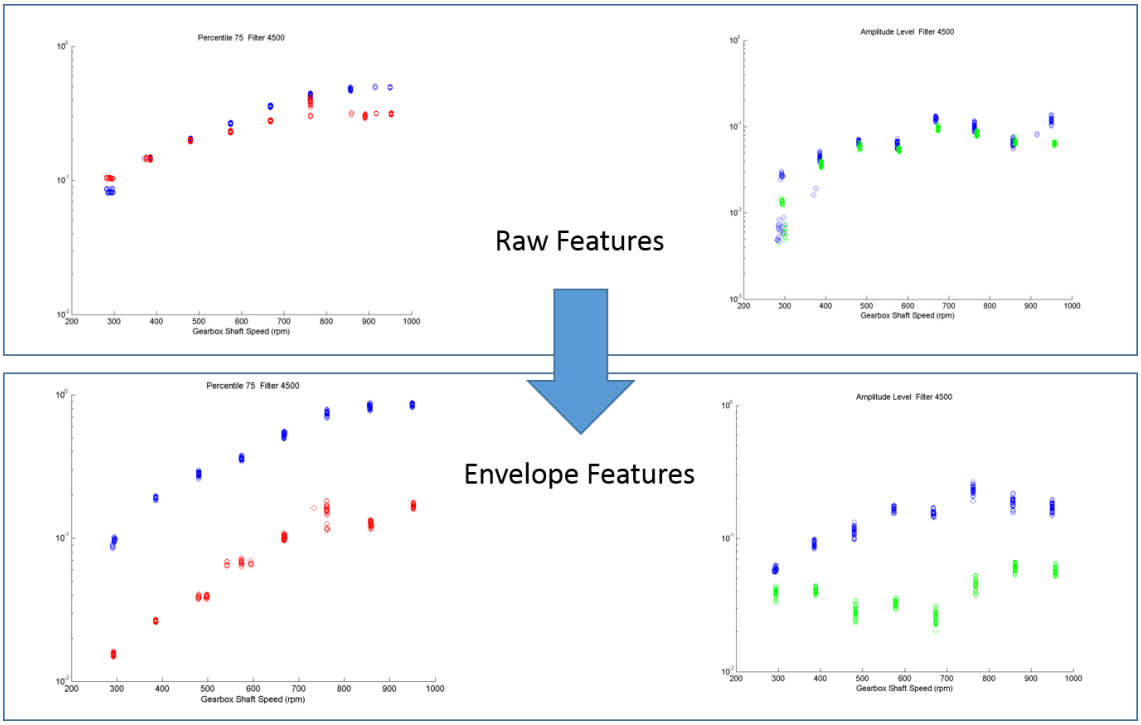

Figure 5.33: Effect of Envelope Analysis on Features.

Figure 5.33 represents the effect filtering had on feature, and the two shown features demonstrate how relevant the correct filter selection is on the classification of faults.

The feature selection was performed according to this procedure, where the features from the filtered data were compared to the raw data. In general, the features showed improved

results.

Based on this criteria, "Engineering knowledge" was used to select a nice subset of 8 features that follow:

1. Speed
2. 75^{th} Percentile (P_{75})
3. Shannon Entropy ($Ent_{shannon}$)
4. Logarithmic Entropy Energy (Ent_{log})
5. Standard Deviation (σ)
6. Peak to Peak (PP)
7. $ENA4$
8. Crest Factor (CF)

5.8.2 Principal Component Analysis

The PCA allows the evaluation of all selected features with the greatest variance content. In the next figures are presented the results for the different features applied to the acoustical and vibration signals, at the different filter parameters.

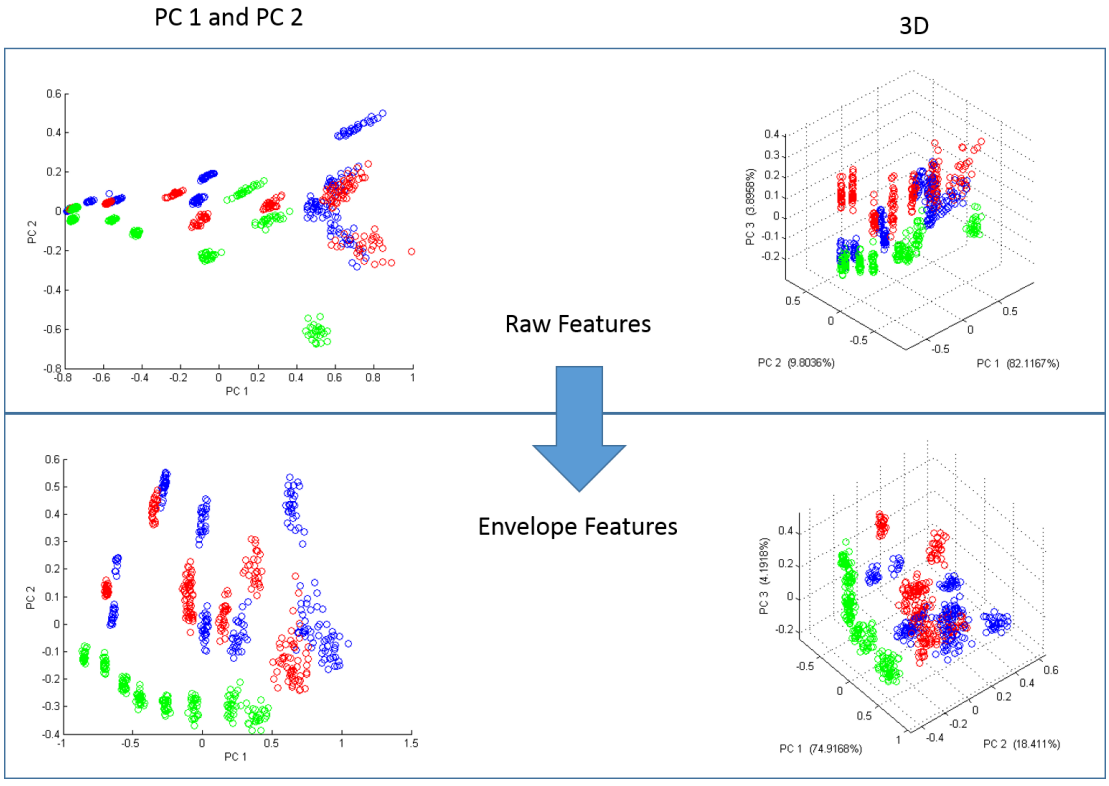

Figure 5.34: PCA of the Acoustical Signals for 1500 Hz bandpass filter.

The Envelope Analysis applied to the signal allows a better classification of the faults. This is seen from Figure 5.34, where the PCA for the Envelope allows classification of the chipped tooth fault by threshold, while the raw features do not provide this classification. The missing tooth could also be classified from the Envelope Analysis for the three lowest

speeds alone, and for the high speeds, the acoustic signals become similar to the healthy case. This is assumed to be the main reason the PCA can not detect the missing tooth.

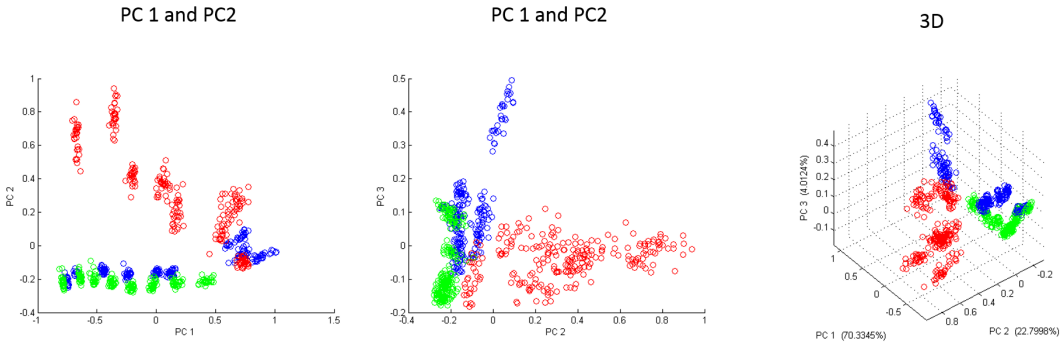

Figure 5.35: PCA of the Acoustical Signals for 8500 Hz bandpass filter.

By filtering around the 8500 Hz band, only the modal frequencies due to the missing tooth impulse are obtained. This results in an attenuation signal for the healthy and chipped cases, and an enhancement for the missing tooth signal, thus turning the classification of the missing tooth fault more evident than for the raw signals.
The principal components of the missing tooth case are mixed together with the healthy signals for the greatest of speeds alone. This can be justified with increasing similarity between the signals as the speed increases, as was already seen from the Wavelet Analysis, that every impulse of the missing tooth was less noticeable as the speed increases, and due to the presence of other sound sources that may be more relevant, thus masking the sound of the gear fault.

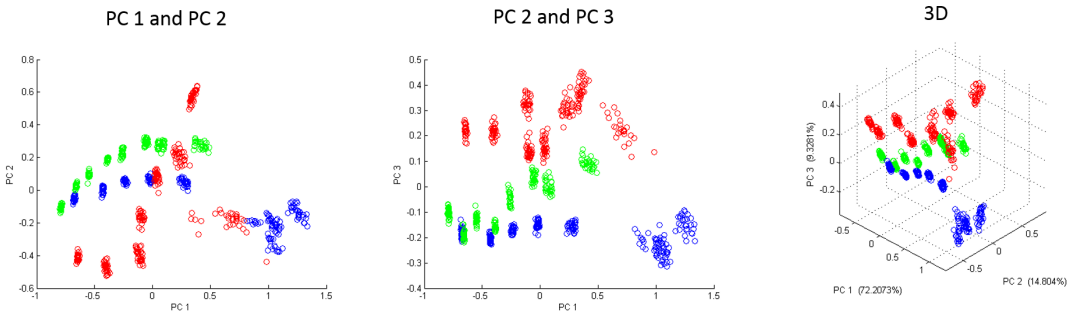

Figure 5.36: PCA of Raw Vibration Signals.

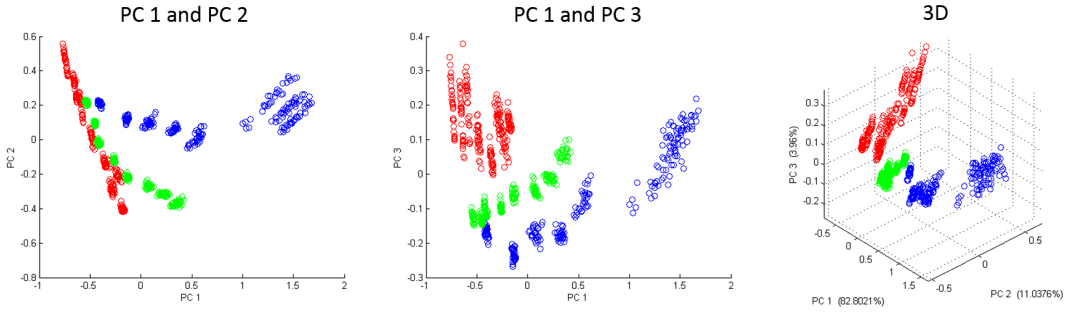

Figure 5.37: PCA of the Vibration Signals for 4500 Hz bandpass filter.

From the PCA of the raw signals, there is already a possibility to detect between the three different faults. This agrees with the raw signals, as they already showed distinct behaviour

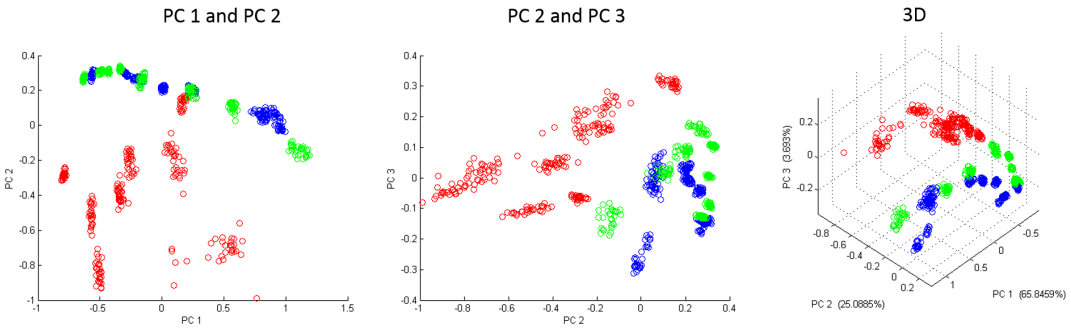

Figure 5.38: PCA of the Vibration Signals for 8500 Hz bandpass filter.

by themselves. Figure 5.36 shows the PCA for the raw vibrations.

PCA for Filter 1 is the one that provides the best classification system. The three level of faults are all distanced from each other for all the speeds, thus providing the best results. This agrees with the analysis so far, as for this filter parameters, and the PCA for this case is shown in Figure 5.37.

The PCA for Filter 2, that selected the frequencies of interest for the missing tooth signal, provides the correct classification of the missing tooth. As seen in Figure 5.38, the principal components correspondent to the missing tooth are completely separated from the other two, and classification of this fault becomes evident for all speeds, with better results than for the raw case.

CHAPTER 6

Conclusion

6.1 Conclusions

At the end of this work it is possible to reach some important conclusions:

- Signal processing techniques are extense and various, and as each one alters the signal in a different way, it is mandatory to spend the time to understand which ones will be more beneficial.
- Faulty signals of rotating machines change from machine to machine, and selected procedures are projected to each case.
- Missing Tooth impulses are more prominent in slow speeds, and could be detected directly on the time-domain. At the highest speeds, the impulse was not detected, as the structure becomes more stable and signals obtained become similar to the healthy case. The chipped similar to the healthy in all speeds, and consistent detection seems difficult with just the Time, Spectral and Wavelet Analysis. It is then the hardest fault to detect, where in the literature cases where the chipped behaves like the missing were also detected.
- TSA method should be applied with care, as the results derived after the TSA showed a weaker performance. This is rare in the literature, but is the case seen when there is no consistent speed reference (tachometer), which was the case. The method seems to remove cyclostationarity from the signal, so use of TSA before the CSC is advised against.
- Envelope Analysis is widely used, as it increases the SNR. However its application depends on the filter selection. CSC returned a strong filter selection for the all Vibration Analysis, and for the Healthy and Chipped cases with the Acoustical Signals.
- CSC for Acoustical signal for the Missing tooth also detected the correct band of demodulation, however as it is not the maximum, the selected filter is wrongly chosen.
- Various features can contain different classification, and the PCA showed good results in classifying the three cases as it used the maximum useful information from the 8 features.
- Acoustics have shown to be more noisy than accelerometers. The used method is proved to be consistent, and looks promising, as it also classified correctly the 3 different faults.

6.2 Future Works

The following works are suggested:

- As the method was applied on one test rig, it is important to validate the method with other test rigs, and with more levels of faults for the gear. The test rig had a magnetic break, where a braking load could be applied, however all the tests were performed without this braking load on the gearbox. As the braking load alters greatly the signals, this condition should also be tested. More data is necessary to have statistical confidence and to further validate the method.
- Bearing Faults should be tested using this method, as it is well advised in the literature. Measurement should be performed with a proper speed reference, so TSA can be correctly applied to obtain the residual signal and compare signals.
- Other Features can be tested, as there are many other that could provide better results. Other methods besides the PCA should be tested for dimensionality reduction, particularly supervised methods that determine the axes by class separation, like the Fisher Discriminant Analysis.
- Advanced Machine Learning Methods should be applied, as they allow the correct classification by threshold.

Bibliography

[1] Principal components analysis, explained visually. http://setosa.io/ev/principal-component-analysis. Accessed 08 January 2017.

[2] L. Rouyu. *Rotating Machine Fault Diagnostics Using Vibratons and Acoustic Emission Sensors*. PhD thesis, Dissertation University of Illinois at Chicago, 2012.

[3] Quora, how do accelerometers work. https://www.quora.com/How-do-accelerometers-work-in-fitness-wearables. Accessed 03 January 2017.

[4] A. Cichon T. Boczar, S. Borucki and M. Lorenc. The analysis of mechanical vibrations and acoustic pressure level of a transformer model. *Optical and Acoustical Methods in Science and Technology*, 114(6):21 – 25, 2008.

[5] Joseph K. Hammond Kihong Shin. *Fundamentals of Signal Processing: for Sound and Vibration Engineers*. Fundamentals of Signal Processing. John Wiley and Sons, Ltd, 2008.

[6] Alessio Figuretti. Rotating machinery condition monitoring: application to rolling bearing and gearbox. Master's thesis, Università Ploitecnica delle Marche, 2012.

[7] Jérôme Antoni and R B Randall. Differential Diagnosis of Gear and Bearing Faults. *Journal of Vibration and Acoustics*, 124, 2002.

[8] Md. Saifullah Khalid Amit Aherwar. Vibration analysis techniques for gearbox diagnostic: A review. *International Journal of Advanced Engineering Technology*, 3(2):308–331, 2012.

[9] Robert B. Randall, Jérôme Antoni, and S Chobsaard. The Relationship Between Spectral Correlation and Envelope Analysis in the Diagnostics of Bearing Faults and Other Cyclostationary Machine Signals. *Mechanical Systems and Signal Processing*, 15(5):945–962, 2001.

[10] Jérôme Antoni, Abboud D, and Xin G. Cyclostationarity in Condition Monitoring: 10 years after. In *Proceedings of ISMA 2016 including USD 2016*, 2016.

[11] J. Antoni. Cyclic spectral analysis in practice. *Mechanical Systems and Signal Processing*, 21:597–630, February 2007.

[12] Robert B. Randall and Jérôme Antoni. Rolling element bearing diagnostics-A tutorial. *Mechanical Systems and Signal Processing*, 25(2):485–520, 2011.

[13] Konstantinos Gryllias. Condition monitoring lectures. Condition Monitoring Lectures, 2016.

[14] Satynarayana Kiran Kumar, Diwakar. Determination of unbalance in rotating machine using vibration signature analysis. *International Journal of Modern Engineering Research*, 2(5):3415 – 3421, 2012.

[15] Why does electric motor fail and what can you do about it?. http://electrical-engineering-portal.com/why-does-electric-motor-fail. Accessed 04 January 2017.

[16] Samieh Abusaad, Ahmed Benghozzi, Ann Smith, Fengshou Gu, and Andrew Ball. *The Detection of Shaft Misalignments Using Motor Current Signals from a Sensorless Variable Speed Drive*, pages 173–182. Springer International Publishing, Cham, 2015.

[17] Eugene E. Shipley. *Gear Failures*. XTEK, Inc, Latham, N.Y., 1967.

[18] Jérôme Antoni. Cyclostationarity by examples. *Mechanical Systems and Signal Processing*, 23(4):987–1036, 2009.

[19] Vijay Karma and Himanshu Borade. Fault diagnosis of single stage spur gearbox using narrow band demodulation technique : effect of spalling. *IMPACT International Journal of Research in Engineering and Technology*, 1(3):11–16, 2013.

[20] T Figlus and M Stańzyk. Diagnosis of wear of gears in the gearbox using wavelet packet transform. *METALURGIJA*, pages 673–676, 2014.

[21] Wade Smith, Yunzhe Yang, and Robert B. Randall. Detecting changes in gear surface roughness using vibration signals. In *Acoustics 2015 Hunter Valley*, 2015.

[22] Songpon Klinchaeam, Nopdanai Ajavakom, and Withaya Yongchareon. Fault detection of a spur gear using vibration signal with multivariable statistical parameters. *Songklanakarin Journal of Science and Technology*, 2014.

[23] L Gelman, I Jennions, and I Petrunin. Detection/Diagnosis of Chipped Tooth in Gears by the Novel Residual Technology. *International Journal of Prognostics and Health Management*, pages 2153–2648, 2011.

[24] Lin Liu, Zhuang Li, and Suri Ganeriwala. Analyzing gearbox degradation using time-frequency signature analysis. Technical report, SpectraQuest, Inc, 2006.

[25] Budhaditya Hazra and Suri Ganeriwala. Effect of torsional load in gear-fault diagnostics using drivetrain diagnostic simulator. Technical report, SpectraQuest, Inc, 2014.

[26] Ahmad Ghasemloonia, Siamak Esmaeel, and Zadeh Khadem. Gear tooth failure detection by the resonance demodulation technique and the instantaneous power spectrum method – A comparative study. *Shock and Vibration*, 18:503–523, 2011.

[27] Zhuang Li. Experimental analyses of vibration and noise of faulted planetary gearbox. In *Inter Noise 2014*, 2014.

[28] Dr. William A. Gardner. *Statistical Spectral Analysis A Nonprobabilistic Theory*. Prentice Hall, Enlewood Cliffs, New Jersey 07632, 1988.

[29] Paulo Jorge Nascimento Morais. Condition Monitoring of Bearings under Low and Medium Speed Rotation. Master's thesis, Faculdade de Engenharia da Universidade do Porto, 2016.

[30] Mohamed Seghir Boucherit Hocine Bendjama, Salah Bouhouche. Application of wavelet transform for fault diagnosis in rotating machinery. *International Journal of Machine Learning and Computing*, 2(1):82–87, February 2012.

[31] Endo Hiroaki and Sawalhi Nader. Gearbox Simulation Models with Gear and Bearing Faults. *Mechanical Engineering*, 2012.

[32] Ming Zhao, Jing Lin, Yonghao Miao, and Xiaoqiang Xu. Feature mining and health assessment for gearboxes using run-up/coast-down signals. *Sensors*, 16(11), 2016.

[33] RB Randall, B Tech, and Ba Bruel. *Cepstrum Analysis and Gearbox Fault Diagnosis*. BK Instruments, Inc, edition 2 edition, 1973.

[34] Michael Kingsley Eric Bechhoefer. A review of time synchronous average algorithms. *Annual Conference of the Prognostics and Health Management Society*, 47(5):50 – 61, 2009.

[35] Labview, vibration time synchronous averaging - forum discussion. http://forums.ni.com/t5/LabVIEW/vibration-time-Synchronous-averaging/td-p/2106372. Accessed 03 January 2017.

[36] Geoffrey Lyall Mcdonald. Vibration Signal-Based Fault Detection for Rotating Machines. Master's thesis, University of Alberta, Department of Electrical and Computer Engineering, 2011.

[37] Jérôme Antoni and R. B. Randall. The spectral kurtosis: Application to the vibratory surveillance and diagnostics of rotating machines. *Mechanical Systems and Signal Processing*, 20(2):308–331, 2006.

[38] J. Antoni, F. Bonnardot, A. Raad, and M. El Badaoui. Cyclostationary modelling of rotating machine vibration signals. *Mechanical Systems and Signal Processing*, 18(6):1285–1314, 2004.

[39] Z K Peng and F L Chu. Application of the wavelet transform in machine condition monitoring and fault diagnostics : a review with bibliography. *Mechanical Systems and Signal Processing*, 18:199–221, 2004.

[40] Z. K. Zhu, Z. H. Feng, and F. R. Kong. Cyclostationarity analysis for gearbox condition monitoring: Approaches and effectiveness. *Mechanical Systems and Signal Processing*, 19:467–482, May 2005.

[41] Ming J Zuo A, Jing Lin, and Xianfeng Fan. Feature separation using ICA for a one dimensional time series and its application in fault detection. *Journal of Sound and Vibration*, 287:614–624, 2005.

[42] Weixiang Sun A, Jin Chen, and Jiaqing Li. Decision tree and PCA-based fault diagnosis of rotating machinery. *Mechanical Systems and Signal Processing*, 21:1300–1317, 2007.

[43] H Alkhadafe and A Lotfi. Condition monitoring of helical gears using automated selection of features and sensors. *Measurement*, 2016.

[44] M H Gharavian, F Almas Ganj, A R Ohadi, and H Heidari Bafroui. Comparison of FDA Based and PCA based Features in Fault Diagnosis of Automobile Gearboxes. *Neurocomputing*, 2013.

[45] Nader Sawalhi and Suri Ganeriwala. Advanced Signal Processing of a Gearbox Vibration Signal with a Defective Rolling Element Bearing. *Technote, SpectraQuest Inc.*, 2015.

[46] Cédric Peeters, Patrick Guillaume, and Jan Helsen. Vibration based bearing fault detection on experimental wind turbine gearbox data. In *Third European Conference of the Prognostics and Health Management Society*, 2016.

[47] W. Bartelmus and R. Zimroz. A new feature for monitoring the condition of gearboxes in non-stationary operating conditions. *Mechanical Systems and Signal Processing*, 2009.

[48] Mitchell Lebold, Katherine Mcclintic, Robert Campbell, Carl Byington, and Kenneth Maynard. Review of vibration analysis methods for gearbox diagnostics and prognostics, 2000.

[49] C. Freitas, P. Morais, and K. Janssens. Condition monitoring of bearings under medium and low rotational speed. Technical report, Siemens Industry Software NV, May 2016.

[50] R. A. Johnson. Miller and freund's probability and statistics for engineers. *Fifth Edition*, pages 1016–1021, April 1994.

[51] Martin H. R. Statistical moment analysis as a means of surface damage detection. *Proceedings of the 7th International Modal Analysis Conference*, pages 1016–1021, April 1989.

[52] FMTC. Vibration based diagnostics of gearboxes. Technical report, FMTC, Inc, 2013.

[53] D. Zappala, P.J. Tavner, C. J. Crabtree, and S. Sheng. Side-band algorithm for automatic wind turbine gearbox fault detection and diagnosis. *Institution of Engineering and Technology Renewable Power Generation*, 8, 2014.

[54] Vikas Sharma and Anand Parey. Fault diagnosis of gearbox using various condition monitoring indicators for non-stationary speed conditions: A comparative analysis. *2nd International and 17th National Conference on Machines and Mechanisms*, 2015.

[55] Marianne Mosher, Anna H. Pryor, and David G. Lweicki. Detailed vibration analysis of pinion gear with time-frequency methods. Technical report, Ames Research Center, NASA, 2003.

[56] Inc. Spectra Quest. Vibration signature of defected gear tooth using spectral analysis. Technical report, SpectraQuest, Inc, 2007.

[57] Edouard Cardenas Cabadas, N. Hamzaoui, and Jérôme Antoni. Acoustic imaging applied to fault detection on a rotating machine bench. In *Proceedings of ISMA 2016 including USD 2016*, 2016.

[58] UK Essays. November 2013. propagation of low frequency acoustic. [online]. https://www.ukessays.com/essays/engineering/propagation-of-low-frequency-acoustic.php?cref=1. Accessed 04 January 2017.

Appendices

APPENDIX A

Tutorial : Gearbox Fault Diagnosis

Gearbox Fault Diagnosis (GFD) is an algorithm developed at Siemens Industry Software, with the objective simplify the analysis of gearbox vibration signals and diagnose three conditions states of the pinion: healthy, with a chipped tooth; and with missing tooth. The algorithm can be opened with Matlab, upon which the following Graphical User Interface appears as seen in figure A.1:

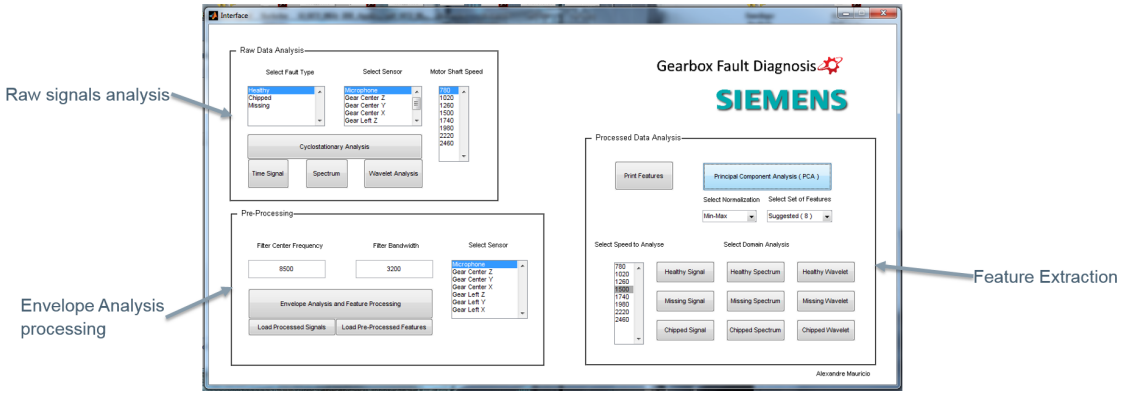

Figure A.1: GFD main interface

The idea of the gearbox fault diagnosis is to detected the frequencies that correspond to each specific fault, filter the signals around these frequencies, and with this minimizing as much as possible other mechanical components signatures. This comes from the vibration theory, that under different operational conditions, different resonant modes of the structure carry the impulse signals of the mechanical components. These resonant modes usually have a high frequency, and are known as carrier waves (a.k.a. carriers). The filter should be made to obtain these frequencies.

A.1 Raw Data Analysis

On the *Raw Data Analysis* window, the raw signals can be analyzed. The selection of the signal is made through the lists available. Here, one of the three fault types can be selected (Healthy, Chipped, Missing), one of the sensor three sensor (Gear Center, Gear Left, Microphone) in one of the three directions, described in the list below:

1. Radial Vertical - Z
2. Radial Horizontal - Y
3. Axial - X

After this, the selected filter can be analyzed in 4 domain. For the selection of the filters, the GFD allows four different representations of the signals, which may expose the information on the carriers of interest. Each method is described by the available buttons, where the most common ones are Time Signal, Spectrum and Wavelet Analysis.

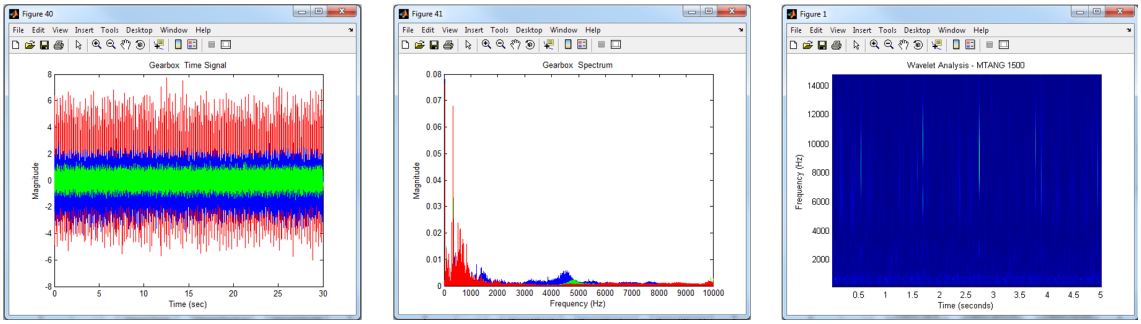

Figure A.2: GFD main interface

Figure A.2 shows the result of each of these three common methods, which are in the Time domain (a.k.a waveform), in the Frequency domain (a.k.a. spectrum) and in the time-frequency domain (wavelet analysis). The plots can be over-posed, for an easy comparison, and the carriers can be seen in either the impulses of the waveform, in frequency bands excited in the spectrum, or in correspondent present frequencies when the impulses take place in the wavelet analysis.

The suggested method is the Cyclostationary Analysis, which is based on the Spectral Correlation. This method was shown to provide consistent results, and declare cyclostationary signatures up to the second level, in an easy to describe map. Pressing the button correspondent to this analysis, the method is calculated and the map is shown, as in Figure A.3

Example 1 *The shown Cyclostationary Analysis is determined from the accelerometer at the center of the gearbox in the vertical direction (GearboxCenterZ) for the healthy pinion at a motor shaft speed of* 1500 *rpm, which is correspondent to a gearbox shaft shaft speed of* 10 *rps/Hz. It can be easily observed that at a cyclic frequency of* $\alpha = 10$ *Hz, the carrier spectral frequency is maximum at around* $f = 4500$ *Hz. Thus the band-pass filter for the healthy impulses is selected with a center frequency of* 4500 *Hz, and a bandwidth of approximately* ± 600 *Hz.*

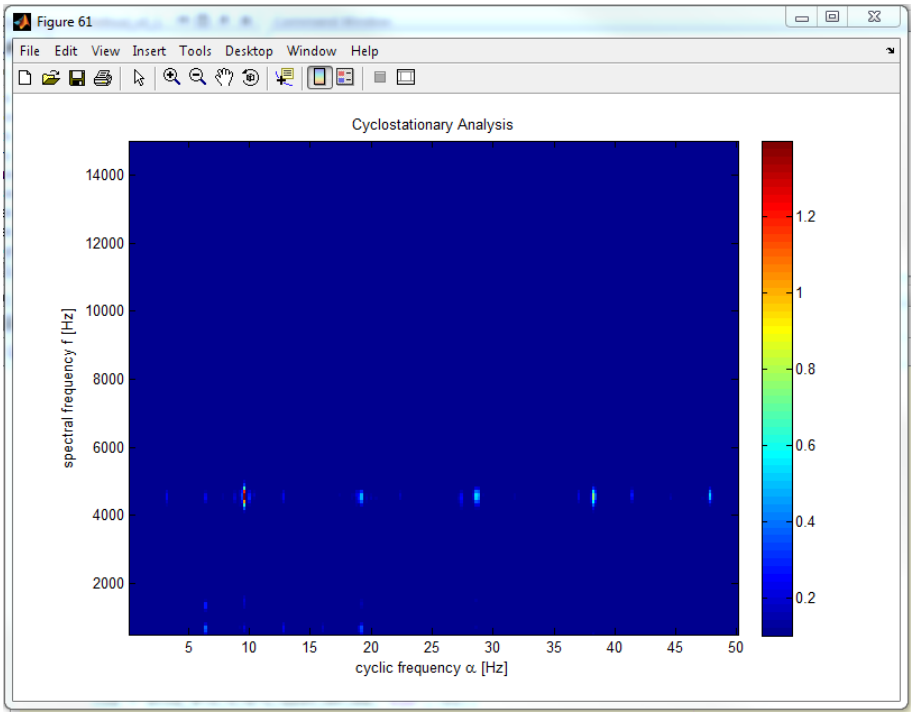

Figure A.3: Cyclostationary Analysis

A.2 Pre-Processing

On the *Pre-Processing* window, the raw signals parameters can be selected for the envelope analysis (band-pass filtering + demodulation). The sensor selections obtains all the measurements at all the available speeds in the database, and filters all signals with the user input filter parameters from the edit boxes 'Filter Center Frequency' and 'Filter Bandwidth'.

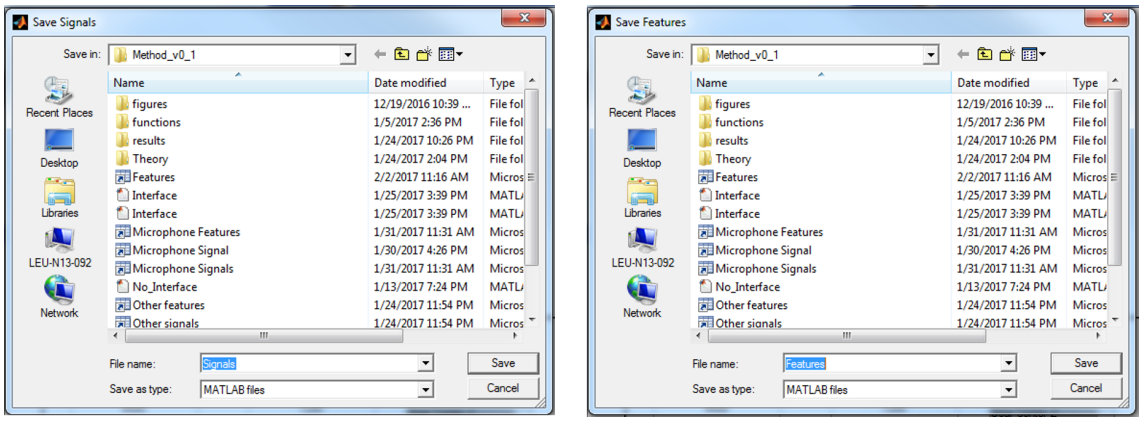

Figure A.4: Save Processed Data

After filter selection, the 'Envelope Analysis and Feature Processing' button processes the signals. After the processing, two windows appear that allow naming and selecting the directory of the processed signals and processed features, as seen in figure A.4. Caution is advised for this processing, as it is computationally expensive, and the processing time rounds up to 22 minutes.

For a fast diagnosis, already processed signals and features can be instantaneously loaded to the algorithm with the buttons 'Load Processed Signals' and 'Load Processed Features'.

A.3 Processed Data Analysis

on the *Processed Data Analysis*, the processed signals can be analyzed, and the fault diagnosed. Similar to the raw data analysis, the three fault causes can be represented in time, spectrum, and time-frequency domain with the wavelet analysis. By selecting the speed to analyze in the available list, and the pressing the button of the fault type and domain represantation, the processed signals can be visualized.

The 'Print Features' button allows visualization of the processed features, and opens a window that allows the user to name the generated pictures and the directory where they will be saved.

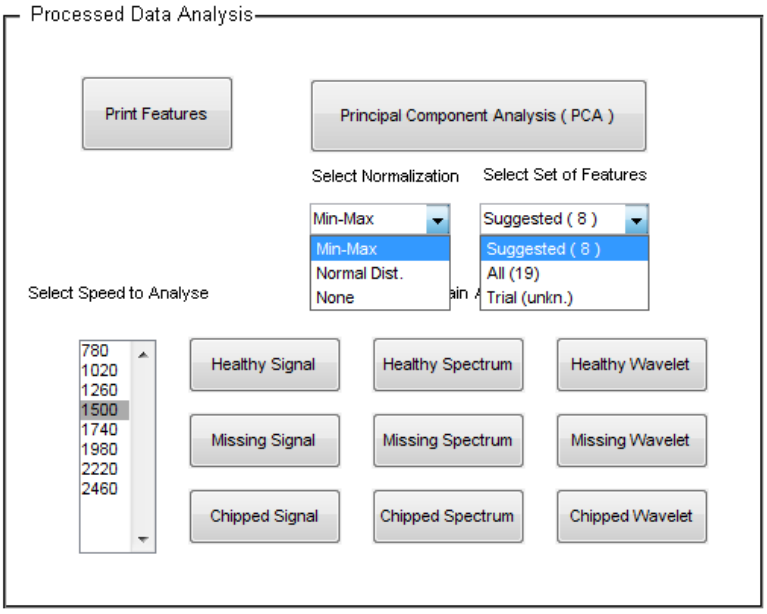

Figure A.5: Processed Data Analysis

The suggested method, that allows differentiation of the different faults, allowing detection, is the Principal Component Analysis. Two pop-up lists are present for the selection of three sets of features and the normalization applied to the features. As seen in figure A.5, the set of features correspond to: *Suggested 8* features that show the best results; *All* the features available in the dataset; *Trial* features that can be selected by changing the correct fields inside Matlab code of the GFD.

When the normalization and set of features is selected, the Principal Component Analysis can be calculated by pressing the *PCA* button. The results are 4 scatter plots, in figure A.6, that represent all possible combinations of the first 3 principal components of the full set of features along the axis with maximum variance. Each fault is represented by a different color, and case the scatter shows aggregation for the same fault case, the diagnosis for that case is assumed viable with the process.

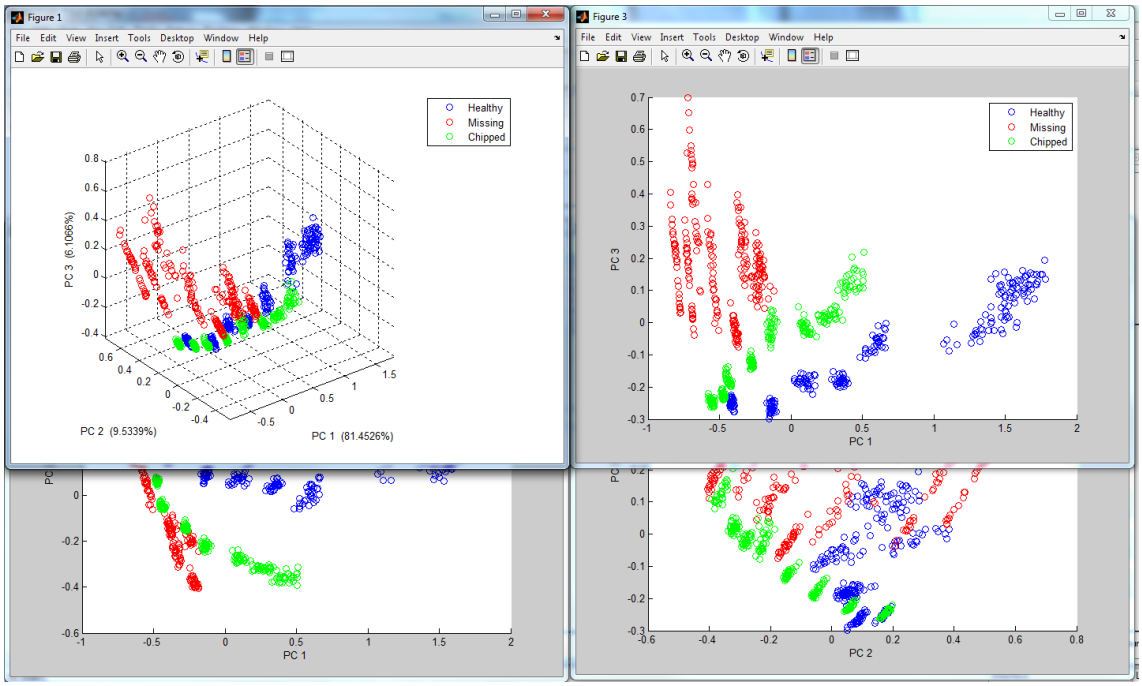

Figure A.6: Principal Component Analysis

Example 2 *The shown PCA figures show the result for the set of 8 features for a band-filter around* 4500 *Hz for the GearboxCenterZ sensor. The 8 features were reduced to 3 dimensions and 2 dimensions, and the first principal component plotted against the third principal component shows separation between the three fault cases. The same is obvious for the 3D plot of the components, where the figure can be rotated to get a better view of the resulting 3 principal components for this signal processing and feature extraction.*